

Chapter 3

Results and discussion

3. Results and Discussion

3.1 Fluoride removal by limestone powder in presence of PA

The author has studied fluoride removal performance using limestone powder in presence of PA. The idea of using powdered limestone and PA for fluoride removal came from earlier works by Nath²⁸⁰. He reported good fluoride removal by acid-enhanced limestone defluoridation (AELD) using PA as the acid in a plug-flow fixed-bed column containing crushed limestone. Therefore, it is thought worthwhile to study the fluoride removal behaviour of limestone powder in presence of PA through batch experiments. The results of batch experiments on fluoride removal by limestone powder in presence of PA as described in the section, *2.4.1 Methods of fluoride removal by limestone powder in presence of PA*, and their interpretations have been presented in this section. Different parameters considered for this experiments were the effect of adsorbent dose, contact time, initial F^- concentrations ($[F^-]_0$) and initial PA concentrations ($[PA]_0$). The kinetics of fluoride removal and the thermodynamic parameters of adsorption of fluoride have also been studied.

3.1.1 Batch study

Batch tests were performed in Erlenmeyer flasks to determine the efficiency of limestone powder in absence and in presence of PA and to optimize the dose of limestone powder and $[PA]_0$. Fluoridated water pre-acidified with PA was added to the flasks containing known amount of limestone powder and were shaken in a thermostated shaker at a speed of 200 rpm for different residence time. The results of this experiment under different operational parameters have been presented below.

3.1.1.1 Effect of adsorbent dose on fluoride removal

The effect of the dose of limestone powder on fluoride removal was studied at fixed conditions of 5 mg/L $[F^-]_0$ concentration and 3 h contact time in absence and in presence of 0.10 M $[PA]_0$ (pH 1.70). The results are given in Table 3.1. and Figure 3.1. The limestone doses were varied from 0.1 g/100 mL to 1 g/100 mL. The fluoride removal in

the presence of PA was found to be much higher than that in the absence and increased on increasing the dose of PA (Figure 3.1A). The amount of fluoride adsorbed per gram in equilibrium decreased gradually with increase in adsorbent dose as shown in Figure 3.1B. On increasing the limestone dose in the presence of PA, the fluoride removal increased from 46% at 0.1 g/100 mL to 92% at 0.5 g/100 mL and then levelled off (Table 3.1). The levelling off may be attributed to two factors. Firstly, overlapping of active sites occurs above a particular dose²⁹⁶. Secondly, there cannot be any appreciable change in the effective surface area due to conglomeration of exchanger particles at higher doses²⁹⁷.

Table 3.1. Remaining $[F^-]$ in the water and amount of fluoride adsorbed in equilibrium (q_e) after treatment by limestone powder in absence and in presence of 0.10 M $[PA]_0$ at different adsorbent dose (g). $[F^-]_0 = 5$ mg/L; contact time = 3 h and $T = 298 \pm 1$ K.

Adsorbent dose (g)	In absence of PA		In presence of 0.10 M PA	
	$[F^-]$ (mg/L)	q_e (mg/g)	$[F^-]$ (mg/L)	q_e (mg/g)
0.1	4.90	0.10	2.70	2.30
0.2	4.70	0.15	1.90	1.55
0.3	4.70	0.10	0.79	1.40
0.4	4.60	0.10	0.66	1.08
0.5	4.40	0.12	0.40	0.92
0.6	4.40	0.10	0.47	0.75
0.7	4.40	0.08	0.47	0.65
0.8	4.40	0.07	0.48	0.57
0.9	4.45	0.06	0.49	0.50
1.0	4.45	0.05	0.51	0.45

3.1.2 Role of sorption in the fluoride removal

The first question is whether the removal of fluoride takes place through precipitation or adsorption. CaF_2 is known to be precipitated by calcium ions generated by dissolution of limestone by acids²⁷⁹. However, the precipitation of CaF_2 is reported to be inhibited by the presence of phosphate ions²⁷⁶. On the other hand, phosphate ions of PA can combine with the calcium ions to form calcium phosphates or HAP which has a high sorption capacity of fluoride^{249, 250}.

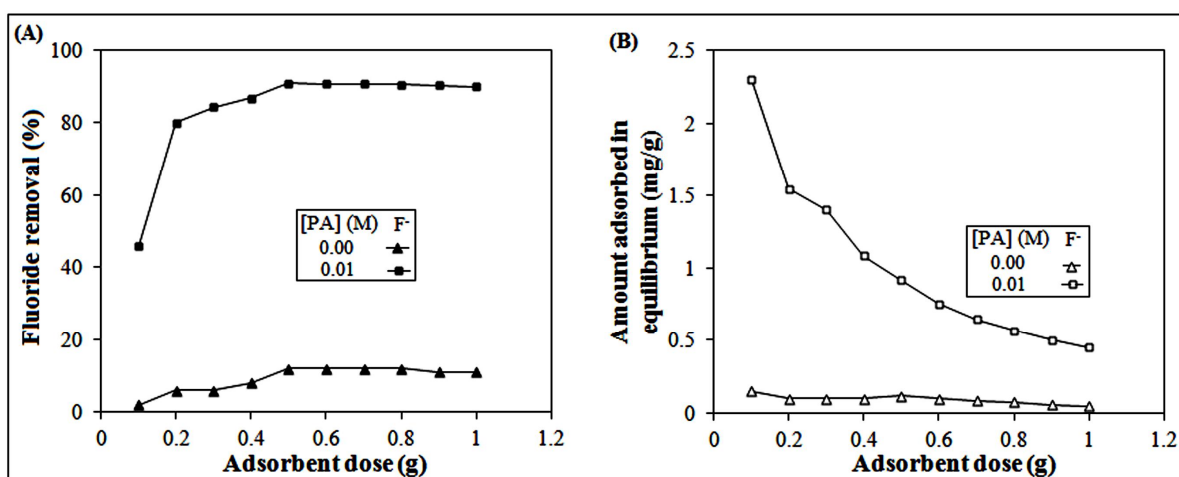


Figure 3.1. Effect of limestone dose on (A) percentage of fluoride removal and (B) the amount of fluoride adsorbed in equilibrium in absence and in the presence of 0.10 M $[PA]_0$ at 298 ± 1 K. $[F^-]_0 = 5$ mg/L.

It is interesting to note that both precipitation by Ca^{2+} ions and adsorption by HAP are known to be selective towards fluoride over other ions commonly present in groundwater²⁴⁹. The actual mechanism of fluoride removal has been assessed from FTIR and XRD analyses and elaborated below.

3.1.2.1 FTIR evidence

The FTIR spectra of fresh limestone powder shows the major characteristic peaks of calcium carbonate^{76, 278} at 1427 , 874 and 708 cm^{-1} (Figure 3.2A). The peak around 3411 cm^{-1} corresponds to the stretching frequency of O-H¹⁹¹. The spectra of the solid obtained after fluoride removal in presence of 0.10 M $[PA]_0$ also show these peaks prominently (Figure 3.2B). The spectra of the solid obtained after use show additional peaks at 1063 and 1137 cm^{-1} which can be attributed to PO_4^{3-} and H- PO_4^{2-} stretching, respectively²⁹⁸. A low intensity peak Ca-F stretching band at 775 cm^{-1} can be attributed to a presence of a small quantity of CaF_2 ²⁹⁹. The author has already mentioned that the precipitation of CaF_2 is inhibited by phosphate ions²⁷⁶. The IR peaks due to CaF_2 may be weak also due to masking by the presence of very large quantity of calcium carbonate and HAP compared to that of CaF_2 . Thus, IR spectra suggest that the solid, obtained after fluoride removal, contains mainly calcium carbonate (limestone) and calcium phosphate in the form of HAP along with a small quantity of CaF_2 .

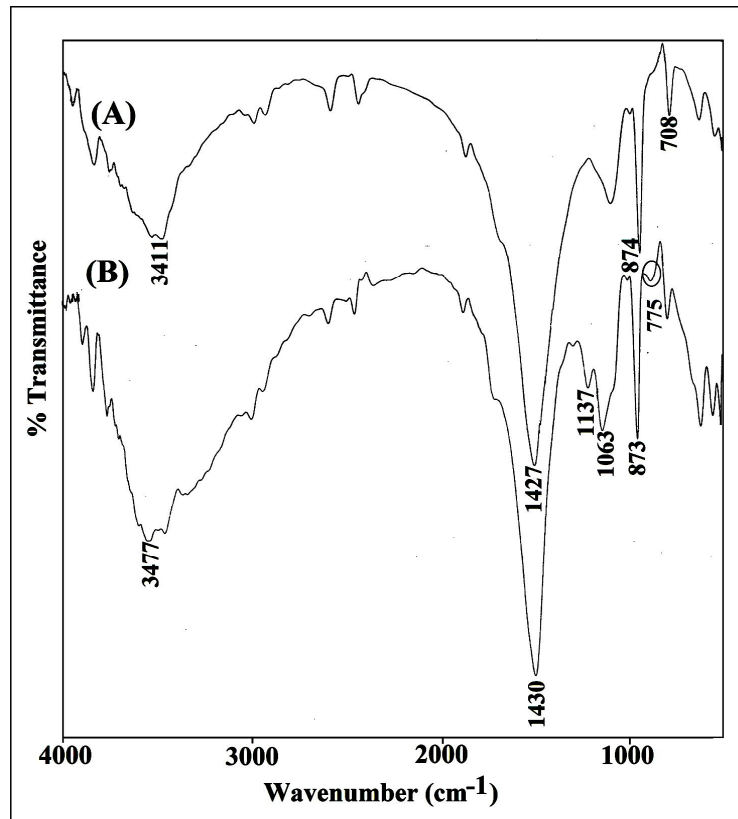


Figure 3.2. FTIR spectra of limestone powder before (A) and after (B) fluoride-loading.

3.1.2.2 XRD evidence

The XRD patterns of the fresh limestone powder and the solid of three samples of used limestone samples obtained from three different sets of experiments in the presence of 0.10 [PA]₀ are shown in Figure 3.3. The peaks with significant intensities at $2\theta = 23^\circ$ (1 0 2), 29.5° (1 0 4) (strong), 36.12° (1 1 0), 39.5° (1 1 3), 43.5° (2 0 2), 47.5° (1 0 8) and 48.5° (1 1 6) corresponding to calcite polymorph of calcium carbonate are seen in the XRD of the fresh limestone powder (Figure 3.3A). The XRD of the solid of three samples of used limestone powder obtained from three sets of experiments shows all these peaks prominently but with some changes in some relative intensities (Figure 3.3B-D). A large increase in the relative peak intensity at 47.5° (1 0 8) in the three solid samples obtained after fluoride removal can be attributed to diffraction from the plane (2 0 2) of fluorite (CaF_2)^{264, 300}. An absence of any significant quantity of fluorite (CaF_2) in the three solid samples obtained after fluoride removal is indicated by the absence of a significant peak of fluorite expected at 46.9° (2 2 0)^{267, 300}. Variations in the relative intensities of the peaks were reported also with limestone after use in AELD with AA, CA and OA²⁷⁷⁻²⁷⁹, which were attributed to adsorption of fluoride on the limestone surfaces.

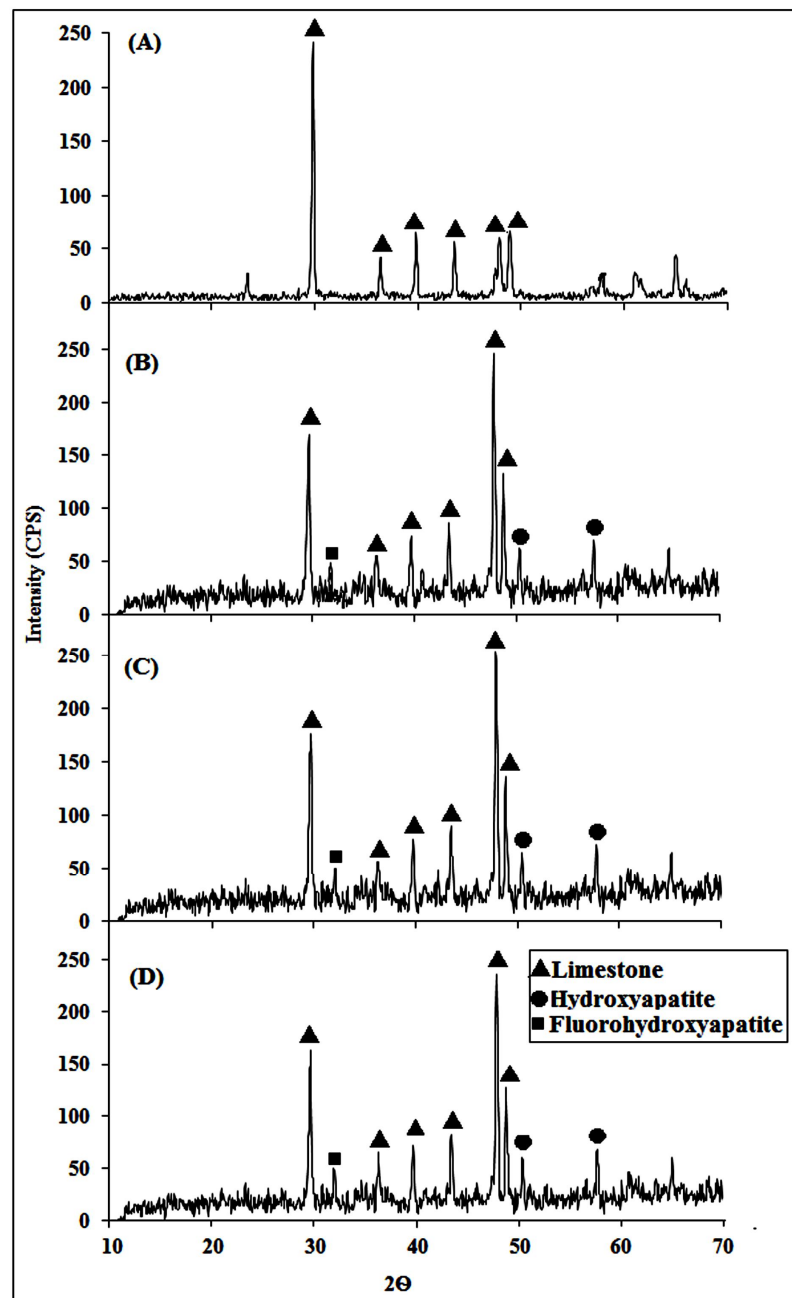


Figure 3.3. XRD of limestone powder before use (A) and after use (B, C and D) obtained from three sets of experiments of fluoride removal in presence of 0.1 M [PA]₀.

Thus, it is possible that the evidences of the presence of fluorite in the solid obtained after fluoride removal is due to fluoride adsorbed on limestone rather than precipitated fluorite.

The large increase in the relative peak intensity observed at 47.5° (1 0 8) after fluoride loading in the three solid samples of limestone may also be attributed to contribution by (1 0 8) plane of HAP¹⁹¹. The peaks at 56.20° (3 2 2) and 50.86° (2 3 1)

also correspond to HAP¹⁹¹. This indicates that a significant formation of HAP takes place in the process. A small peak at 31.93° (2 1 1) in all three solid samples of limestone obtained from three sets of experiments, corresponds to FAP¹⁹² (JCPDS card no. 87-2462). It can be mentioned here that the (2 1 1) peak of FAH observed at 31.93°, occurs at a slightly higher angle than a corresponding (2 1 1) peak of HAP observed at 31.7° (JCPDS card no. 89-6438). The FAP may have formed due to adsorption of fluoride by HAP since HAP has a very strong affinity for adsorption of fluoride^{192, 193}. Thus, the above evidences suggest that the fluoride removal in the present process is dominated by adsorption by two adsorbents. The major adsorbent is HAP which forms FAP after sorption of fluoride through ion-exchange and the minor adsorbent is the limestone itself. The mechanism will be clear from the subsequent studies on adsorption equilibrium and kinetics.

3.1.3 Kinetics of neutralization of PA by limestone powder

The initial pH of 0.10 M PA is 1.70, which finally increases to above 6.00 after neutralization by limestone. The equilibrium pH of treated water is found to be in the range 6.00-6.50. However, remaining pH of the treated water can be increased to pH 7 by treatment of the effluent with another crushed limestone reactor²⁵¹. The kinetics of neutralization of PA by limestone powder have been studied and presented in Table 3.2 and Figure 3.4.

Table 3.2. The results of neutralization of 0.10 M PA by limestone powder with time (s) at 298±1 K.

Time (sec)	[PA] (M)	Time (sec)	[PA] (M)
1	0.002955	40	1.81x10 ⁻⁵
2	0.000269	50	1.76x10 ⁻⁵
4	0.000216	60	6.29x10 ⁻⁵
6	6.02x10 ⁻⁵	120	1.55x10 ⁻⁵
10	5.39x10 ⁻⁵	180	1.38x10 ⁻⁶
12	5.09x10 ⁻⁵	240	1.18 x10 ⁻⁶
14	4.73x10 ⁻⁵	300	1.14 x10 ⁻⁶
16	4.12x10 ⁻⁵	600	1.11x10 ⁻⁶
18	3.77x10 ⁻⁵	900	1.08x10 ⁻⁶
20	3.14x10 ⁻⁵	1200	9.96x10 ⁻⁷
22	2.51x10 ⁻⁵	1500	8.97x10 ⁻⁷
30	2.28x10 ⁻⁵	1800	7.86x10 ⁻⁷

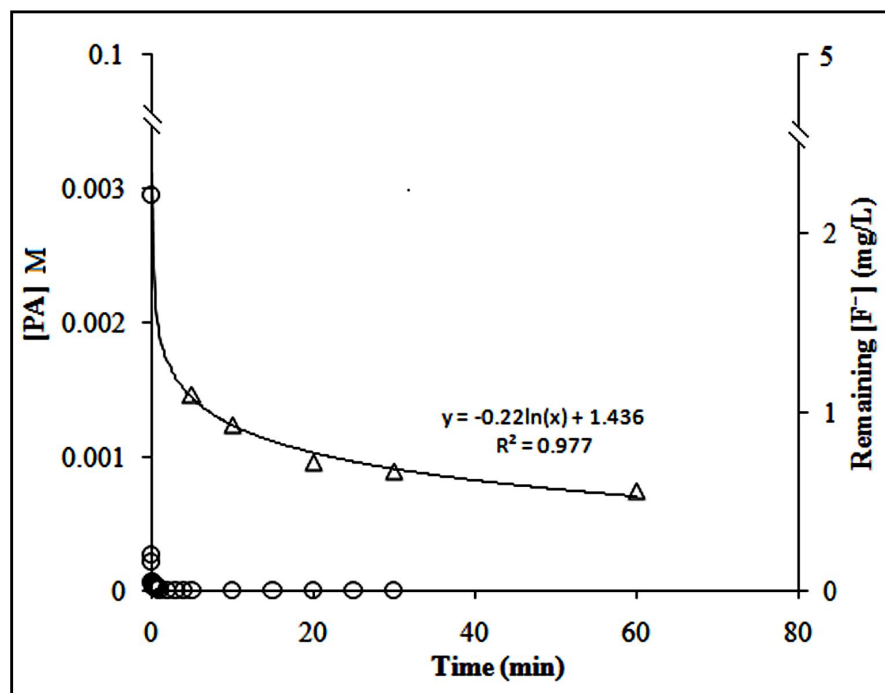


Figure 3.4. A plot of neutralization of PA and remaining $[F^-]$ in the water after treatment with limestone powder vs. time. $[PA]_0 = 0.10$ M and $[F^-]_0 = 5$ mg/L.

It has been seen that the acid is almost neutralized within a minute whereas the fluoride removal, though faster initially, continues for hours. Therefore, the dissolution of limestone by PA and the precipitation of calcium phosphates is a rapid process and it is quite possible that the dominant mechanism of fluoride removal is a slower adsorption or sorption by the co-produced calcium phosphates. However, the validity of this assumption and the role and nature of sorption will be clear from the results of the experiments described in the next sections.

3.1.4 Effect of contact time on fluoride removal

The removal of fluoride as a function of contact time for different $[PA]_0$ and $[F^-]_0$ have been studied and the results have been summarized in Table 3.3 and Figure 3.5, respectively. The figures show that the removal of fluoride continued to increase on increasing contact time up to 50 min and the equilibrium is reached within 3 h (Table 3.3A and Figure 3.5A). The same trend was observed with other $[PA]_0$ and $[F^-]_0$. Thus, the fluoride removal increases with increase in $[PA]_0$ but decreases with increase in $[F^-]_0$ (Table 3.3B and Figure 3.5B) as was reported with other acids²⁷⁷⁻²⁷⁸.

Table 3.3A. Remaining $[F^-]$ (mg/L) in the water at different contact time (min) after treatment with limestone powder in absence and in presence of different $[PA]_0$. * $[F^-]_0 = 5$ mg/L; adsorbent dose = 0.5 g/100 mL and $T = 298 \pm 1$ K.

Time (min)	$[PA]$ (M)					
	0.00 M	0.01 M	0.03 M	0.05 M	0.07 M	0.10 M
Remaining $[F^-]$ (mg/L)						
5	4.80	2.00	1.90	1.70	1.70	0.97
10	4.70	1.80	1.60	1.35	1.30	0.85
20	4.60	1.50	1.50	1.20	1.10	0.74
30	4.60	1.40	1.20	1.00	0.96	0.64
60	4.60	1.20	1.00	0.85	0.72	0.59
120	4.50	1.20	0.93	0.75	0.57	0.50
180	4.40	1.10	0.82	0.65	0.51	0.40
240	4.35	1.10	0.82	0.65	0.51	0.42
300	4.40	1.10	0.82	0.65	0.51	0.42

*Error limit: $[F^-] = \pm 0.2$ mg/L

Table 3.3B. Results of remaining $[F^-]$ (mg/L) in the water and percentage of fluoride removal at different contact time (min) after treatment with limestone powder in presence of 0.10 M $[PA]_0$ at varying $[F^-]_0$. * Adsorbent dose = 0.5 g/100 mL and $T = 298 \pm 1$ K.

Time (min)	$[F^-]_0$ (mg/L)					
	5		10		15	
	$[F^-]$ (mg/L)	F^- (%)	$[F^-]$ (mg/L)	F^- (%)	$[F^-]$ (mg/L)	F^- (%)
5	0.97	81	2.70	73	4.80	68
10	0.85	83	2.50	75	4.65	69
15	0.81	84	2.30	77	4.35	71
20	0.74	85	2.10	79	4.05	73
30	0.64	87	1.90	81	3.90	74
60	0.59	88	1.70	83	3.60	76
120	0.50	90	1.60	84	3.30	78
180	0.40	92	1.50	85	3.00	80
240	0.42	92	1.50	85	3.00	80
300	0.42	92	1.50	85	3.00	80

*Error limit: $[F^-] = \pm 0.2$ mg/L

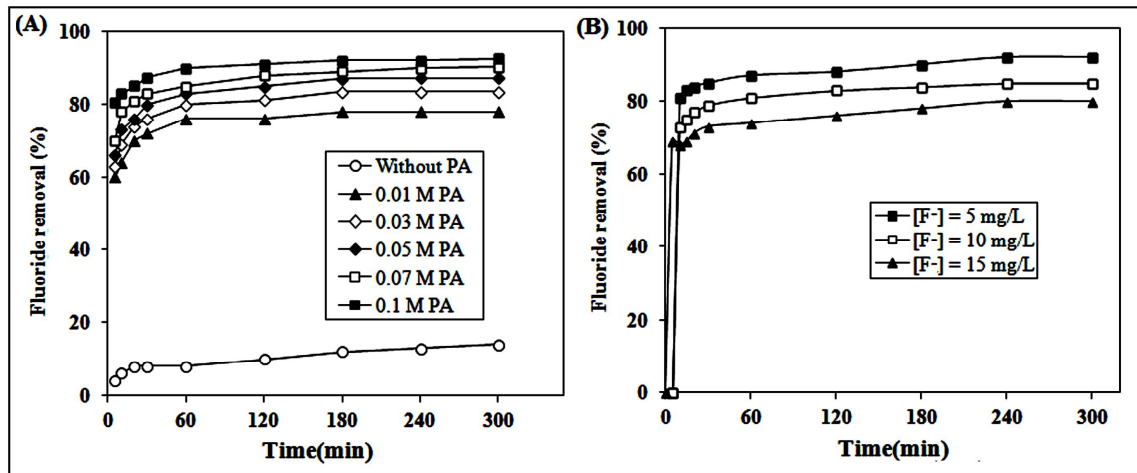


Figure 3.5. Effect of contact time on fluoride removal by limestone powder in presence of varying $[PA]_0$ (A) and $[F^-]_0$ (B) at 298 ± 1 K.

3.1.5 Adsorption kinetics

Kinetics of fluoride removal by limestone powder in presence of PA has been investigated using various kinetic models at different $[F^-]_0$. The results of remaining fluoride concentration with contact time after treatment by limestone powder at different $[F^-]_0$ are presented in Table 3.4.

Table 3.4 Results of remaining $[F^-]$ (in mg/L) at different contact time (min) after treatment with limestone powder with adsorbent dose of 0.5 g/100 mL at different $[F^-]_0$. $T = 298\pm 1$ K.

Time (min)	$[F^-]_0$ (mg/L)								
	3	4	5	6	7	8	9	10	15
	$[F^-]$ (mg/L)	$[F^-]$ (mg/L)	$[F^-]$ (mg/L)	$[F^-]$ (mg/L)	$[F^-]$ (mg/L)	$[F^-]$ (mg/L)	$[F^-]$ (mg/L)	$[F^-]$ (mg/L)	$[F^-]$ (mg/L)
5	0.69	0.78	0.97	1.10	1.40	1.70	1.80	2.70	4.80
10	0.57	0.71	0.85	0.98	1.10	1.50	1.70	2.50	4.65
20	0.49	0.66	0.74	0.91	0.97	1.30	1.50	2.10	4.05
30	0.40	0.61	0.64	0.85	0.83	1.10	1.30	1.90	3.90
60	0.29	0.57	0.59	0.69	0.72	0.96	1.00	1.70	3.60
120	0.27	0.43	0.50	0.54	0.61	0.80	0.97	1.60	3.30

The plots of different kinetic models, *viz.*, pseudo-first-order, pseudo-second-order, intra-particle diffusion and Elovich models have been evaluated using the results presented in Table 3.4 and are described below.

3.1.5.1 Pseudo-first-order equation

The pseudo first-order equation is expressed by Eq. (3.1.1)²⁸⁶:

$$\ln(q_e - q_t) = \ln(q_e) - (k_1)t \quad (3.1.1)$$

where, q_e and q_t are the fluoride adsorption capacities of sorbent at equilibrium and at time t , respectively, and k_1 (min^{-1}) is the pseudo-first-order rate constant. The values of q_e and k_1 have been determined from the slope and the intercept of the linear plot of $\ln(q_e - q_t)$ against t . The results are shown in Figure 3.6A and Table 3.5.

The correlation coefficient values (Table 3.5) obtained from the linear pseudo first-order plot (Figure 3.6A) are poor (<0.952) and the adsorption capacity (q_e , cal) calculated from the plot does not match well with experimental values which indicate a poor fitting of pseudo first-order model in the present process.

3.1.5.2 Pseudo-second-order equation

The pseudo-second-order kinetic rate equation can be expressed by the Eq. (3.1.2)²⁸⁶:

$$t/q_t = (1/k_2).(1/q_e^2) + (t/q_e) \quad (3.1.2)$$

where, q_e and q_t are the fluoride adsorption capacities of sorbent at equilibrium and at time t , respectively, and k_2 is the second order rate constant (g/mg min)

The values of k_2 and q_e were calculated from the slope and the intercept of the plot of t/q_t vs. t and listed in Table 3.5. In case of the pseudo second-order plot (Figure 3.6B), the correlation coefficient values are found to be in the range between 1.000-0.999 which is much better than that of pseudo first-order plots (Table 3.5). The calculated equilibrium capacities (q_e , cal) values are also match well to those obtained from experiment indicating the feasibility of the model.

It can be noted here that both the pseudo first-order rate constant (k_1) and the pseudo second-order rate constant (k_2) decreased with increasing $[F^-]_0$ (Table 3.5) which may be due to decrease in the solid/solute ratio on increasing the $[F^-]_0$.

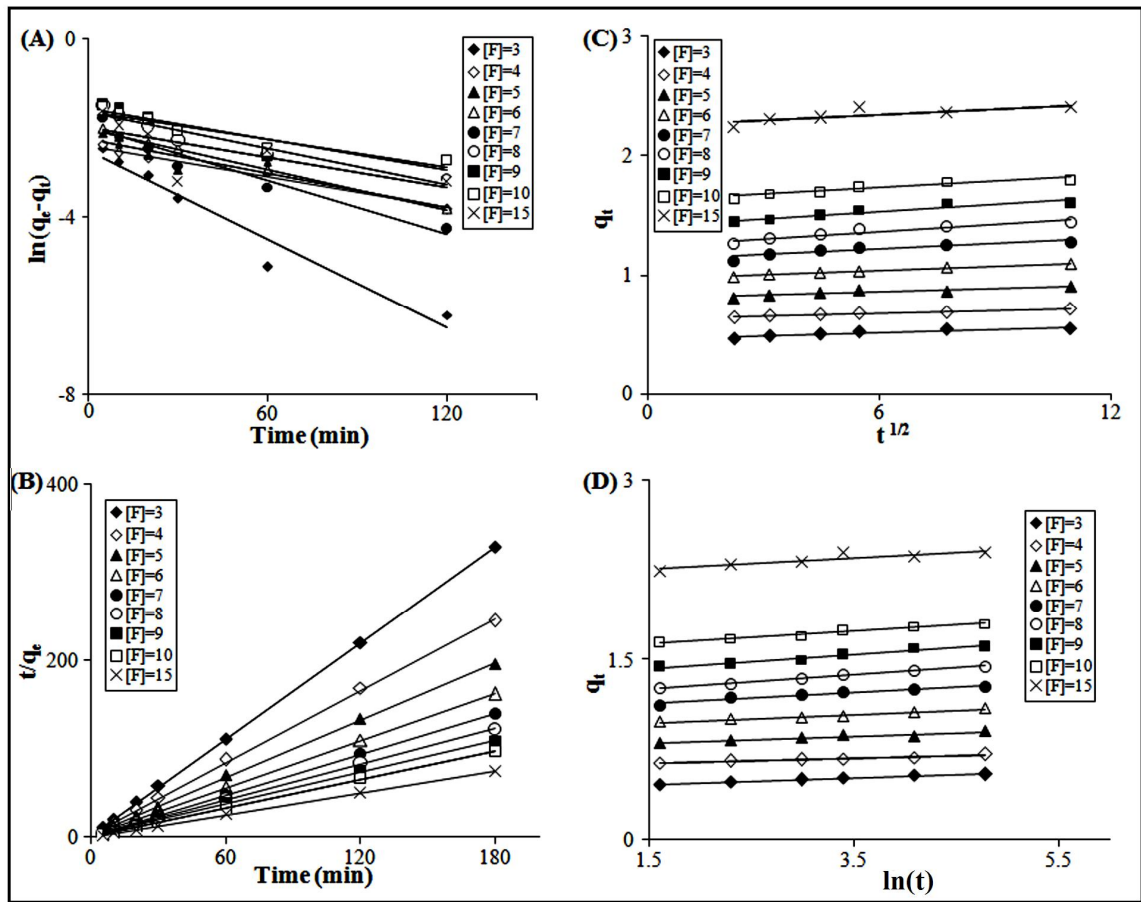


Figure 3.6. Plots of pseudo first-order (A), pseudo second-order (B), intra-particle diffusion (C) and Elovich (D) kinetic model of fluoride adsorption in Limestone-PA systems at different $[F^-]_0$ with fixed $[PA]_0$ (0.10 M) and fixed adsorbent dose (0.5 g/100 mL) at 298 ± 1 K.

3.1.5.3 Intra-particle diffusion model

The intra-particle diffusion model has been used to evaluate the actual rate-limiting step of the adsorption process²⁸⁷. The intra-particle diffusion model can be expressed by the Eq. (3.1.3)²⁸⁷:

$$q_t = k_i t^{1/2} + C \quad (3.1.3)$$

where, k_i ($\text{mg/g min}^{1/2}$) is the intra-particle diffusion rate constant and C gives an idea of the boundary of the thickness. The values of k_i can be evaluated from the plot of q_t vs. $t^{1/2}$ (Figure 3.6C).

Table 3.5. Adsorption parameters obtained from pseudo first-order, pseudo second-order, intra-particle diffusion and Elovich models for adsorption of fluoride by limestone powder in the presence of PA with varying $[F^-]_0$. $[PA]_0 = 0.10$ M and adsorbent dose = 0.5 g/100 mL at 298 ± 1 K.

Parameter	$[F^-]_0$ (mg/L)								
	3	4	5	6	7	8	9	10	15
<i>Pseudo first-order model</i>									
k_1	0.033	0.014	0.012	0.014	0.020	0.013	0.011	0.010	0.007
q_e (cal)	0.081	0.094	0.104	0.133	0.137	0.194	0.208	0.168	0.197
q_e (exp)	0.548	0.736	0.924	1.114	1.292	1.482	1.675	1.864	2.446
R^2	0.952	0.948	0.878	0.945	0.947	0.929	0.830	0.893	0.904
<i>Pseudo second-order model</i>									
k_2	1.225	0.737	0.617	0.562	0.473	0.567	0.326	0.295	0.435
q_e (cal)	0.552	0.737	0.925	1.118	1.298	1.485	1.672	1.865	2.444
q_e (exp)	0.548	0.736	0.924	1.114	1.292	1.482	1.675	1.864	2.446
R^2	1.000	0.999	0.999	0.999	0.999	0.999	0.999	0.999	0.999
<i>Intra-particle diffusion model</i>									
k_i	0.009	0.007	0.009	0.012	0.016	0.020	0.020	0.018	0.015
R^2	0.862	0.974	0.845	0.982	0.834	0.904	0.896	0.915	0.656
<i>Elovich model</i>									
A	1.54	5.50	5.63	1.93	1.79	3.28	3.95	5.15	2.63
	$\times 10^5$	$\times 10^{11}$	$\times 10^{10}$	$\times 10^{10}$	$\times 10^8$	$\times 10^7$	$\times 10^8$	$\times 10^{12}$	$\times 10^{18}$
1/B	0.027	0.020	0.027	0.034	0.048	0.058	0.059	0.052	0.048
R^2	0.970	0.963	0.913	0.979	0.960	0.988	0.957	0.981	0.798

The intra-particle diffusion rate constant (k_i) for various $[F^-]_0$ were determined from the slope of respective plots (Table 3.5). The observed linearity of the curves indicates the occurrence of intra-particle diffusion. However, the intra-particle diffusion may not be the only rate-controlling step because the plots did not pass through the origin. Perhaps, the precipitation of calcium salts also complicates the process. Since the values of k_i increases with increasing $[F^-]_0$, the intra-particle diffusion may be considered as concentration dependent diffusion²⁹⁶.

3.1.5.4 Elovich model

The Elovich rate equation is used for describing kinetics of chemisorptions²⁷⁵ and the equation can be represented by Eq. (3.1.4)²⁸⁸:

$$q_t = (1/B) \ln(AB) + (1/B) \ln(t) \quad (3.1.4)$$

where, A (mg/g min) is the sorption constant of the fluoride ions and B (g/mg) is the desorption constant of the fluoride ions. The slope of the plots of q_t vs. $\ln(t)$ (Figure 3.6D) gives the values of $1/B$. The desorption constant ($1/B$) values ranged from 0.027 to 0.059 mg/g at different $[F^-]_0$, which suggests that the number of available active sites to sorb fluoride decreases with increasing $[F^-]_0$ (Table 3.5). The correlation coefficient values lie between 0.913-0.988 (except with highest $[F^-]_0$) indicating suitability of this model.

From the correlation coefficient values, the order of the appropriateness of the kinetic models for adsorption of fluoride on limestone in presence of PA has been found to be: pseudo second-order > pseudo first-order > Elovich > intra-particle diffusion.

3.1.6 Adsorption isotherms

In order to understand the ability of limestone to adsorb fluoride in absence and in presence of PA, different isotherm plots have been studied. The Freundlich, Langmuir, Dubinin-Radushkevich (D-R) and Temkin isotherm models have been studied by considering different operational parameters. The results are summarized in Table 3.6.

Table 3.6. Remaining $[F^-]$ (mg/L) in the treated water and amount of fluoride adsorbed at equilibrium using limestone powder in absence and in presence of different $[PA]_0$. Adsorbent dose = 0.5 g/100 mL and $T = 298 \pm 1$ K.

$[F^-]_0$ (mg/L)	$[PA]$ (M)					
	0.00	0.01	0.03	0.05	0.07	0.10
	$[F^-]$ (mg/L)	$[F^-]$ (mg/L)	$[F^-]$ (mg/L)	$[F^-]$ (mg/L)	$[F^-]$ (mg/L)	$[F^-]$ (mg/L)
3	2.00	0.55	0.42	0.32	0.28	0.26
5	4.40	1.40	0.82	0.68	0.51	0.40
7	6.40	2.00	1.00	0.94	0.64	0.54
9	9.40	2.50	1.70	1.30	0.98	0.68
10	11.70	3.10	2.40	2.50	2.10	1.50
15	14.70	4.80	4.20	4.00	3.50	3.00

The plots of different isotherm models have been studied using the results presented in Table 3.6 and are described below.

3.1.6.1 Freundlich isotherm

The linear forms of Freundlich isotherm can be expressed by Eq. (3.1.5)²⁸⁹:

$$\ln(q_e) = \ln(K_F) + 1/n \ln(C_e) \quad (3.1.5)$$

where, q_e , C_e , K_F and n are the amount of fluoride adsorbed at equilibrium (mg/g), the fluoride concentration at equilibrium (mg/L), the Freundlich adsorption capacity (mg/g) and adsorption intensity, respectively. The values of K_F and n have been evaluated from the intercept and slope of the linear plot of $\ln(q_e)$ vs. $\ln(C_e)$ (Figure 3.7A) (Table 3.7). Values of n lie between 1 and 10 confirm the existence of favourable conditions for Freundlich isotherm. In the absence of PA, limestone shows a poor adsorption capacity of 0.988 (mg/g) with a correlation coefficient (R^2) of 0.951. The correlation coefficients values are good (≈ 0.974) but the adsorption capacity values are low in the presence of 0.01 M PA. The correlation coefficients values however gradually decrease to 0.834 on increase in the concentration of PA up to 0.10 M. The adsorption capacity (q_e) value increases with increasing $[PA]_0$ which may be due to two factors. Firstly, due to increase in adsorption on renewed limestone surface due to dissolution of limestone by the acid²⁷⁷⁻²⁷⁹ and secondly, due to adsorption of fluoride by newly formed calcium phosphates like HAP, through reaction between limestone and PA^{249, 250}.

3.1.6.2 Langmuir isotherm

The Langmuir isotherm can be represented by Eq. (3.1.6)²⁸⁹:

$$C_e/q_e = C_e/Q_0 + 1/bQ_0 \quad (3.1.6)$$

where Q_0 (mg/g) and b (L/mg) are the Langmuir adsorption capacity and the Langmuir isotherm constant related to the affinity of the binding sites, respectively. The values of Q_0 and b have been calculated from the linear plots of C_e/q_e vs. C_e (Figure 3.7B). The calculated values are included in Table 3.7. The R^2 values in presence of PA decreased on increasing $[PA]_0$ in a similar way as was observed with the Freundlich model.

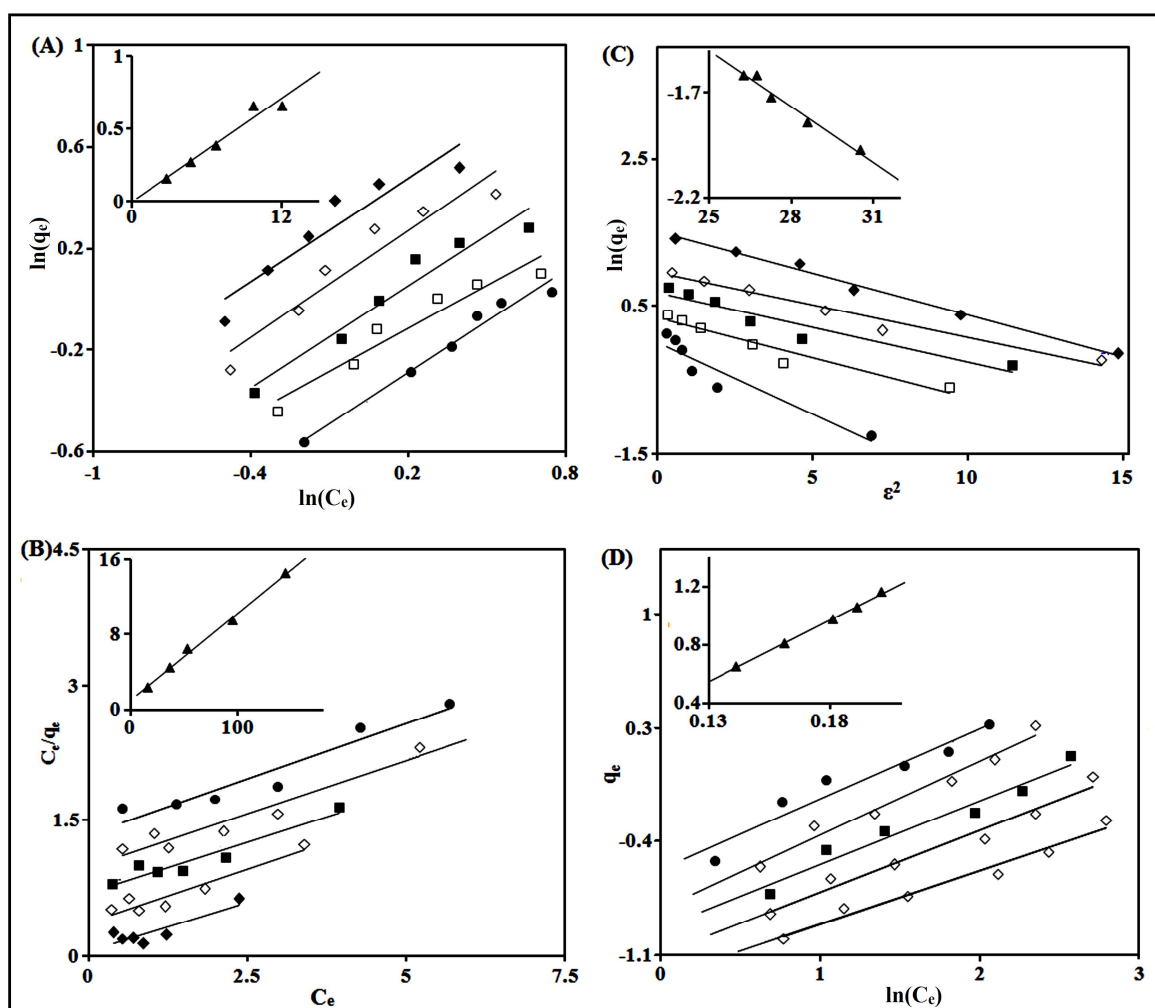


Figure 3.7. Freundlich (A), Langmuir (B), Dubinin–Radushkevich (C) and Temkin (D) isotherms for fluoride adsorption on limestone powder at fixed adsorbent dose (0.5 g/100 mL) and contact time (3 h) at 298 ± 1 K. $[F^-]_0$: 3–15 mg/L, $[PA]_0$: 0.01 M (●) 0.03 M (□), 0.05 M (■), 0.07 M (◇), 0.10 M (◆), 0.00 M (inset, ▲).

The maximum fluoride adsorption capacities of limestone powder in absence and in the presence of 0.10 M PA have been found to be 1.10 and 4.38 mg/g, respectively. It is interesting to note a four-fold higher fluoride removal capacity of PA-enhanced limestone powder compared to the crude limestone powder.

Table 3.7. Values of Freundlich, Langmuir, Dubinin–Radushkevich and Temkin isotherm parameters for fluoride adsorption on limestone in absence and presence of [PA]₀ at 298±1 K.

Isotherm Model	[PA] ₀ /M					
	0.00	0.01	0.03	0.05	0.07	0.10
<i>Freundlich</i>						
K _F (mg/g)	0.988	0.997	1.020	1.208	1.489	1.932
n	1.497	1.044	1.550	1.531	1.490	1.307
R ²	0.951	0.974	0.932	0.942	0.917	0.834
<i>Langmuir</i>						
Q ₀ (mg/g)	1.104	4.032	3.400	3.802	4.000	4.380
b (L/mg)	0.093	0.155	0.483	0.493	0.636	0.748
R ²	0.996	0.924	0.927	0.920	0.891	0.768
<i>Dubinin-Radushkevich</i>						
B _D (mol ² /kJ ²)	0.088	0.284	0.162	0.120	0.112	0.112
Q _D (mg/g)	2.691	1.702	2.029	2.088	2.442	2.992
E (KJ/mol)	6.743	1.327	1.756	2.041	2.113	2.113
R ²	0.971	0.889	0.937	0.903	0.968	0.989
<i>Temkin</i>						
A _T (L/g)	0.860	0.740	0.452	0.439	0.392	0.485
B _T	8.441	0.468	0.548	0.512	0.479	0.391
R ²	0.998	0.927	0.971	0.955	0.970	0.957

The results suggest that the adsorption behaviour of fluoride on limestone in the presence of PA does not fit well to either of the Freundlich and the Langmuir models. However, the Freundlich model fits somewhat better than the Langmuir model. This behaviour can be explained by considering the fluoride removal by both physical adsorption on limestone or HAP and ion-exchange between F⁻ and CO₃²⁻ ions inside limestone particle or between F⁻ and OH⁻ ions inside HAP as shown in the Eq. 3.1.7 and Eq. 3.1.8^{112, 191}.



Such fluoride removal by combination of adsorption and ion-exchange mechanisms is reported in fluoride removal by HAP and n-HAP^{112, 191}. It can be seen from Table 3.7 that the adsorption coefficient, b which is related to the apparent energy of adsorption, is increased from 0.155 to 0.748 L/mg on increasing $[\text{PA}]$ from 0.01 to 0.10 M. The increase in b with $[\text{PA}]_0$ may be attributed to increased quantity of the actual major adsorbent produced in situ, i.e., HAP.

The feasibility of the Langmuir isotherm is expressed in terms of dimensionless equilibrium parameter, R_L defined by the Eq. 3.1.9²⁸⁹:

$$R_L = 1 / (1 + bC_0) \quad (3.1.9)$$

where, C_0 is the $[\text{F}^-]_0$. The R_L values (Table 3.8) are smaller than 1 at the experimental $[\text{F}^-]_0$ and $[\text{PA}]_0$ and decrease with increase in the initial concentrations of both. This indicates that the adsorption is favourable and increases with the concentrations of both fluoride and PA.

Table 3.8. The values of R_L obtained from the Langmuir constant, b at different $[\text{F}^-]_0$ and $[\text{PA}]_0$ at 298 ± 1 K.

$[\text{F}^-]_0/(\text{mg/L})$	$[\text{PA}]_0/\text{M}$				
	0.01	0.03	0.05	0.07	0.10
3	0.683	0.408	0.043	0.344	0.308
5	0.563	0.293	0.287	0.239	0.211
7	0.479	0.229	0.225	0.183	0.160
10	0.392	0.172	0.168	0.136	0.118
15	0.301	0.121	0.119	0.095	0.081

3.1.6.3 Dubinin-Radushkevich (D-R) isotherm

The linear form of D-R isotherm equation can be expressed by the Eq. (3.1.10)²⁹⁰:

$$\ln(q_e) = \ln(Q_D) - B_D \varepsilon^2 \quad (3.1.10)$$

where, Q_D is the adsorption capacity (mg/g), B_D is the activity constant related to mean sorption energy (mol^2/kJ^2) and ϵ is the Polanyi potential.

The mean free energy of adsorption, E (kJ/mol) can be calculated from B_D using Eq. (3.1.11)²⁹⁰:

$$E = 2B_D^{-0.5} \quad (3.1.11)$$

The plot of $\ln(q_e)$ vs. ϵ^2 is shown in Figure 3.7C and the values of the constants Q_D and B_D calculated from the slope and the intercept, respectively, are included in Table 3.7. The reasonably good R^2 values indicate that the adsorption of fluoride by limestone powder in presence of PA fits well to the D-R model. The fitting improved with increase in $[\text{PA}]_0$. The calculated E values have been found to be in the range between 1 and 7 kJ/mol (Table 3.7), which suggest that the adsorption of fluoride on limestone in presence or absence of PA takes place through physisorption.

3.1.6.4 Temkin isotherm

The linear form of Temkin isotherm equation can be represented by Eq. (3.1.12):

$$q_e = B_T \ln(A_T) + B_T \ln(C_e) \quad (3.1.12)$$

A_T (L/g) is the binding constant that represents the maximum binding energy, $B_T = (RT)/b$ is the Temkin constant related to heat of sorption. The plot of q_e vs. $\ln(C_e)$ generates a straight line (Figure 3.7D). These constants have been evaluated from the plots of q_e vs. $\ln(C_e)$ (Table 3.7). The R^2 values indicate that the present system fits well to the Temkin model. The B_T values in the presence of PA are considerably lower than that in the absence of PA. Temkin isotherm equation assumes that the heat of adsorption decreases linearly with coverage due to adsorbate-adsorbate interactions, and that the adsorption is characterized by a uniform distribution of the binding energies, up to some maximum binding energy²⁹¹. The enthalpy of ion-exchange can be as low as the enthalpy of physisorption³⁰¹. The observed lower values in B_T in the presence of PA may indicate a lower heat of exchange of OH^- ions of HAP by F^- ions than the adsorption of F^- ions on limestone. It may be noted here that fluoride ions replace OH^- ions of HAP to form FAP in the present case. Therefore, in the present case, B_T is probably a function of the enthalpy of exchange of OH^- ions by F^- ions rather than simple adsorption of the latter.

Based on the R^2 values, the suitability of the adsorption isotherms follow the order: Temkin > Freundlich > D-R > Langmuir. Thus, it appears from the adsorption isotherms that the removal of fluoride in the PA-enhanced limestone powder takes place through exchange of OH^- ions of HAP by F^- ions which is energetically comparable to physisorption³⁰¹.

3.1.7 Impact of calcium and phosphate ions on fluoride removal

It is evident from above discussion that HAP produced in situ by the reaction between limestone and PA. However, it will be clear more by examining the remaining calcium and phosphate ions in the treated water. The plots of the concentrations of calcium and phosphate as phosphorous remaining in the treated water as a function of $[\text{PA}]_0$ are shown in Figure 3.8. The deviations in the curves of the plots of the concentrations of calcium and phosphate as phosphorous vs. $[\text{PA}]_0$ from linearity suggest increased in the formation of HAP at higher $[\text{PA}]_0$.

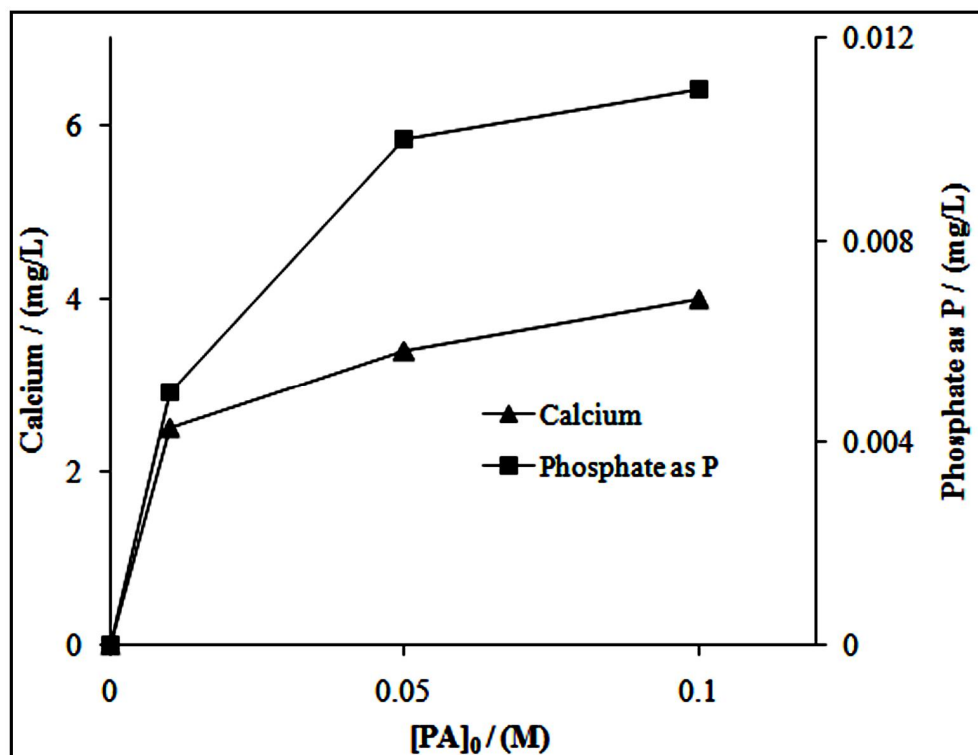


Figure 3.8. Plots of the concentrations of residual calcium and phosphate (as P) in the treated water vs. $[\text{PA}]_0$.

3.1.8 The thermodynamic of adsorption

To see the effect of temperature on the process of fluoride adsorption on the limestone powder in absence and in presence of PA, various thermodynamic parameters *viz.*, standard free energy change (ΔG^0), standard enthalpy change (ΔH^0) and standard entropy change (ΔS^0) are evaluated using the equations (3.1.13) and (3.1.14), respectively²⁹².

$$\Delta G^{\circ} = -RT \ln(K_c) \quad (3.1.13)$$

$$\ln(K_c) = \Delta S^{\circ}/R - \Delta H^{\circ}/RT \quad (3.1.14)$$

where, K_c is the standard equilibrium constant of adsorption. The values of equilibrium concentration of fluoride (C_e), amount adsorbed in equilibrium (q_e) and K_c (ratio of q_e/C_e) at different temperature have been evaluated and are listed in Table 3.9.

Table 3.9. Equilibrium concentration of fluoride (C_e), amount adsorbed fluoride at equilibrium (q_e) and K_c (ratio of q_e/C_e) obtained after treatment with limestone powder in absence and in presence of different $[PA]_0$ at different temperatures. $[F^-]_0 = 5$ mg/L and adsorbent dose = 0.5 g/100 mL.

T (K)	Without PA			0.01 M PA			0.05 M PA			0.10 M PA		
	C_e (mg/L)	q_e (mg/g)	K_c	C_e (mg/L)	q_e (mg/g)	K_c	C_e (mg/L)	q_e (mg/g)	K_c	C_e (mg/L)	q_e (mg/g)	K_c
298	4.40	0.12	0.02	1.10	0.78	0.71	0.65	0.87	1.33	0.40	0.92	2.30
303	2.20	0.56	0.25	0.50	0.90	1.80	0.28	0.94	3.37	0.23	0.95	4.14
308	2.00	0.60	0.30	0.38	0.92	2.43	0.17	0.96	5.68	0.15	0.97	6.46
318	1.80	0.64	0.36	0.32	0.93	2.93	0.11	0.97	8.89	0.05	0.99	19.8
328	1.20	0.76	0.63	0.27	0.95	3.50	0.05	0.99	19.80	0.02	0.99	49.8

A plot of $\ln(K_c)$ vs. $1/T$ for 5 mg/L $[F^-]_0$ in presence or absence of PA gives a straight line and the values of ΔH^0 and ΔS^0 have been estimated from the slope and the intercept, respectively (Figure 3.9). The values of thermodynamic parameters are listed in Table 3.10.

The negative value of ΔG^0 at all temperatures in presence of PA implies that the reaction is spontaneous (Table 3.10). The free energy becomes more negative with increase in $[PA]_0$ and the temperature. The free energy of adsorption is low but sufficiently high to provide a favourable equilibrium fluoride adsorption, as has been observed. However, the values of ΔG^0 are positive at all temperatures for the adsorption of fluoride on limestone in absence of PA, which confirms that adsorption of fluoride on

limestone powder, is very weak. The positive values of ΔH° suggest that the adsorption of fluoride on limestone in all cases is endothermic in nature²⁹². Li et al.³⁰² attributed similar increase in adsorption with temperature to positive ΔH° . The positive ΔS° actually makes the ΔG° more and more negative on increasing temperature which causes the adsorption to increase with increase in the temperature. The entropy change is positive and increased with increase in the $[PA]_0$. This indicates an increase in the randomness after sorption and the sorption is entropy driven.

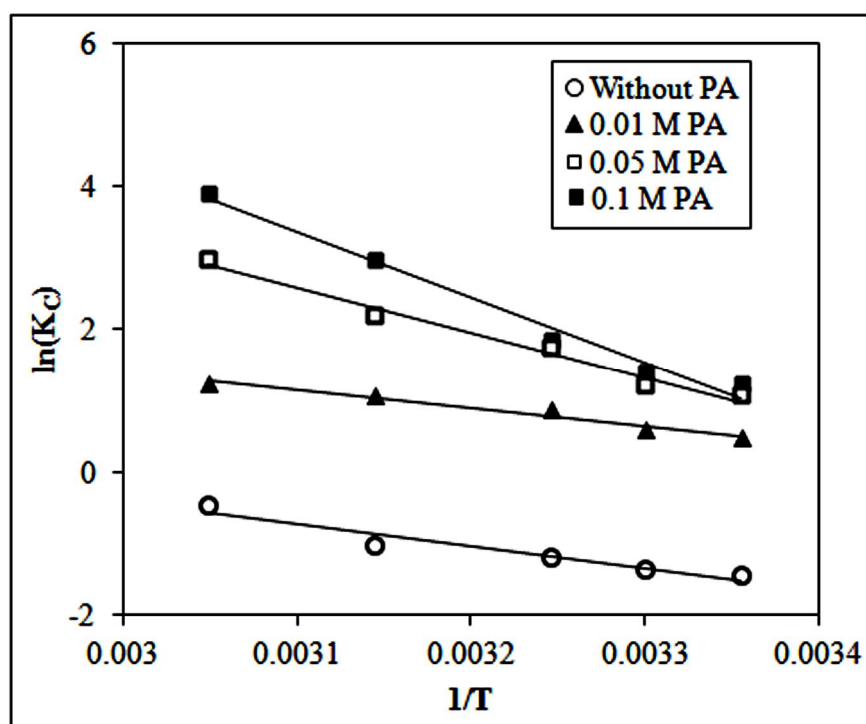


Figure 3.9. Plots of $\ln(K_c)$ vs. $1/T$ for the adsorption of fluoride by limestone powder from aqueous solution in the presence/absence of $[PA]_0$.

Table 3.10. Thermodynamic parameters for the adsorption of fluoride on limestone powder in absence/presence of PA at different $[PA]_0$.

$[PA]_0/M$	$\Delta S^\circ/$ {J/(Kmol)}	$\Delta H^\circ/$ (kJ/mol)	$\Delta G^\circ/(kJ/mol)$				
			298 K	303 K	308 K	318 K	328 K
0.00	0.073	25.64	3.886	3.521	3.156	2.426	1.696
0.01	0.076	21.41	-1.238	-1.618	-1.998	-2.758	-3.518
0.05	0.183	52.03	-2.504	-3.419	-4.334	-6.164	-7.994
0.10	0.262	75.60	-2.476	-3.786	-5.096	-7.716	-10.34

3.1.9 Competitiveness of the present adsorbent

The PA-treated limestone powder which shows comparable fluoride adsorption capacity with HAP and brushite (Table 3.11.), can be of great potential for application in the severely fluoride-affected regions like south Asia where limestone is readily available but HAP and brushite do not occur naturally. The PA-treated limestone powder is advantageous over other modified adsorbent materials (Table 3.11.) such as Al₂O₃/carbon nanotube, surfactant-modified pumice, tamarind fruit-shell carbon, calcined PA-treated limestone, graphene, etc., as the present process does not involve any sophisticated or energy-intensive and can be used without electricity.

Table 3.11. Comparison of monolayer adsorption capacity of limestone from the present work with some reported adsorbents.

Adsorbent	Capacity (mg/g)	Reference
Quartz	0.19	112
Calcite	0.39	112
Magnesite	0.71	146
Gypsum	0.85	146
Laterite	0.86	149,150
Bauxite	1.05	146
Activated alumina	1.45	115
Clays	1.69	303, 304
Fluorspar	1.79	112
Bone char	2.50	305
Nano-HAP chitin composite	2.80	171
Carbon nano-tubes	4.50	132
Hydroxyapatite (HAP)	4.54	112
<i>Powdered limestone-PA</i>	<i>4.38</i>	<i>Present work</i>
Nano-HAP	5.50	192
Brushite	6.59	253
Al ₂ O ₃ /carbon nanotube	13.5	131
Graphene	17.65	302
Calcined PA-treated limestone	22	249
Tamarind fruit-shell carbon	22.33	251
Surfactant-modified pumice	41.00	158

3.1.10 Summary

The findings of this work can be summarised as follows:

- The present study reveals that addition of PA to water along with limestone powder considerably increases the fluoride removal which gives a maximum fluoride adsorption capacity of 4.38 mg/g.
- Analysis of the solid after sorption experiment also showed sorption of fluoride on limestone surface along with the presence of HAP and FAP.
- The experimental observations suggest that fluoride sorption takes place through physisorption and ion-exchange between F^- and OH^- of HAP.
- The kinetics of sorption of fluoride fits the different kinetic models in the following order: pseudo second-order > pseudo first-order > Elovich > intra-particle diffusion.
- The fluoride adsorption fits to different adsorption models in the order: Temkin > Freundlich > D-R > Langmuir.
- The thermodynamic calculation shows that the adsorption and/or ion-exchange of fluoride on limestone powder in presence of PA is spontaneous, endothermic and irreversible in nature.

3.2 Fluoride removal by hydrothermally modified limestone powder using PA

Since hydroxyapatite (HAP) having high affinity towards fluoride adsorption is formed in the reaction between limestone and PA, it is thought worthwhile to modify low-cost limestone hydrothermally using aqueous PA and examine the fluoride adsorption behaviour of the product. This section presents the results of hydrothermal modification of limestone powder using aqueous PA of different concentrations at a fixed Ca/P ratio of 1.66 as described in the section, *2.4.2 Methods of fluoride removal by hydrothermally modified limestone powder using PA*, the characterization of the products and evaluation of its ability to remove fluoride from water with respect to adsorbent dose, contact time, initial fluoride concentration and pH. The fluoride adsorption behaviour of the product has also been studied using various kinetic and thermodynamic models.

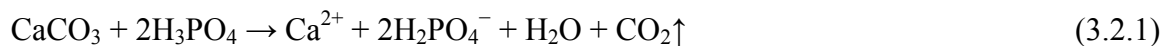
3.2.1 Characterization of the modified limestone

The modified limestone samples were characterized through FTIR, XRD and SEM-EDX analyses.

3.2.1.1 FTIR analysis

The FTIR spectra of fresh limestone powder (L0) and the modified limestone powder samples prepared in the presence of PA concentrations of 0.30 M (M3), 0.60 M (M6) and 0.90 M (M9) are shown in Figure 3.10. The major characteristic peaks for calcium carbonate were observed around 2375, 1417, 878 and 710 cm^{-1} in fresh limestone powder (L0). The characteristic peaks observed at 3571 cm^{-1} and 1798 cm^{-1} correspond to bending mode of adsorbed water¹⁹¹. The peaks at around 2375 cm^{-1} and 1417 cm^{-1} correspond to CO_3^{2-} ion of fresh limestone³⁰⁶. The intensities of the CO_3^{2-} peaks were found to decrease in the order L0 > M3 > M6 > M9, i.e., with increase in the concentration of PA used in the hydrothermal treatment. This may be due to an incorporation of PO_4^{3-} ion replacing CO_3^{2-} ions in that order. In the cases of all three modified limestone powder samples, there are intense peaks at around 1084 cm^{-1} and 615 cm^{-1} indicating formation of hydroxyapatite (HAP)¹⁹². The ratio of the intensities of the peaks at 1084 cm^{-1} (phosphate) to 1417 cm^{-1} (carbonate) gradually increased in the order

L0 < M3 < M6 < M9, i.e., on going from pure limestone towards modified limestone powder with increasing concentration of PA used in the hydrothermal treatment. The formation of phosphates may take place during the hydrothermal treatment through the following reaction:



The sample M9 was used for batch adsorption study as it contains the highest presence of phosphates and hence is expected to highest fluoride adsorption. The FTIR spectra of M9 after fluoride adsorption, MF has been included in Figure 3.10. A weak band appears at around 775 cm^{-1} corresponds to Ca-F stretching of CaF_2 ²⁹⁹.

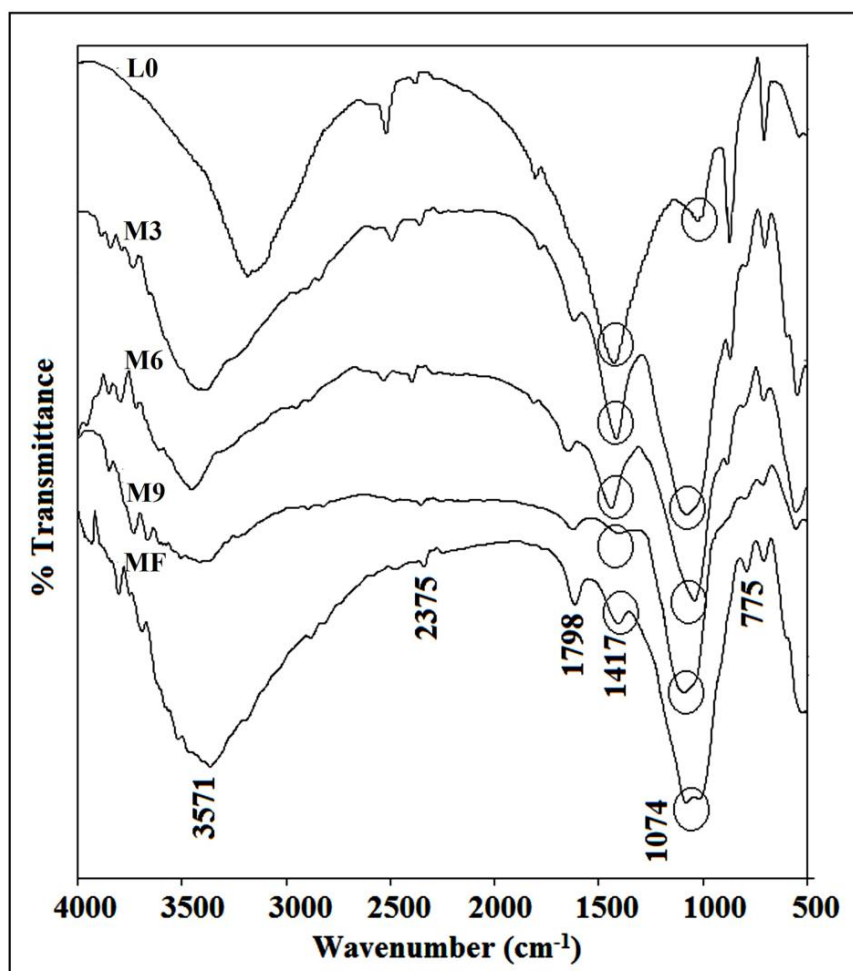


Figure 3.10. FTIR spectra of fresh limestone (L0), hydrothermally synthesized limestone powder at 0.30 M (M3), 0.60 M (M6), 0.90 M (M9) and fluoride-loaded HAP (MF).

3.2.1.2 XRD analysis

The XRD spectra of fresh limestone and modified limestone powder at different PA concentrations have been shown in Figure 3.11. Sharp diffraction peaks in the spectra of modified materials indicate crystalline nature. The peaks at $2\theta = 29.5^\circ$ (1 0 4), 36° (1 1 0), 39° (1 1 3), 43° (2 0 2), 47.5° (1 0 8) and 48° (1 1 6) correspond to calcite polymorph of calcium carbonate²⁷⁷⁻²⁷⁹ in sample L0 (Figure 3.11). The XRD spectra of M3 did not show any characteristic peak for HAP. But in the case of M6, two additional peaks appeared at 25.8° (0 0 2) and 31.7° (2 1 1) which correspond to HAP indicating the formation of HAP¹⁹² (JCPDS card no. 89-6438). The formation of HAP in sample M9 is clear from the peaks at around 25.8° (0 0 2), 31.7° (2 1 1), 49.4° (2 1 3) and 53° (0 0 4) (JCPDS card no. 89-6438).

The crystalline size, τ , of the samples L0 and M9 was calculated from the XRD pattern using the Debye–Scherrer equation (Eq. 3.2.2)³⁰⁷:

$$\tau = \frac{\lambda}{d \cdot \cos\theta} \quad (3.2.2)$$

where, ' λ ' is the wavelength of the Cu-K α radiation, d is the half width of the peak at maximum intensity and θ is the Bragg angle. The characteristic peaks observed for L0 at 29.5° , 39.5° , 47.5° showed the crystalline size of 59, 52 and 48 nm, respectively, which were well-matched to the crystalline size of limestone reported by Babou-Kammoe et al.³⁰⁷. The crystalline sizes of the sample M9 were smaller compared to L0 and found to be 43, 40, 43 and 45 nm for 29.5° , 39° , 47.5° and 48° , respectively, which agreed well with the crystalline size reported for HAP³⁰⁸. There are losses of the planes of limestone with simultaneous formation of respective planes on the hydrothermal modification.

Thus, FTIR and XRD analysis indicated formation of HAP from limestone during the hydrothermal treatment. The sample M9 showed formation of maximum HAP and hence is expected to show maximum adsorption of fluoride. In the fluoride loaded HAP (MF), no marked change was observed except appearance of two small intensity peaks at 33.1° (3 0 0) and 60.3° (2 4 0), which may be attributed to formation of FAP¹⁹² (JCPDS card no. 87-2462).

3.2.1.3 SEM-EDX analysis

The SEM and EDX spectra of the samples L0, M9 and MF were compared and shown in Figure 3.12.

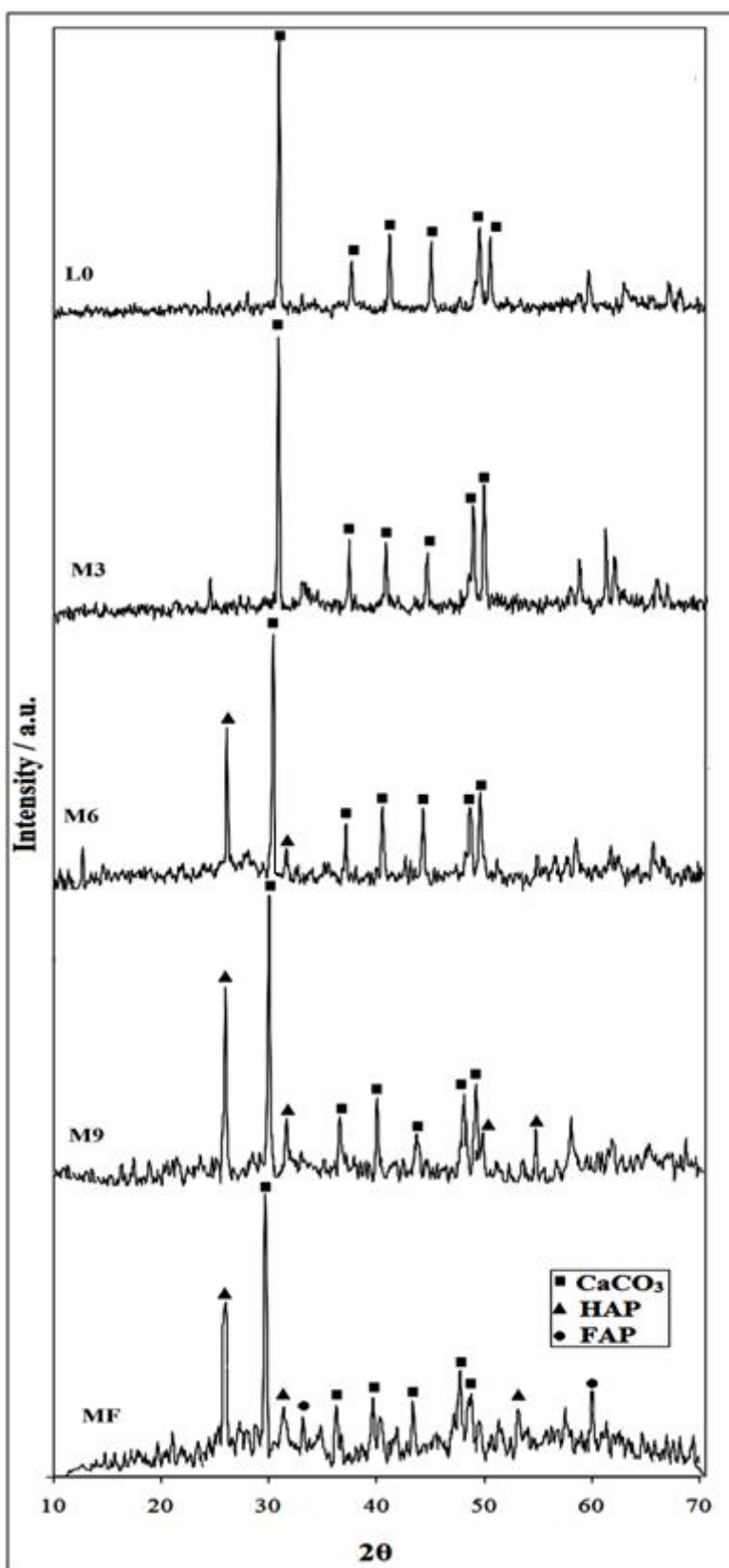


Figure 3.11. XRD spectra of fresh limestone (L0); modified limestone (M3, M6, and M9) and fluoride-loaded HAP (MF).

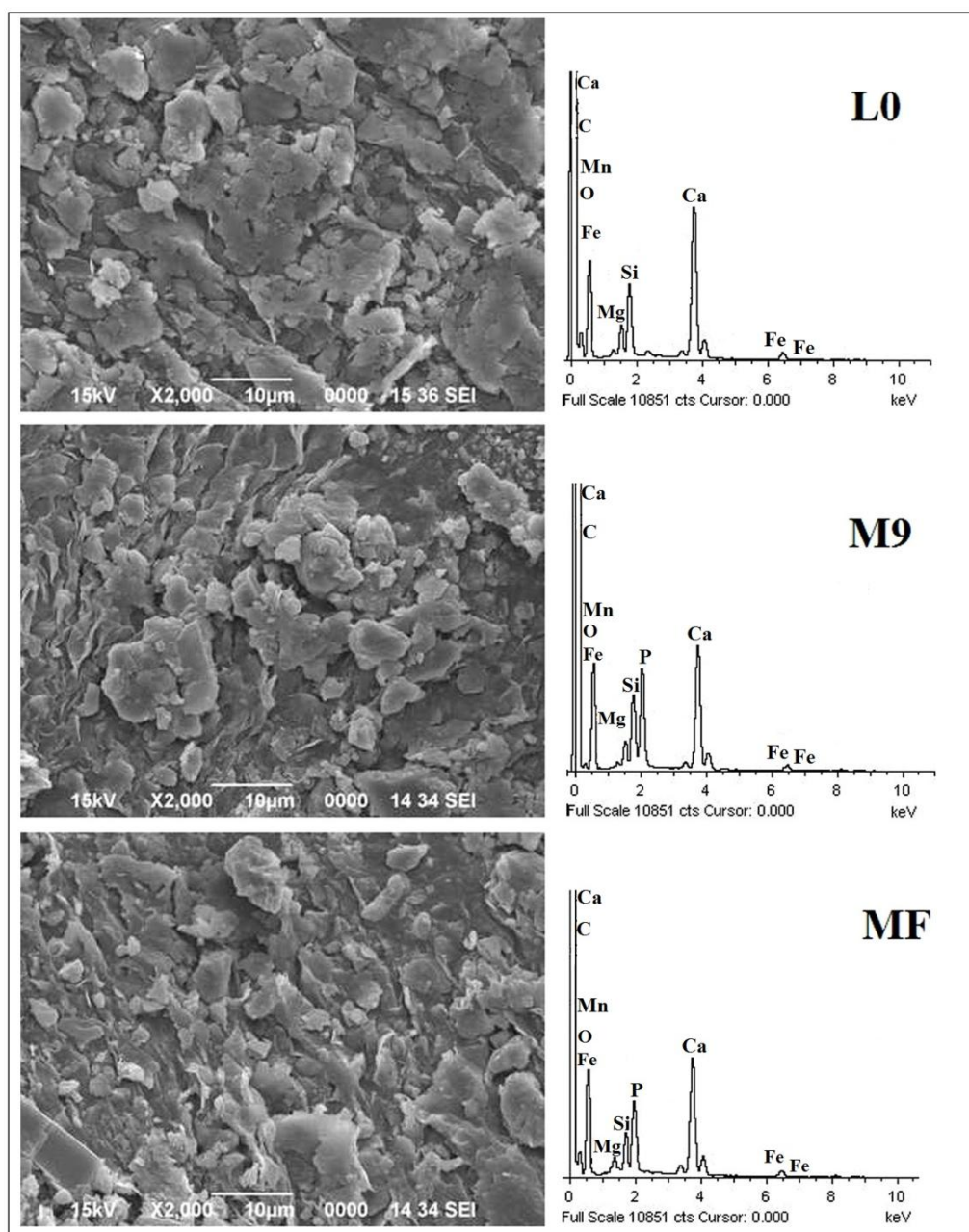


Figure 3.12. SEM and EDX spectra of fresh limestone (L0), modified limestone powder (M9) and fluoride-loaded HAP (MF).

The samples M9 and MF showed the surface modification in comparison to arranged randomly. However, the nanotrac wave particle size distribution analysis showed that the particle sizes of all three samples were mostly within $\leq 1 \mu\text{m}$. The EDX spectra of M9 clearly showed the presence of Ca and P. The atomic weight percent of P in MF was found to be lower than that in M9, which may be due to presence of small amount of F.

3.2.2 Batch study on fluoride removal

3.2.2.1 Fluoride removal by modified limestone

The performance of fluoride removal using the sample L0, M3, M6 and M9 was studied at fixed conditions of adsorbent dose and initial fluoride concentration ($[F^-]_0$). The results are shown in Table 3.12 and Figure 3.13A. A 32% fluoride removal observed with the fresh limestone powder was found to increase to 93% with M9. The fluoride removal increased considerably on changing the adsorbents in the order: L0 < M3 < M6 < M9 as expected. The increase in the fluoride removal in this order may be attributed to a gradual increase in the formation of HAP, which is a much stronger fluoride adsorbent than limestone¹¹².

The plots of variation of pH with time after mixing the adsorbents with adsorbent dose of 0.5 g/150 mL of water are shown in Table 3.12 and Figure 3.13B. Initially, the pH decreased rapidly and then slowed down but continued to decrease slowly till 3 h. The final pH of the water after treatment with the samples M3, M6 and M9 was within 7.10-7.90. The pH of the treated water decreased on changing the adsorbent in the order: M9 < M6 < M3 < L0. The decrease in the pH of the water with time has a correspondence with increase in the removal of fluoride with time as can be seen in Figure 3.13A.

Table. 3.12. Remaining $[F^-]$ (mg/L) and final pH of water after treatment with different adsorbents at adsorbent dose of 0.5 g per 150 mL of water containing 10 mg/L $[F^-]_0$ at $T = 298 \pm 1$ K.

Time (min)	L0		M3		M6		M9	
	$[F^-]$ (mg/L)	pH	$[F^-]$ (mg/L)	pH	$[F^-]$ (mg/L)	pH	$[F^-]$ (mg/L)	pH
2	9.00	8.54	8.10	7.93	7.50	7.81	4.00	7.75
5	8.50	8.45	7.50	7.87	6.10	7.69	3.00	7.58
10	8.40	8.38	6.90	7.81	5.40	7.66	2.50	7.44
15	7.90	8.25	6.40	7.77	4.50	7.61	1.80	7.41
20	7.80	8.17	5.40	7.73	3.80	7.60	1.50	7.39
30	7.20	7.98	4.80	7.70	2.70	7.51	1.20	7.29
60	7.00	7.98	4.10	7.67	2.10	7.38	1.00	7.18
120	6.90	7.98	3.50	7.54	1.80	7.37	0.98	7.20
180	6.80	7.97	3.10	7.45	1.5	7.24	0.75	7.10

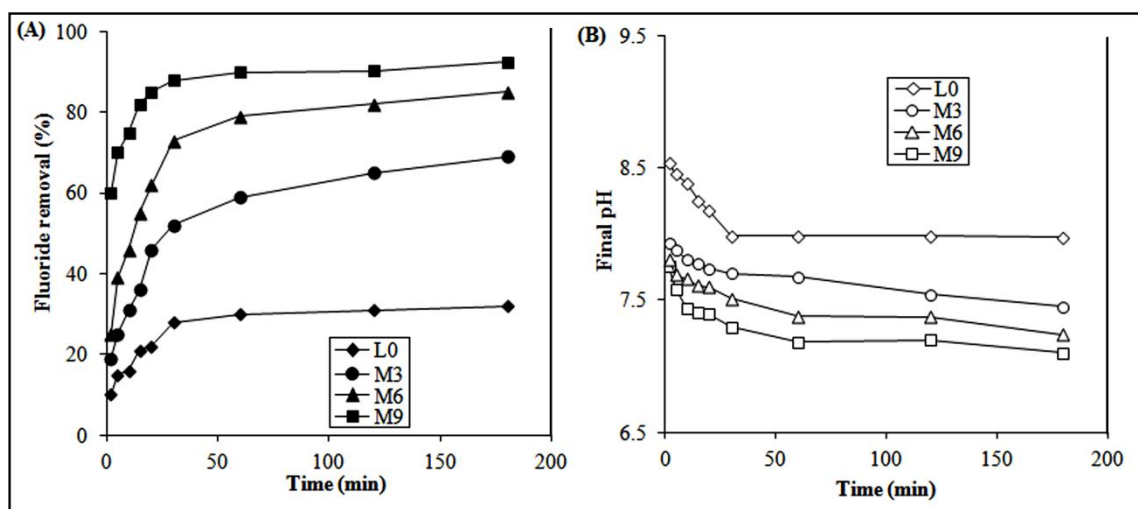


Figure 3.13. The plots of (A) fluoride removal performance and (B) final pH of treated water of the fresh (L0) and the modified limestone powders (M3, M6 and M9) vs. contact time with adsorbent dose of 0.5 g/150 mL at 298 ± 1 K. $[F^-]_0 = 10$ mg/L.

3.2.2.2 Effect of initial fluoride concentration

A batch experiment was carried out using a fixed dose of 0.5 g/150 mL of adsorbent M9 at different initial fluoride concentrations of 5, 10 and 20 mg/L to see the effects of the initial fluoride concentration and contact time. The results are shown in Table 3.13 and Figure 3.14.

Table 3.13. Remaining $[F^-]$ (mg/L) after treatment with adsorbent M9 at different $[F^-]_0$ (mg/L) as a function of contact time (min). Adsorbent dose = 0.5 g/150 mL of water at 298 ± 1 K.

Time (min)	$[F^-]_0$ (mg/L)		
	5	10	20
	$[F^-]$ (mg/L)	$[F^-]$ (mg/L)	$[F^-]$ (mg/L)
2	2.90	6.50	15.00
5	2.10	5.20	12.00
10	1.50	4.00	10.00
15	1.20	3.10	8.90
20	1.00	2.50	7.50
30	0.94	2.20	5.00
60	0.81	1.00	4.20
120	0.21	0.75	3.80
180	0.21	0.75	3.80
240	0.22	0.76	3.70
300	0.21	0.75	3.80

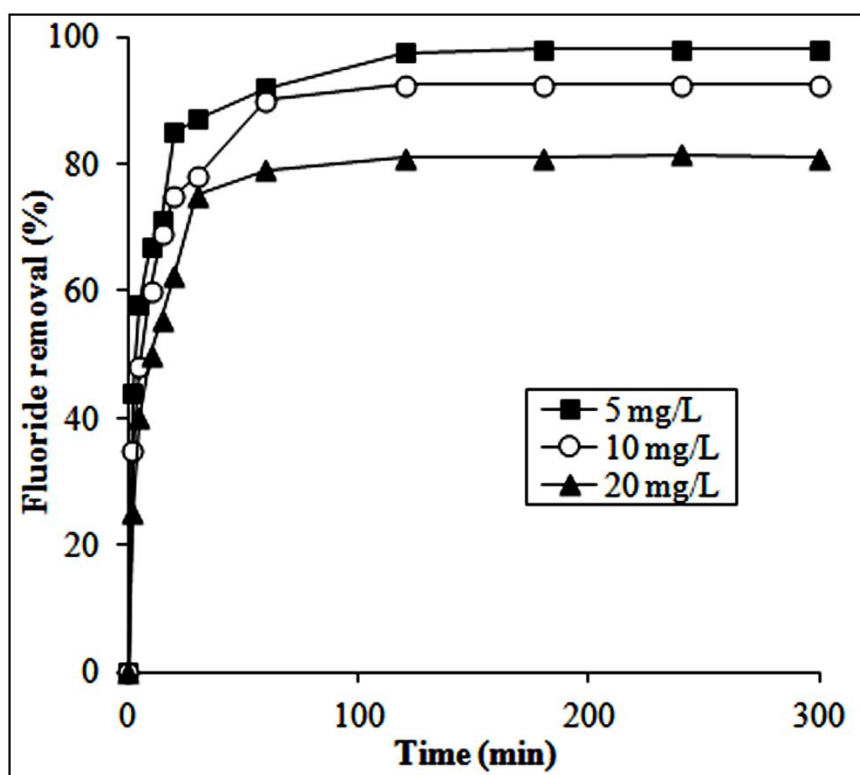


Figure 3.14. Effect of initial fluoride concentration ($[F^-]_0$) and contact time on fluoride removal by M9 with adsorbent dose of 0.5 g/150 mL of water at 298 ± 1 K.

It has been found that the fluoride removal initially increased rapidly with increase in contact time (Table 3.13 and Figure 3.14). The increase in fluoride removal gradually slowed down after ≈ 1 h until reaching equilibrium at ≈ 3 h. The percentage fluoride removal gradually decreased with increase in $[F^-]_0$ and was found to be up to 98%, 93% and 80% with $[F^-]_0$ of 5, 10 and 20 mg/L, respectively. Similar observation was reported with limestone powder in presence of PA.

3.2.2.3 Effect of adsorbent dose

The effect of adsorbent dose M9 on the fluoride removal from initial fluoride concentration of 10 mg/L with contact time of 3 h has studied. The results are shown in Table 3.14 and Figure 3.15. The fluoride removal increased gradually from 75% at the dose of 0.1 g/150 mL of water to 93% at the dose 0.5 g/150 mL of water and levelled off above that dose. However, with increase in the dose, there was a gradual decrease in the amount of fluoride adsorbed per g of the adsorbent. The increase in fluoride removal with adsorbent dose is due to increase in available active fluoride adsorption sites. Similar

observation was reported earlier in batch experiment with limestone powder in presence of PA.

Table. 3.14. Remaining $[F^-]$ (mg/L), percentage of fluoride removal and fluoride adsorbed on adsorbent M9 at different adsorbent dose (g). $[F^-]_0 = 10$ mg/L; contact time = 3 h and $T = 298 \pm 1$ K.

Adsorbent dose (g)	Remaining $[F^-]$ (mg/L)	Fluoride removal (%)	Fluoride adsorbed (mg/g)
0.1	2.50	75	7.50
0.2	2.10	79	3.95
0.3	1.50	85	2.83
0.4	1.00	90	2.25
0.5	0.75	93	1.85
0.6	0.76	92.4	1.54
0.7	0.75	92.5	1.32
0.8	0.74	92.6	1.15
0.9	0.75	92.5	1.02
1.0	0.76	92.4	0.92

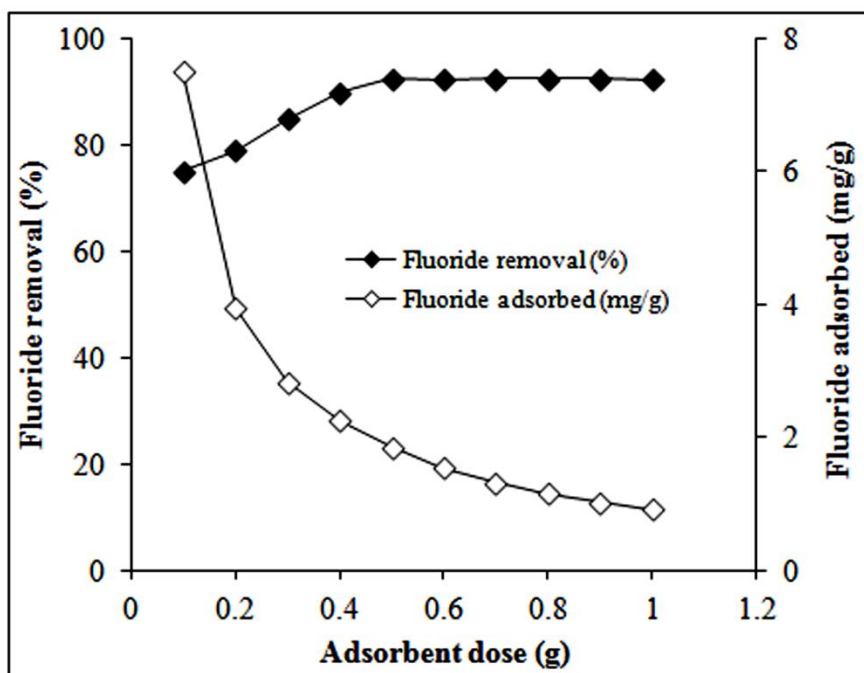


Figure 3.15. The fluoride removal and the amount of fluoride adsorbed in mg/g of the adsorbent vs. the dose of adsorbent M9.

3.2.2.4 Effect of pH

The adsorption of fluoride on adsorbent M9 has been evaluated at varying pH by adjusting the pH with 0.10 M HCL or 0.10 M NaOH in the range of 3-11. The results have been shown in Table 3.15 and Figure 3.16.

Table 3.15. Remaining $[F^-]$ (mg/L) and fluoride removal (%) using adsorbent M9 at different pH. Adsorbent dose = 0.5 g/150 mL; contact time = 3 h and $T = 298 \pm 1$ K.

$[F^-]_0$ (mg/L)	pH	Remaining $[F^-]$ (mg/L)	Fluoride removal (%)
10	3	0.40	96
	4	0.52	94.8
	5	0.54	94.6
	6	0.62	93.8
	7	0.70	93
	8	3.10	69
	9	5.10	49
	10	6.60	34
	11	7.90	21

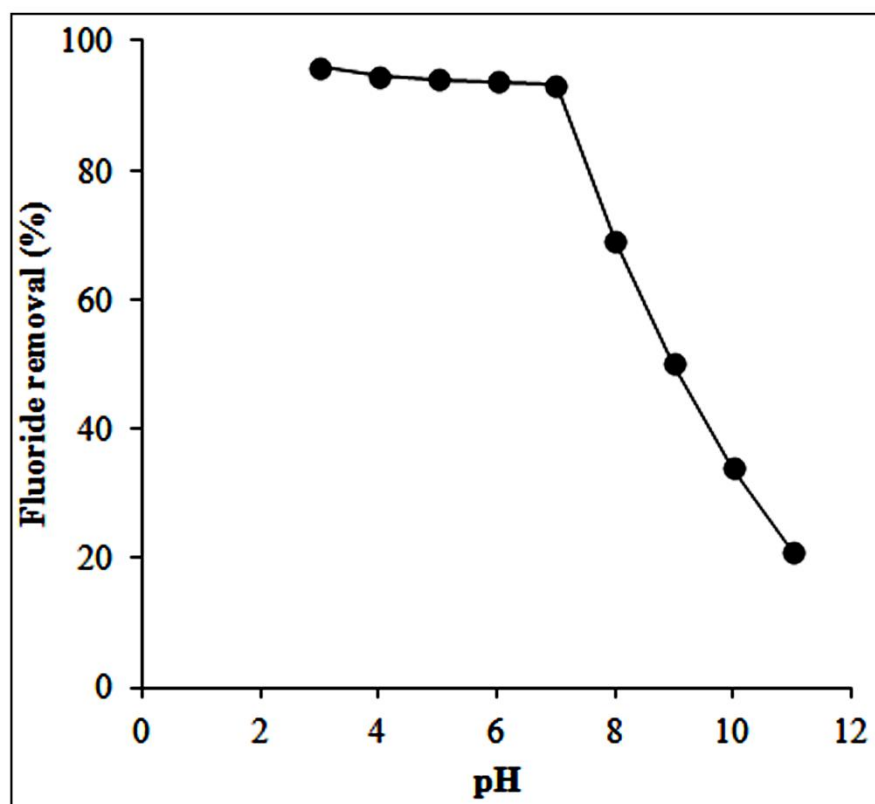


Figure 3.16. Effect of pH on fluoride removal (%) by M9 sample with adsorbent dose of 0.5 g/150 mL of water at 298 ± 1 K. $[F^-]_0 = 10$ mg/L and contact time = 3 h.

With initial fluoride concentration of 10 mg/L, 96% fluoride removal was achieved at pH 3 which, upon increasing the pH, decreased very slowly up to pH 7 (Table 3.15 and Figure 3.16). However, the fluoride removal was found to decrease rapidly above pH 7, which can be attributed to increasing competition by OH ions for adsorption sites with increase in pH. Similar observations are reported in the literature¹⁹¹.

3.2.3 Adsorption kinetics

The fluoride adsorption kinetics was studied for evaluating the rate of adsorption of fluoride by the modified limestone, M9 using various kinetics models at varying $[F^-]_0$. The results of remaining fluoride concentration after treatment with adsorbent (M9) at different treatment time are presented in Table 3.16.

Table 3.16. Remaining $[F^-]$ (in mg/L) after treatment with adsorbent dose (M9) of 0.5 g/150 mL at different $[F^-]_0$. T = 298±1 K.

Time(min)	$[F^-]_0$ (mg/L)						
	3	5	7	9	10	15	20
	$[F^-]$ (mg/L)	$[F^-]$ (mg/L)	$[F^-]$ (mg/L)	$[F^-]$ (mg/L)	$[F^-]$ (mg/L)	$[F^-]$ (mg/L)	$[F^-]$ (mg/L)
5	0.85	1.50	1.60	1.70	2.00	2.50	3.00
10	0.65	0.95	1.10	1.50	1.50	2.10	2.30
20	0.54	0.84	0.98	1.00	1.10	1.50	1.70
30	0.42	0.62	0.75	0.95	0.98	1.10	1.20
60	0.35	0.54	0.62	0.78	0.84	1.00	1.10
120	0.12	0.21	0.41	0.52	0.75	0.98	1.00

The plots of different kinetic models are evaluated using the results presented in Table 3.16 and are described below.

3.2.3.1 Pseudo-first-order equation

The pseudo-first-order equation is described by the Eq. 3.2.3²⁸⁶:

$$\ln(q_e - q_t) = \ln(q_e) - (k_1)t \quad (3.2.3)$$

where, q_e and q_t are the fluoride adsorption capacities of sorbent in mg/g at equilibrium and at time t , respectively, and $k_1(\text{min}^{-1})$ is the pseudo-first-order rate constant. The parameters correspond to pseudo-first-order equation have been evaluated from the slope and intercept of the plot of $\ln(q_e - q_t)$ vs. time (Fig. 3.17A). The results obtained from the

plots for different initial fluoride concentrations in the range of 3-20 mg/L are shown in Table 3.17. The correlation coefficients (R^2) of the plots were poor and found to be in the range of 0.953 to 0.741. The calculated q_e values were different from the experimental q_e values indicating that the data did not fit well to the pseudo-first-order model to predict the adsorption kinetics.

3.2.3.2 Pseudo-second-order equation

The pseudo-second-order kinetic rate equation is expressed by the Eq. (3.2.4)²⁸⁶:

$$t/q_t = (1/k_2) \cdot (1/q_e^2) + (t/q_e) \quad (3.2.4)$$

where, q_e and q_t are the fluoride adsorption capacities of sorbent at equilibrium and at time t , respectively, and k_2 is the second order rate constant (g/mg min). The pseudo-second-order rate constant, k_2 , and adsorption capacity at equilibrium (q_e) were calculated from the slope and the intercept of the plot of t/q_t vs. t (Figure 3.17B). The R^2 values of the pseudo-second-order plots were found to be between 0.990 and 1.000 which are much better than that of pseudo-first-order plots (Table 3.17.). The equilibrium adsorption capacities (q_e , cal) calculated by this model were also found close to those obtained from experiments (q_e , exp). Thus, the adsorption of fluoride fitted much better to the pseudo-second-order kinetics than the pseudo-first-order kinetics. It has been observed from the Table 3.17 that both pseudo-first-order rate constant (k_1) and pseudo-second-order rate constant (k_2) values decrease with increase in $[F^-]_0$. The observed decrease in the rate constant with increase in $[F^-]_0$ is may be attributed to a decrease in the solid/solute ratio.

3.2.3.3. Intra-particle diffusion model

The actual rate-limiting step of the adsorption process can be determined by intra-particle diffusion model using Eq. (3.2.5)²⁸⁷.

$$q_t = k_i t^{1/2} + C \quad (3.2.5)$$

where, k_i (mg/g min^{1/2}) is the intra-particle diffusion rate constant and C provides an idea of the boundary layer thickness. The intra-particle diffusion rate constant (k_i) for various $[F^-]_0$ values have been determined from the slope of the q_t vs. $t^{1/2}$ plots (Figure 3.17C).

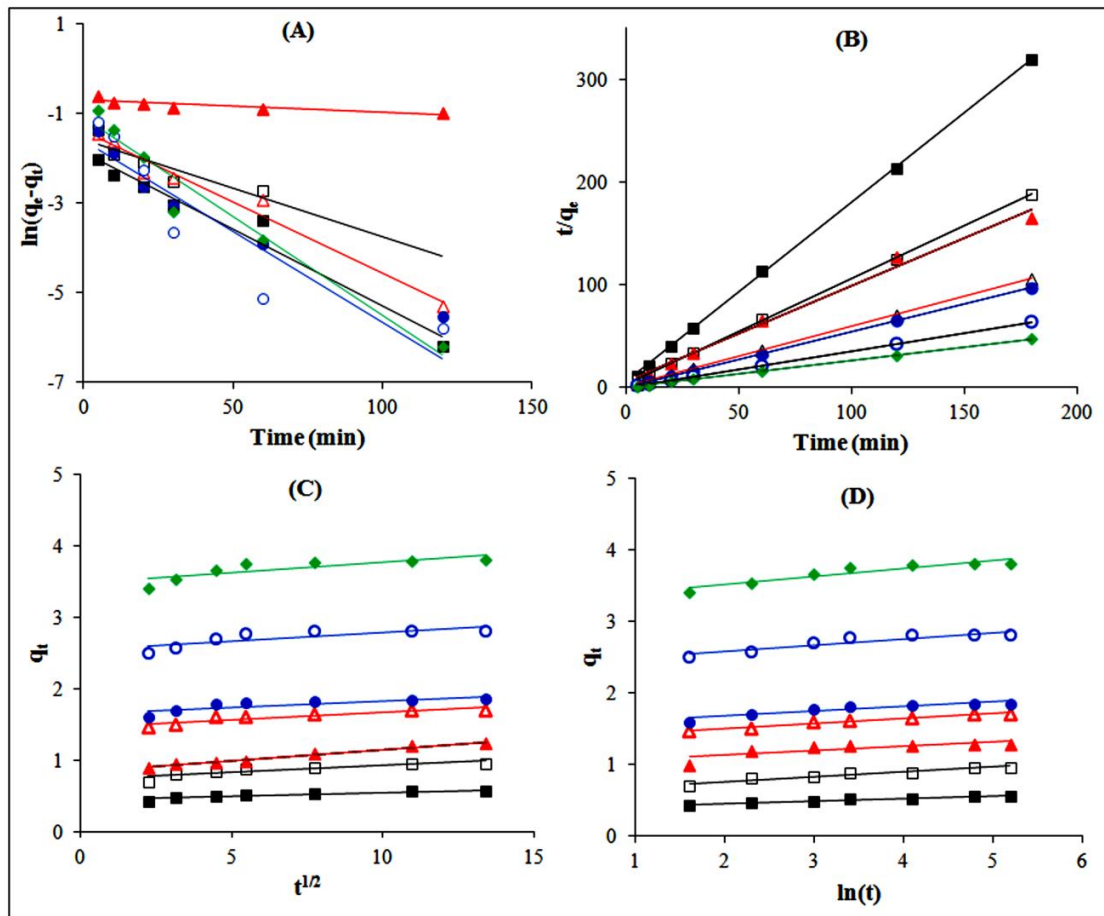


Figure 3.17. Plots of pseudo-first-order (A), pseudo-second-order (B), intra-particle diffusion (C) and Elovich (D) kinetic models at different $[F^-]_0$ (mg/L): 3 (■), 5 (□), 7 (▲), 9 (△), 10 (●), 15 (○), 20 (◆), respectively, with adsorbent dose (M9) of 0.5 g/150 mL and at 298 ± 1 K.

The R^2 values found from by intra-particle diffusion model were not satisfactory (Table 3.17). The curves also did not pass through the origin, indicating that intra-particle diffusion is not be the controlling factor in determining the kinetics of the process. In this case intra-particle diffusion may be considered as concentration dependent diffusion as the values of k_i were found to increase with increasing $[F^-]_0$ ²⁹⁶.

3.2.3.4 Elovich model

The Elovich model can be represented by the Eq. (3.2.6)²⁸⁸:

$$q_t = (1/B) \ln(AB) + (1/B) \ln(t) \quad (3.2.6)$$

where, A (mg/g min) is the sorption constant of the fluoride ions and B (g/mg) is the desorption constant of the fluoride ions for a particular experiment.

Table 3.17. The kinetic parameters obtained from pseudo-first-order, pseudo-second-order, intra-particle diffusion and Elovich models for adsorption of fluoride on M9 at different $[F^-]_0$ with adsorbent dose of 0.5 g/150mL at 298 ± 1 K.

Parameter	$[F^-]_0$ (mg/L)						
	3	5	7	9	10	15	20
<i>Pseudo first-order model</i>							
k_1	0.078	0.048	0.004	0.071	0.066	0.052	0.041
q_e (exp)	0.564	0.958	1.320	1.698	1.852	2.806	3.802
q_e (cal)	0.081	0.272	0.199	0.042	0.021	0.026	0.081
R^2	0.965	0.800	0.741	0.972	0.953	0.839	0.958
<i>Pseudo second-order model</i>							
k_2	0.615	0.602	0.592	0.587	0.589	0.535	0.392
q_e (exp)	0.564	0.958	1.320	1.698	1.852	2.806	3.802
q_e (cal)	0.572	0.963	1.324	1.691	1.853	2.820	3.805
R^2	0.999	0.999	0.990	0.999	1.000	1.000	1.000
<i>Intra-particle diffusion model</i>							
k_i	0.011	0.019	0.021	0.020	0.028	0.029	0.030
R^2	0.871	0.818	0.978	0.830	0.671	0.643	0.658
<i>Elovich model</i>							
A	0.086	0.150	0.172	0.206	0.208	0.289	0.375
1/B	0.037	0.067	0.061	0.068	0.066	0.087	0.110
R^2	0.978	0.939	0.634	0.955	0.867	0.843	0.857

The values of A and 1/B can be obtained from the slope and intercept of the plots of q_t vs. $\ln(t)$ (Figure 3.17D). The desorption constant (1/B) values were found to increase from 0.037 to 0.110 mg/g with increase in $[F^-]_0$ from 3 to 20 mg/L indicating that the number of available active sites to adsorb fluoride decreases with increase in $[F^-]_0$ (Table 3.17). The R^2 values were also slightly higher than that obtained in the case of intra-particle diffusion model suggesting the suitability of this model.

3.2.4 Adsorption isotherm

Adsorption isotherm is one of the most important models to evaluate the adsorption capacity of sorbent and to understand the mechanism of adsorption. The Freundlich,

Langmuir, Dubinin-Radushkevich (D-R) and Temkin isotherm models for the adsorption of fluoride on the modified materials are studied using the results obtained under different operational parameters as shown in Table 3.18.

Table 3.18. Remaining $[F^-]$ (mg/L) in the treated water and amount of fluoride adsorbed at equilibrium using different adsorbents, L0, M3, M6 and M9 with varying $[F^-]_0$ (mg/L).

$[F^-]_0$ (mg/L)	L0		M3		M6		M9	
	$[F^-]$ (mg/L)	q_e (mg/g)	$[F^-]$ (mg/L)	q_e (mg/g)	$[F^-]$ (mg/L)	q_e (mg/g)	$[F^-]$ (mg/L)	q_e (mg/g)
3	2.00	0.19	2.10	0.27	3	1.50	0.19	0.84
5	4.40	0.18	3.50	0.45	5	2.50	0.21	1.45
7	6.00	0.30	5.00	0.60	7	3.80	0.52	1.94
9	7.00	0.60	6.50	0.75	9	4.70	0.67	2.49
10	6.80	0.96	7.40	0.78	10	5.20	0.75	2.77
15	11.00	1.20	11.20	1.14	15	8.50	1.90	3.93
20	14.00	1.80	15.00	1.50	20	12.00	3.80	4.86

The plots of different isotherm models have been studied using the results presented in Table 3.18 and are described below.

3.2.4.1 Freundlich isotherm

Freundlich isotherm model can be represented by the linearised Eq. (3.2.7)²⁸⁹:

$$\ln(q_e) = \ln(K_F) + 1/n \ln(C_e) \quad (3.2.7)$$

where, q_e , C_e , K_F and n are the amount of fluoride adsorbed at equilibrium (mg/g), the fluoride concentration at equilibrium (mg/L), the Freundlich adsorption capacity (mg/g) and adsorption intensity, respectively. The values of the equilibrium data were determined by plotting $\ln(q_e)$ vs. $\ln(C_e)$ (Figure 3.18) and listed in Table 3.19. The observed values of $1/n$ between 0.1 and 1.0 and R^2 in the range 0.992-0.958 indicated favourable conditions for Freundlich adsorption. The agreement with Freundlich type adsorption decreases in the order: L0 > M3 > M6 > M9 as indicated by the decrease in R^2 in that order. The equilibrium adsorption capacity increased in the order: L0 < M3 < M6 < M9, which is indicative of an increase in the formation of HAP in the same order during the hydrothermal treatment.

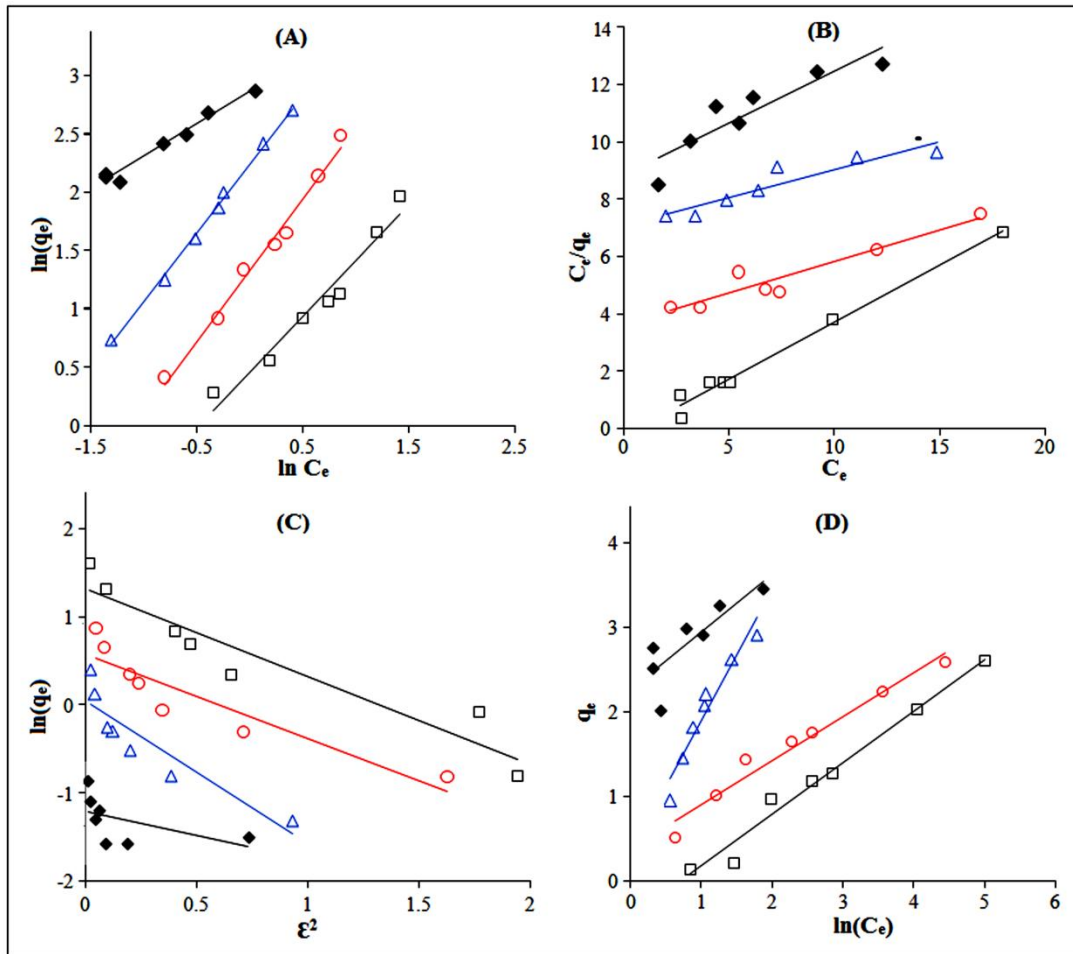


Figure 3.18. Plots of Freundlich (A), Langmuir (B), Dubinin–Radushkevich (C) and Temkin (D) isotherm models for sorption of fluoride on L0 (◆), M3 (Δ), M6 (○) and M9 (□) at different $[F]_0$. Adsorbent dose = 0.5 g/150 mL at 298 ± 1 K.

3.2.4.2 Langmuir isotherm

The linear form of Langmuir isotherm can be represented by Eq. (3.2.8)²⁸⁹:

$$C_e/q_e = C_e/Q_0 + 1/bQ_0 \quad (3.2.8)$$

where Q_0 (mg/g) and b (L/mg) are the Langmuir adsorption capacity and the Langmuir isotherm constant related to the affinity of the binding sites, respectively. The values of Q_0 and b have been calculated from the linear plots of C_e/q_e vs. C_e (Figure 3.18B) and are included in Table 3.19. The R^2 values of the Langmuir plots were poorer than those of the Freundlich plots suggesting the adsorption to be primarily physisorption. The R^2 values of the Langmuir plots improved in the order: L0 < M3 < M6 < M9 which is exactly the reverse of the order observed for the Freundlich plots.

Table 3.19. Various isotherm parameters for adsorption of fluoride on unmodified and modified limestone powder at 298±1 K.

<i>Kinetic parameters</i>	L0	M3	M6	M9
<i>Freundlich</i>				
K _F (mg/g)	2.017	2.370	3.789	5.847
1/n	1.823	0.853	0.822	0.589
R ²	0.992	0.990	0.986	0.958
<i>Langmuir</i>				
Q ₀ (mg/g)	0.479	5.150	6.329	6.450
b (L/mg)	0.014	0.026	0.052	0.975
R ²	0.824	0.873	0.909	0.984
<i>Dubinin-Radushkevich</i>				
B _D (mol ² /kJ ²)	0.405	1.621	0.958	0.068
Q _D (mg/g)	0.264	1.048	1.787	3.998
E (KJ/mol)	3.141	2.669	2.043	1.571
R ²	0.255	0.825	0.846	0.899
<i>Temkin</i>				
A _T (L/g)	0.989	1.450	1.170	0.045
B _T	8.314	1.550	1.013	0.768
R ²	0.682	0.932	0.965	0.979

The maximum monolayer fluoride adsorption capacity was found to be 6.45 mg/g for M9 which is about seventeen-fold higher than that reported for fresh limestone¹¹². The binding energy constant (b) increased in the order: M3 < M6 < M9 indicating higher HAP formation in the same order.

The adsorption efficiency of Langmuir isotherm can be calculated using the Eq. (3.2.9)²⁸⁹:

$$R_L = 1 / (1 + bC_0) \quad (3.2.9)$$

where, C₀ is the initial fluoride concentration ([F⁻]₀). The calculated R_L values have been included in Table 3.20. All R_L values were between 0 and 1 suggesting a favoured Langmuir adsorption.

Table 3.20. The values of R_L obtained from the Langmuir constant, b , at different $[F^-]_0$ for different modified limestone powder at 298 ± 1 K.

$[F^-]_0$ /(mg/L)	M3	M6	M9
3	0.927	0.865	0.254
5	0.884	0.794	0.170
7	0.846	0.733	0.127
9	0.810	0.681	0.102
10	0.793	0.657	0.093
15	0.719	0.561	0.064
20	0.657	0.490	0.048

3.2.4.3 Dubinin-Radushkevich (D-R) isotherm

Dubinin-Radushkevich (D-R) isotherm equation which predicts whether the adsorption is physisorption or chemisorptions, can be expressed by the Eq. (3.2.10)²⁹⁰:

$$\ln(q_e) = \ln(Q_D) - B_D \varepsilon^2 \quad (3.2.10)$$

where, Q_D is the adsorption capacity (mg/g), B_D is the activity constant related to mean sorption energy (mol^2/kJ^2) and ε is the Polanyi potential. The values of maximum adsorption capacity (Q_D), activity coefficient related to mean sorption energy (B_D) have been calculated from the slope and intercept of the plots of $\ln(q_e)$ vs. ε^2 (Figure 3.18C) and included in Table 3.19.

The mean free energy of adsorption, E (kJ/mol) can be determined using Eq. (3.2.11)²⁹⁰:

$$E = 2B_D^{-0.5} \quad (3.2.11)$$

If the value of mean free energy of adsorption (E) ranges from 1.0-8.0 kJ/mol, then the sorption process is physisorption and if it is in between 9.0-16.0 kJ/mol, then the sorption process is chemical in nature. The E value in the present case has been found to be between 1 and 3 kJ/mol (Table 3.19) which suggest the adsorption to be primarily physisorption. However, the observed poor R^2 values indicate that the mechanism of adsorption in the present case cannot be described well by D-R model.

3.2.4.4 Temkin isotherm

The Temkin isotherm equation can be represented by Eq. (3.2.12)²⁹¹:

$$q_e = B_T \ln(A_T) + B_T \ln(C_e) \quad (3.2.12)$$

where, A_T (L/g) and $B_T = (RT)/b$ are Temkin constants. These constants have been evaluated from the plots of q_e vs. $\ln(C_e)$ (Figure 3.18D). The R^2 values were better than those of Langmuir and D-R isotherms which suggested that the Temkin model suits the adsorption of fluoride by modified limestone (Table 3.19). The lower values of B_T indicate a favourable lower heat of exchange of OH^- ions of HAP by F^- ions than that of the adsorption of F^- ions on the modified materials. The observed decrease in the B_T values in the order: M9 < M6 < M3 < L0 indicates an increase in the ion exchange in the same order.

3.2.5 Thermodynamic investigation

To see the effect of temperature on the process of fluoride adsorption on the modified limestone powders, various thermodynamic parameters *viz.*, standard free energy change (ΔG^0), standard enthalpy change (ΔH^0) and standard entropy change (ΔS^0) were evaluated using the equations (3.2.13) and (3.2.14), respectively²⁹².

$$\Delta G^0 = -RT \ln(K_c) \quad (3.2.13)$$

$$\ln(K_c) = \Delta S^0/R - \Delta H^0/RT \quad (3.2.14)$$

where, R is the gas constant, T is the temperature and K_c is the standard equilibrium constant of adsorption. The values of equilibrium concentration of fluoride (C_e), amount adsorbed in equilibrium (q_e) and K_c (ratio of q_e/C_e) at different temperature have been evaluated and are listed in Table 3.21. The van't Hoff plots of $\ln(K_c)$ vs. $1/T$ are shown in Figure 3.19 and the thermodynamic parameters at different temperatures obtained from the respective plots have been listed in Table 3.22. The negative ΔG^0 and positive ΔH^0 for all of the modified limestone samples suggest that the adsorption process is spontaneous and endothermic in nature. The positive entropy change indicates an increased randomness at the adsorbent/solution interface after sorption of fluoride.

Table 3.21. Equilibrium concentration of fluoride (C_e), amount adsorbed fluoride at equilibrium (q_e) and K_c (ratio of q_e/C_e) obtained by the treatment with different adsorbents at different temperatures. $[F^-]_0 = 10$ mg/L and adsorbent dose = 0.5 g/150 mL.

T (K)	M3			M6			M9		
	C_e (mg/L)	q_e (mg/g)	K_c	C_e (mg/L)	q_e (mg/g)	K_c	C_e (mg/L)	q_e (mg/g)	K_c
298	7.40	0.78	0.11	5.20	1.44	0.28	0.75	2.78	3.70
303	5.20	1.44	0.28	3.20	2.04	0.64	0.63	2.81	4.46
308	4.20	1.74	0.41	2.60	2.22	0.85	0.41	2.88	7.02
318	3.10	2.07	0.67	2.10	2.37	1.12	0.12	2.96	24.70
328	2.70	2.19	0.81	1.50	2.55	1.70	0.10	2.97	29.70

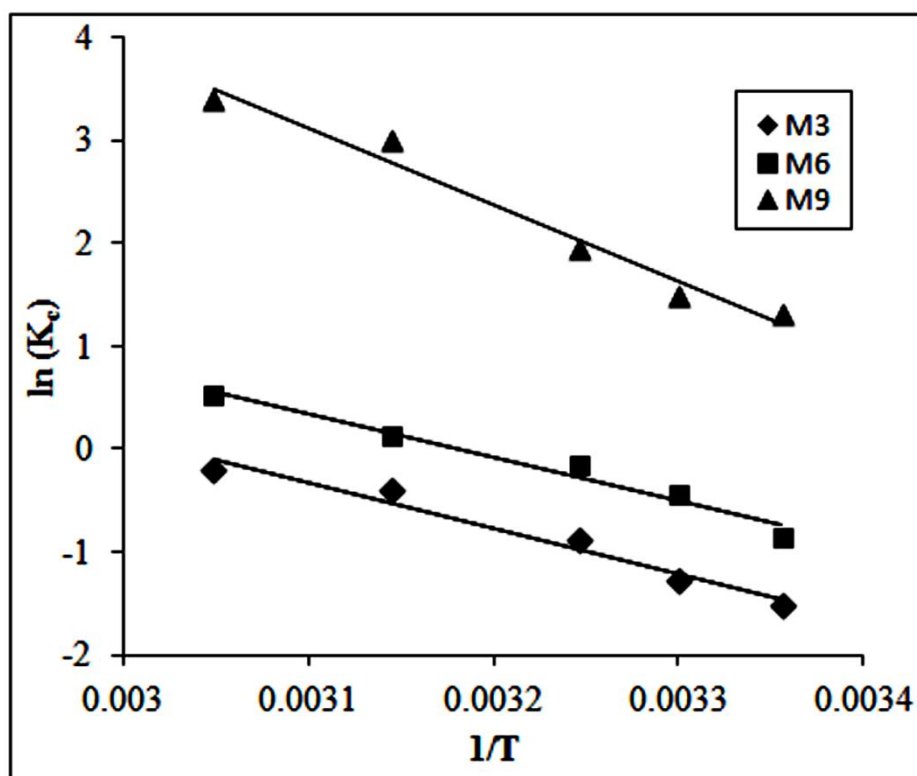


Figure 3.19. Plots of $\ln(K_c)$ vs. $1/T$ (K^{-1}) for sorption of fluoride on the modified limestone samples with $[F^-]_0 = 10$ mg/L, adsorbent dose = 0.5 g/150 mL.

Table 3.22. The standard thermodynamic parameters of the sorption of fluoride on different modified limestone with $[F^-]_0 = 10 \text{ mg/L}$, adsorbent dose = 0.5 g/150 mL.

Adsorbent	ΔS° (J/Kmol)	ΔH° (kJ/mol)	ΔG° (kJ/mol)				
			298 K	303 K	308 K	318 K	328 K
M3	0.123	35.00	-1.65	-2.26	-2.88	-4.11	-5.34
M6	0.132	37.07	-2.26	-2.92	-3.58	-4.90	-6.23
M9	0.216	61.54	-2.82	-3.90	-4.98	-7.14	-9.30

3.2.6 Desorption of fluoride

A desorption study has been done to check the reusability of fluoride-loaded material. The procedure of desorption study has been explained in the section, 2.4.2.3 *Desorption study*. The results have been shown in Table 3.23 and Figure 3.20. The desorption of F^- was found to be low in acidic and neutral conditions but increased rapidly from $\approx 5\%$ at pH 7 to $\approx 72\%$ at pH 12. The higher desorption in the alkaline condition suggests exchange of F^- ions with OH^- ions and indicates regeneration-ability of the adsorbent^{145, 150}.

Table 3.23. Effluent $[F^-]$ (mg/L) and desorption of fluoride (%) from fluoride-loaded adsorbent M9 at different pH.

pH	Effluent $[F^-]$ (mg/L)	Desorption of F^- (%)
3	2.4	4.2
5	2.9	5.1
7	3.2	5
9	31	39
12	40.9	72

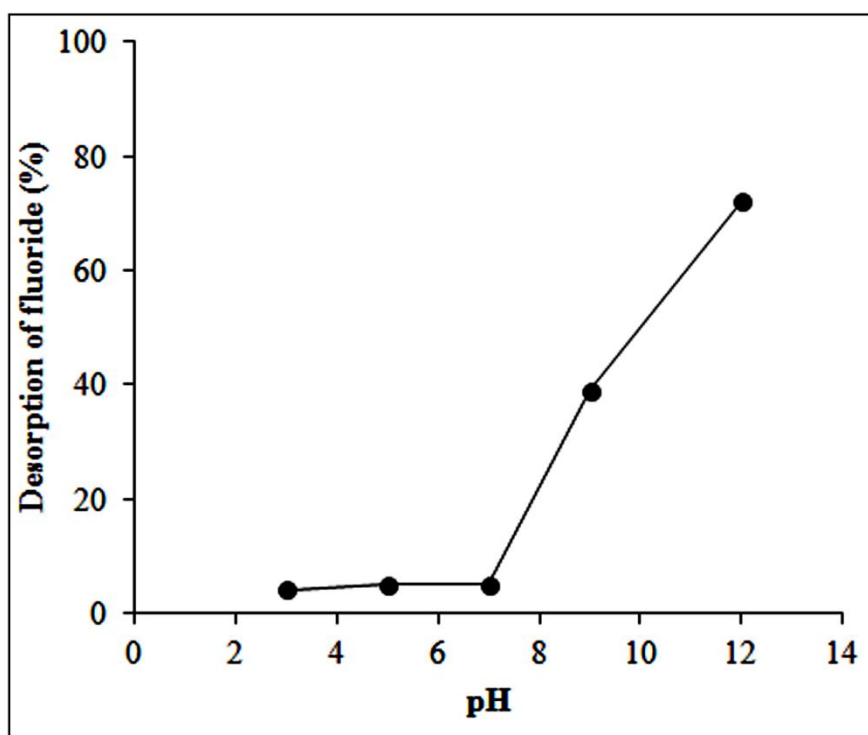


Figure 3.20. Effect of pH on desorption of fluoride from fluoride-loaded M9 sample. Adsorbent dose = 0.25 g/75 mL and contact time = 3 h at 298 ± 1 K.

3.2.7 Disposal of sludge

The leaching of fluoride from used adsorbent was determined as per the toxicity characteristic leaching procedure (TCLP) test²⁹⁵. This showed a leaching of only 0.20 mg/L fluoride which is much lower than the permissible value of 150 mg/L for disposal in landfill³⁰⁹.

3.2.8 Competitiveness of the present adsorbent

Limestone is a low-cost and natural material which is readily available in all fluoride affected areas in the world (Figure 1.1) and PA is recommended by USEPA²⁷⁰ for drinking purpose. A comparison of different reported adsorbent based on adsorption capacities with the present adsorbent has been listed in Table 3.24. The adsorption capacity of the present modified limestone was found to be better than that of all abundant and common adsorbents, *viz.*, calcite, magnesite, bauxite, laterite, gypsum, clays, activated alumina, bone char and HAP and comparable to that of brushite (Table 3.24.). Though the value of adsorption capacities of certain adsorbents, *viz.*, $\text{Al}_2\text{O}_3/\text{carbon}$

nanotube, graphene, tamarind fruit-shell carbon and calcined PA-treated limestone have been reported to be higher than the present adsorbent, the later has an edge over the others either in terms of cost or availability.

Table 3.24. Comparison of adsorption capacity of the present adsorbent with various reported adsorbents.

Adsorbent	Capacity (mg/g)	Reference
Calcite	0.39	112
Magnesite	0.71	146
Gypsum	0.85	146
Laterite	0.86	146
Bauxite	1.05	146
Activated alumina	1.45	115
Clays	1.69	303, 304
Bone char	2.50	305
HAP	4.54	112
Nano-HAP	5.50	192
<i>Hydrothermally modified limestone</i>	<i>6.45</i>	<i>present study</i>
Brushite	6.59	253
Al ₂ O ₃ /carbon nanotube	13.5	131
Graphene	17.65	302
Calcined PA-treated limestone	22	249
Tamarind fruit-shell carbon	22.33	251

3.2.9 Summary

The findings of this work can be summarised as follows:

- Hydrothermal modification of limestone powder in presence of PA leads to formation of HAP.
- The HAP formation increased with increase in the concentration of the PA used by keeping the Ca/P ratio constant at 1.66.
- The hydrothermal modification with 0.90 M PA gave a product with a fluoride adsorption capacity of 6.45 mg/g.
- Fluoride adsorption on M9 sample has been found to be higher at pH 3 and decreases rapidly after pH 7.

- The adsorption of fluoride on the modified powder is predominantly a physisorption through pseudo-second-order kinetics and exchange of OH^- ions with F^- ions.
- The higher desorption of fluoride in the alkaline condition indicates the regeneration-ability of the adsorbent.
- Thermodynamic investigation showed that the adsorption of fluoride on the modified limestone powder is spontaneous, endothermic and irreversible.

3.3 Fluoride removal by phosphoric acid-crushed limestone treatment in continuous-flow mode

Nath studied fluoride removal from water using PA and crushed limestone in a plug-flow fixed-bed column²⁸⁰. The influent fluoride containing water is pre-acidified with PA before treatment with crushed limestone bed of chip size 2-3 mm. He reported that fluoride can be removed from 10 mg/L to below 1.0 mg/L with a residence time of 3 h using 0.01 M [PA]₀. The fluoride removal takes place through precipitation of calcium fluoride and adsorption of fluoride by HAP produced in situ in the reactor. Based on these results, the author has planned to study the performance of phosphoric acid-crushed limestone treatment (PACLT) in a continuous-flow mode so that the author can evaluate the method for an on-line domestic application. The fluoride removal performance by PACLT in a continuous-flow mode, as described in the section, *2.4.3 Methods of continuous-flow column experiment*, has been studied by considering various operational parameters, viz., effects of [PA]₀ and [F⁻]₀, effects of flow rates and effect of co-existing ions. Regeneration of exhausted limestone and the ability of regenerated limestone for fluoride removal have also been studied. The results have been presented here.

3.3.1 Effect of influent PA concentration

The effect of [PA]₀ on fluoride removal by PACLT in a continuous-flow mode has been investigated using 5 mg/L [F⁻]₀ by varying [PA]₀ at the flow rate of 100 mL/h. The influent water is fed into the column from the bottom of the column containing 1.0-1.5 cm size limestone as shown in Figure 2.1. Remaining fluoride concentration of the treated water has been analysed at regular intervals after discharge of water of every 5 L. The pH of the treated water was also measured after every 5 L of discharged water. The results and the breakthrough curves are shown in Table 3.25 and Figure 3.21. The breakthrough curves for a columns has been analyzed by plotting the remaining fluoride concentration along with the ratio of the C_t/C_0 vs. throughput volume (total collected water volume), where, C_t and C_0 are the effluent and influent fluoride concentrations, respectively. The results showed that using the same limestone bed, about 300 L, 420 L and 450 L of water could be defluoridated before the breakthrough in presence of 0.01 M, 0.03 M and 0.05 M [PA]₀, respectively.

Table 3.25. Remaining fluoride concentration (mg/L) along with throughput volume (L) after treatment by the PACLT in continuous-flow mode at different $[PA]_0$. $*[F^-]_0 = 5$ mg/L and flow rate = 100 mL/h.

Throughput volume (L)	$[PA]_0$ (M)			Throughput volume (L)	$[PA]_0$ (M)		
	0.01 M	0.03 M	0.05 M		0.01 M	0.03 M	0.05 M
	$[F^-]$ (mg/L)				$[F^-]$ (mg/L)		
5	0.01	0.010	0.009	185	0.23	0.22	0.20
10	0.008	0.006	0.003	190	0.28	0.25	0.24
15	0.10	0.098	0.096	195	0.29	0.26	0.25
20	0.12	0.094	0.093	200	0.32	0.27	0.24
25	0.21	0.10	0.098	205	0.33	0.30	0.29
30	0.29	0.19	0.15	210	0.35	0.31	0.30
35	0.20	0.18	0.17	215	0.38	0.33	0.31
40	0.26	0.06	0.03	220	0.39	0.35	0.34
45	0.33	0.25	0.21	225	0.42	0.36	0.35
50	0.20	0.19	0.17	230	0.45	0.41	0.39
55	0.12	0.17	0.16	235	0.54	0.42	0.38
60	0.10	0.11	0.10	240	0.47	0.45	0.42
65	0.13	0.11	0.10	245	0.50	0.46	0.44
70	0.14	0.12	0.11	250	0.52	0.48	0.42
75	0.10	0.09	0.08	255	0.65	0.48	0.45
80	0.15	0.36	0.21	260	0.74	0.62	0.61
85	0.21	0.32	0.20	265	0.80	0.70	0.65
90	0.27	0.24	0.24	270	0.89	0.75	0.74
95	0.27	0.45	0.21	275	0.91	0.76	0.75
100	0.28	0.44	0.22	280	0.93	0.80	0.77
105	0.26	0.24	0.22	285	0.93	0.89	0.80
110	0.24	0.25	0.24	290	0.95	0.87	0.81
115	0.21	0.21	0.20	295	0.96	0.92	0.90
120	0.19	0.14	0.10	300	1.50	0.94	0.92
125	0.19	0.17	0.18	305	1.60	0.93	0.93
130	0.18	0.15	0.14	305	1.80	0.92	0.90
135	0.17	0.14	0.13	315	3.20	0.91	0.94
140	0.16	0.15	0.12	320	3.50	0.95	0.91
145	0.08	0.10	0.15	325	3.60	0.96	0.95
150	0.17	0.13	0.12	330	4.10	0.97	0.94
155	0.17	0.14	0.13	335	4.40**	0.96	0.95
160	0.15	0.15	0.14	340		0.96	0.96
165	0.24	0.15	0.16	345		0.95	0.98
170	0.18	0.17	0.17	350		0.97	0.97
175	0.20	0.18	0.17	355		0.98	0.96
180	0.21	0.20	0.19	360		0.95	0.97

Continued to the next page-

Continued from the previous page-

Throughput volume (L)	0.01 M	0.03 M	0.05 M	Throughput volume (L)	0.01 M	0.03 M	0.05 M
	[F ⁻] (mg/L)				[F ⁻] (mg/L)		
365		0.96	0.95	430		1.80	0.97
370		0.97	0.96	435		3.20	1.00
375		0.98	0.97	440		3.50	1.10
380		0.99	0.97	445		3.60	1.00
385		0.98	0.97	450		4.10	1.50
390		0.97	0.98	455		4.40	2.00
395		0.91	0.97	460		4.80**	2.10
400		0.98	0.98	465			2.50
405		0.99	0.95	470			3.00
410		1.00	0.93	475			3.50
415		1.20	0.89	480			4.00
420		1.50	0.87	485			4.50
425		1.60	0.88	490			5.00**

*Error limit: [F⁻] = ±0.2 mg/L; **Discontinued due to poor fluoride removal

The observed good fluoride removal performance indicating a major contribution to the removal by calcium phosphates formed in the column due to reaction between the phosphate ions of PA and calcium ions formed by the dissolution of limestone. The breakthrough was reached sooner at lower [PA]₀. However, 0.01 M influent PA is sufficient to reduce fluoride concentration from influent 5 mg/L to less than 1.5 mg/L. Further experiments were performed with 0.01 M PA concentrations as low acid concentration is more suitable in field applications. The result of statistical analysis has been shown in Table 3.26. It has been found that the fluoride removal increases significantly with increase in [PA]₀ with an LSD value 0.018 at p<0.05.

Table 3.26. The results of one-way analysis of variance of fluoride removal with different [PA]₀. [F⁻] = 5 mg/L and flow rate = 100 mL/h.

[PA] ₀ (M)			LSD	p*
0.01	0.03	0.05		
**[F ⁻] (mg/L)	**[F ⁻] (mg/L)	**[F ⁻] (mg/L)	0.018	<0.05
0.33	0.44	0.49		
0.34	0.40	0.50		
0.38	0.42	0.52		

*p- Pearson's correlation is significant at <0.05 level.

**The results are average of three experiments

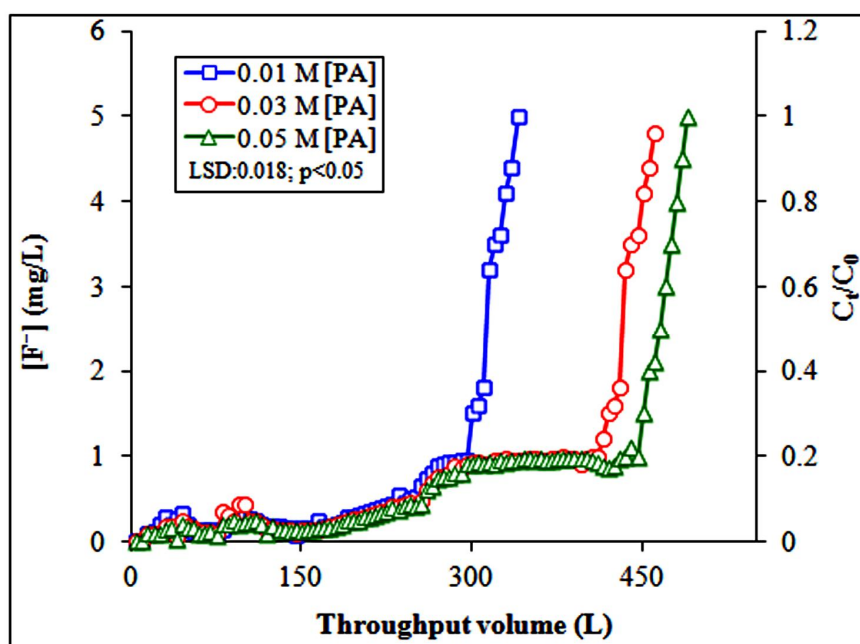


Figure 3.21. The breakthrough curves for fluoride removal at different $[PA]_0$ at $[F^-]_0 = 5$ mg/L and flow rate = 100 mL/h.

3.3.2 Effect of influent fluoride concentration

The results of fluoride removal with different $[F^-]_0$ at a fixed $[PA]_0$ of 0.01 M and a fixed flow rate of 100 mL/h have been shown in Table 3.27 and Figure 3.22. The breakthrough was observed sooner with higher $[F^-]_0$. With $[F^-]_0$ of 5 mg/L, a total volume of 300 L of fluoride free water was obtained without regeneration of the limestone. The results of statistical analysis are presented in Table 3.28. It has been observed from the performance of fluoride removal that the throughput volume was significantly decreased with increasing $[F^-]_0$ with LSD value 0.032 at $p < 0.05$.

Table 3.28. The results of one-way analysis of variance of fluoride removal with different $[F^-]_0$. $[PA]_0 = 0.01$ M and flow rate = 100 mL/h.

$[F^-]_0$ (mg/L)			LSD	p^*
5	7	10		
** $[F^-]$ (mg/L)	** $[F^-]$ (mg/L)	** $[F^-]$ (mg/L)	0.032	<0.05
0.33	0.74	0.89		
0.34	0.79	0.87		
0.38	0.82	0.80		

*p- Pearson's correlation is significant at <0.05 level.

**The results are average of three experiments

Table 3.27. The breakthrough results of fluoride removal at different influent fluoride concentrations ($[F^-]_0$) at fixed $[PA]_0 = 0.01$ M and a fixed flow rate = 100 mL/h. *

Throughput volume (L)	$[F^-]_0$ (mg/L)			Throughput volume (L)	$[F^-]_0$ (mg/L)	
	5	7	10		5	7
	Remaining $[F^-]$ (mg/L)	Remaining $[F^-]$ (mg/L)	Remaining $[F^-]$ (mg/L)		Remaining $[F^-]$ (mg/L)	Remaining $[F^-]$ (mg/L)
5	0.01	0.54	0.74	190	0.28	0.84
10	0.008	0.47	0.79	195	0.29	1.10
15	0.10	0.21	0.81	200	0.32	1.10
20	0.12	0.25	0.87	205	0.33	1.20
25	0.21	0.35	0.87	210	0.35	1.40
30	0.29	0.39	0.84	215	0.38	1.80
35	0.20	0.48	0.85	220	0.39	2.10
40	0.26	0.51	0.84	225	0.42	2.50
45	0.33	0.59	0.87	230	0.45	2.80
50	0.20	0.62	0.88	235	0.54	3.00
55	0.12	0.67	0.90	240	0.47	3.40
60	0.10	0.68	0.94	245	0.50	4.50
65	0.13	0.74	0.97	250	0.52	4.80**
70	0.14	0.71	0.98	255	0.65	
75	0.10	0.59	0.98	260	0.74	
80	0.15	0.65	1.00	265	0.80	
85	0.21	0.67	1.10	270	0.89	
90	0.27	0.68	1.20	275	0.91	
95	0.27	0.69	1.60	280	0.93	
100	0.28	0.87	2.10	285	0.93	
105	0.26	0.87	2.90	290	0.95	
110	0.24	0.79	3.20	295	0.96	
115	0.21	0.81	3.80	300	1.50	
120	0.19	0.85	4.10**	305	1.60	
125	0.19	0.87		310	1.80	
130	0.18	0.89		315	3.20	
135	0.17	0.85		320	3.50	
140	0.16	0.87		325	3.60	
145	0.08	0.75		330	4.10	
150	0.17	0.79		335	4.40**	
155	0.17	0.85				
160	0.15	0.86				
165	0.24	0.84				
170	0.18	0.82				
175	0.20	0.81				
180	0.21	0.85				
185	0.23	0.76				

*Error limit: $[F^-] = \pm 0.2$ mg/L.

**Discontinued due to poor fluoride removal

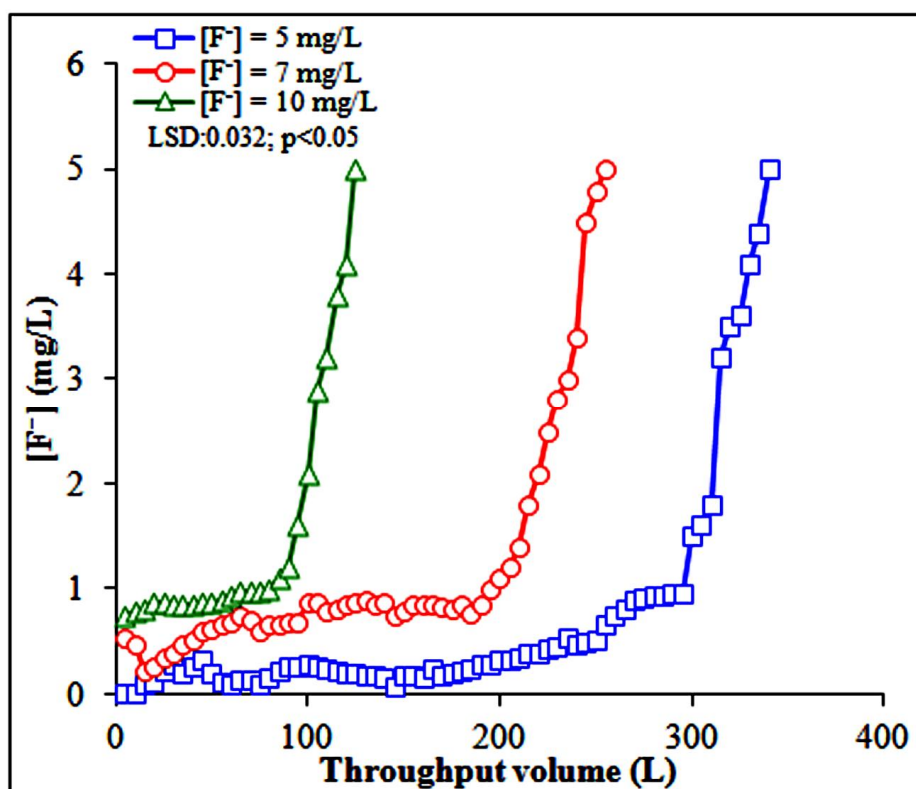


Figure 3.22. The breakthrough curves for defluoridation of water at different influent fluoride concentrations at fixed $[PA]_0 = 0.01$ M and flow rate = 100 mL/h.

3.3.3 Effect of flow rates

The fluoride removal performance was examined at different flow rates of the feed, and hence of the output also, at $[F^-]_0$ of 5 mg/L in presence of 0.01 M $[PA]_0$. The results are summarized in Figure 3.23A and Table 3.29. About 300, 225 and 55 L breakthrough volume (V_B) s of water were obtained at flow rates of 100, 200 and 300 mL/h, respectively, until the $[F^-]$ in the effluent reached 1.5 mg/L, the WHO guideline value.

The service time at breakthrough (t_b) and empty bed contact time (EBCT) have been evaluated using the Eqs. (3.3.1) and (3.3.2), respectively^{293, 294}.

$$t_b = V_B/Q \quad (3.3.1)$$

$$EBCT = V_v/Q \quad (3.3.2)$$

where, V_v (mL) and Q (mL/h) are void volume (1500 mL) and flow rate.

The results indicate that a decrease in flow rate increased the breakthrough volume or breakthrough time due to an increase in empty bed contact time, which was

3000, 1150 and 183 min for flow rates at 100, 200 and 300 mL/h, respectively (Table 3.30).

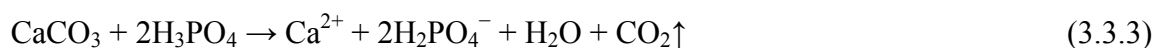
Table 3.30. Summary of breakthrough results for fluoride removal in fixed-bed column PACLT at varying flow rates.

Flow rate (mL/h)	Pore volume (V in mL)	Service time at breakthrough (t_b in h)	Breakthrough volume (V_B in L)	Empty bed contact time (EBCT in min)
100	650	3000	300	900
200	650	1150	230	450
300	650	183	55	300

3.3.4 The pH of effluent water

The final pH of the treated water is an important parameter. The pH of the treated water of each sample measured till the onset of breakthrough and the results were shown in Table 3.29 and Figure 3.23B for different flow rates.

The influent pH was 2.34 at $[PA]_0$ of 0.01 M. As the influent water enters into the column containing limestone bed, the acidified water gets neutralized by limestone through a reaction as shown in Eq. (3.3.3).



The pH of the effluent from the reactor was found in the range of 6.5-5.2. The effluent pH was found to increase with decrease in flow rate suggesting the neutralization to be a slow process. The pH decreased with increase in the throughput volume indicating inhibition of the neutralization reaction at the limestone surface by some process, e.g., sorption of fluoride, which decreases the contact between limestone surface and PA of water. The slightly acidic effluent pH is corrected to 7.4-7.7 (acceptable range for drinking) by the treatment in a four layered sand-limestone-sand-gravel filter (Figure 2.1) for a residence time of 1 h. The results obtained from the one-way ANOVA show that the fluoride removal significantly increases with decreasing flow rate with LSD value 0.037 at $p < 0.05$ (Table 3.31).

Table. 3.29. Remaining $[F^-]$ and pH of treated water after PACLT in continuous-flow mode at different flow rates of the feed.* $[F^-]_0 = 5 \text{ mg/L}$ and $[PA]_0 = 0.01 \text{ M}$.

Throughput volume (L)	$[PA]_0 = 0.01 \text{ M}$ & $[F^-]_0 (\text{mg/L}) = 5 \text{ mg/L}$					
	Flow rate (mL/h)					
	100 mL/h		200 mL/h		300 mL/h	
	$[F^-]$ (mg/L)	pH	$[F^-]$ (mg/L)	pH	$[F^-]$ (mg/L)	pH
5	0.01	6.50	0.38	6.39	0.15	6.24
10	0.008	6.52	0.02	6.38	0.14	6.13
15	0.10	6.53	0.29	6.37	0.13	6.09
20	0.12	6.49	0.28	6.36	0.85	5.98
25	0.21	6.47	0.29	6.37	0.91	5.97
30	0.29	6.45	0.37	6.38	1.00	5.95
35	0.20	6.46	0.35	6.37	1.10	5.93
40	0.26	6.45	0.41	6.39	1.20	5.90
45	0.33	6.43	0.39	6.37	1.40	5.90
50	0.20	6.42	0.27	6.32	1.30	5.89
55	0.12	6.44	0.24	6.25	1.50	5.87
60	0.10	6.45	0.21	6.21	1.70	5.89
65	0.13	6.42	0.25	6.20	2.20	5.84
70	0.14	6.28	0.29	5.94	2.50	5.81
75	0.10	6.24	0.31	5.84	2.80	5.45
80	0.15	6.01	0.30	5.56	3.00	5.40
85	0.21	6.00	0.33	5.53	5.00**	5.39
90	0.27	5.98	0.27	5.51		
95	0.27	5.89	0.29	5.49		
100	0.28	5.79	0.31	5.41		
105	0.26	5.74	0.29	5.39		
110	0.24	5.71	0.28	5.32		
115	0.21	5.69	0.29	5.31		
120	0.19	5.70	0.27	5.33		
125	0.19	5.71	0.28	5.32		
130	0.18	5.68	0.27	5.31		
135	0.17	5.67	0.29	5.30		
140	0.16	5.57	0.28	5.31		
145	0.08	5.48	0.27	5.30		
150	0.17	5.46	0.26	5.32		
155	0.17	5.41	0.25	5.33		
160	0.15	5.42	0.23	5.32		
165	0.24	5.39	0.22	5.30		
170	0.18	5.38	0.21	5.31		
175	0.20	5.36	0.18	5.32		
180	0.21	5.35	0.36	5.31		
185	0.23	5.34	0.39	5.30		
190	0.28	5.37	0.45	5.31		
195	0.29	5.35	0.55	5.32		
200	0.32	5.36	0.84	5.31		
205	0.33	5.34	0.99	5.30		

Continued to the next page-

Continued from the previous page-

Throughput volume (L)	100 mL/h		200 mL/h		300 mL/h	
	[F ⁻] (mg/L)	pH	[F ⁻] (mg/L)	pH	[F ⁻] (mg/L)	pH
210	0.35	5.38	1.10	5.30		
215	0.38	5.39	1.00	5.30		
220	0.39	5.37	1.10	5.29		
225	0.42	5.36	1.50	5.28		
230	0.45	5.35	1.80	5.28		
235	0.54	5.34	2.00	5.29		
240	0.47	5.37	2.50	5.28		
245	0.50	5.34	3.00	5.27		
250	0.52	5.32	3.20	5.28		
255	0.65	5.31	3.50	5.25		
260	0.74	5.30	3.60	5.26		
265	0.80	5.31	4.10	5.27		
270	0.89	5.32	4.40	5.26		
275	0.91	5.31	4.80**	5.25		
280	0.93	5.30				
285	0.93	5.32				
290	0.95	5.31				
295	0.96	5.30				
300	1.50	5.32				
305	1.60	5.28				
310	1.80	5.27				
315	3.20	5.26				
320	3.50	5.25				
325	3.60	5.24				
330	4.10	5.23				
335	4.40	5.21				
340	5.00	5.17				

*Error limits: [F⁻] = ±0.2 mg/L and pH = ±0.1

**Discontinued due to poor fluoride removal

Table 3.31. The results of one-way analysis of variance of fluoride removal with different flow rates of the influent water. $[PA]_0 = 0.01$ M and $[F^-]$ (mg/L) = 5 mg/L.

100 mL/h	200 mL/h	300 mL/h	LSD	p*
**[F ⁻] (mg/L)	**[F ⁻] (mg/L)	**[F ⁻] (mg/L)		
0.33	0.39	0.69	0.037	<0.05
0.34	0.43	0.74		
0.38	0.50	0.79		

*p- Pearson's correlation is significant at <0.05 level.

**The results are average of three experiments

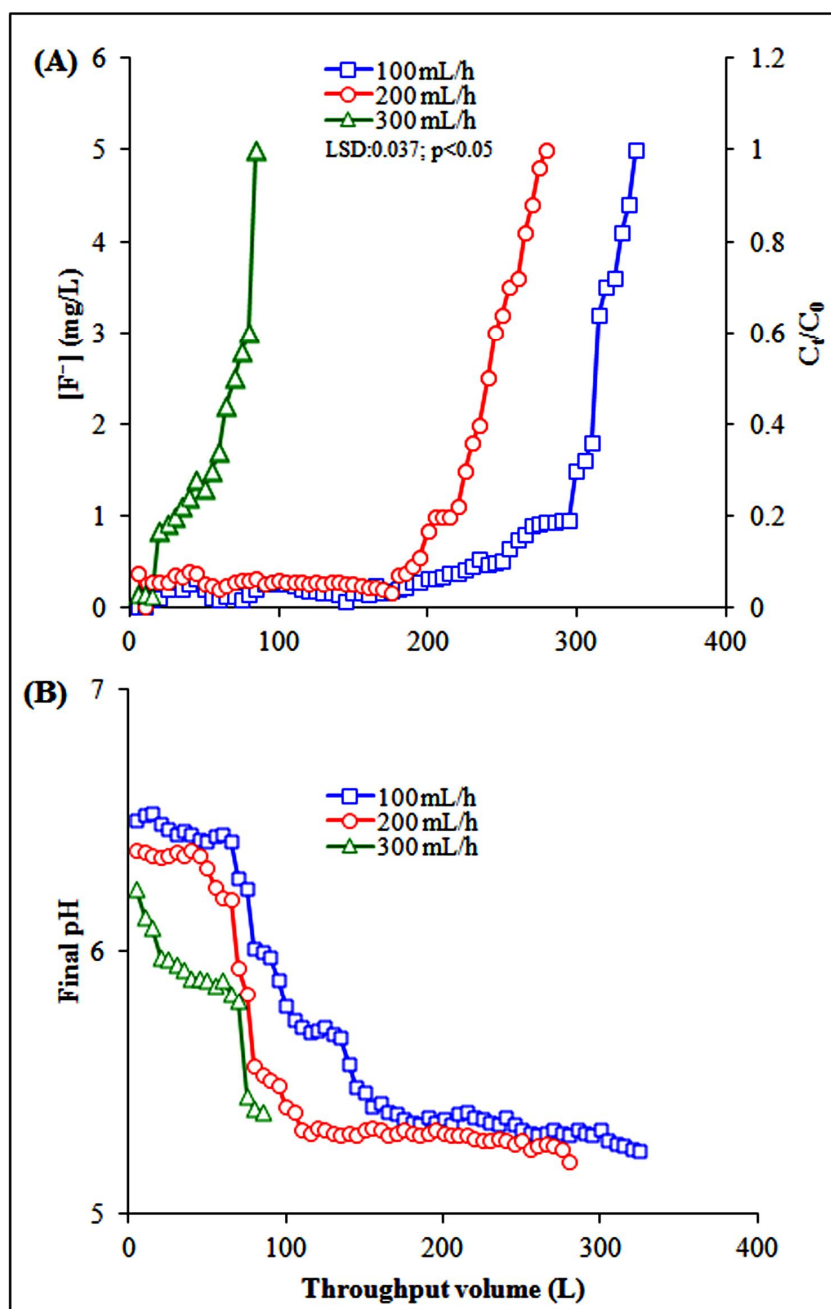


Figure 3.23. The plots of (A) breakthrough curves and (B) final pH of effluent water vs. throughput volume (L), at different flow rates with $[PA]_0 = 0.01$ M and $[F^-]_0 = 5$ mg/L.

3.3.5 The effect of co-existing ions

The interference of co-existing SO_4^{2-} , NO_3^- , Cl^- and Br^- ions on fluoride removal was investigated and results were shown in Figure 3.24. It has been observed from the results that the percentage of fluoride removal remains within in the range of 96-95% in the presence of anions *viz.*, NO_3^- , Cl^- and Br^- . This indicates that NO_3^- , Cl^- and Br^- ions have little influence on fluoride removal. However, in the presence of SO_4^{2-} ions the

fluoride removal decreases to 82% and thus it has some influence on fluoride removal. There is only slight gradual decrease in the fluoride removal on increasing concentrations of anions.

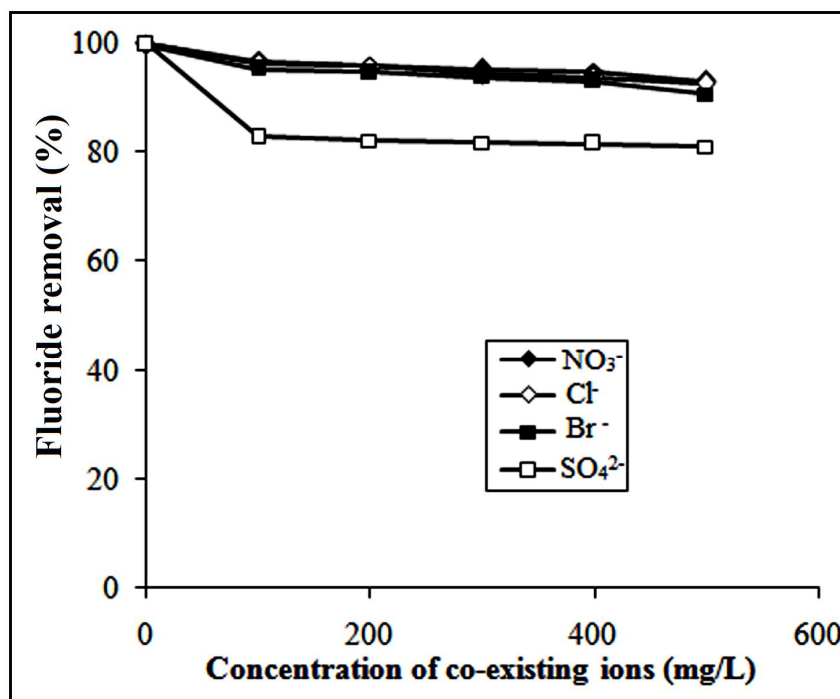


Figure 3.24. Effects of different competing anions on fluoride removal by PACLT in continuous-flow column experiment. $[F^-]_0 = 5$ mg/L; $[PA]_0 = 0.01$ M and flow rate = 100 mL/h.

3.3.6 Column regeneration

Since regeneration increases the commercial viability and environmental acceptability of a water purification technology, the author regenerated the exhausted limestone by feeding 0.30 M NaOH solution through the column at different flow rates until $[F^-]$ attained equilibrium. The breakthrough results of PACLT with limestone after the first time regeneration at three different flow rates at $[F^-]_0$ of 5 mg/L and $[PA]_0$ of 0.01 M have been shown in Table 3.32 and Figure 3.25A. The first-time regenerated limestone showed fluoride removal activity of about 73% compared to fresh limestone. The activity of the regenerated limestone was found to decrease with increasing flow rates. To see the activity of exhausted limestone, the author has performed three times regeneration experiment after completion of each regeneration cycle. The results are presented in Table 3.33 and Figure 3.25B. The activity of the regenerated limestone was found to decrease more with repeated regeneration as shown in Figure 3.25B.

Table 3.32. Remaining $[F^-]$ in the treated water after treatment with the first-time regenerated limestone in the PACLT at different flow rates of feed.* $[F^-]_0 = 5 \text{ mg/L}$ and $[PA]_0 = 0.01 \text{ M}$.

Throughput volume (L)	$[F^-]$ (mg/L)		
	100 mL/h	200 mL/h	300 mL/h
5	0.15	0.23	0.16
10	0.12	0.20	0.10
15	0.35	0.39	0.41
20	0.31	0.41	0.45
25	0.31	0.45	0.48
30	0.31	0.41	0.50
35	0.34	0.47	0.90
40	0.32	0.49	0.95
45	0.34	0.46	1.50
50	0.33	0.48	1.80
55	0.32	0.49	2.10
60	0.31	0.51	2.30
65	0.34	0.52	2.50
70	0.35	0.56	3.00
75	0.35	0.64	3.30**
80	0.45	0.71	
85	0.51	0.75	
90	0.55	0.82	
95	0.56	0.85	
100	0.62	0.84	
105	0.67	0.82	
110	0.70	0.86	
115	0.73	0.89	
120	0.75	0.91	
125	0.80	0.91	
130	0.85	0.92	
135	0.86	0.94	
140	0.89	0.95	
145	0.98	0.97	
150	0.99	0.98	
155	0.97	0.99	
160	0.89	0.98	
165	0.91	1.00	
170	1.00	1.30	
175	1.10	1.40	
180	1.00	1.50	
185	0.98	2.00	
190	0.99	2.50	
190	0.99	2.50	
195	1.10	2.80	
200	1.20	3.20**	
205	1.30		
210	1.30		
215	1.20		
220	1.50		
225	1.60		
235	2.00		
230	1.90		
240	2.00		
245	2.20		
250	2.50		
255	2.90		
260	3.40**		

*Error limits: $[F^-] = \pm 0.2 \text{ mg/L}$; **Discontinued due to poor fluoride removal

Table 3.33. Remaining $[F^-]$ in the treated water after treatment with first, second and third-time regenerated limestone in the PACLT at a fixed flow rate of 100 mL/h.* $[F^-]_0 = 5$ mg/L and $[PA]_0 = 0.01$ M.

Throughput volume (L)	$[F^-]$ (mg/L)		
	Regeneration cycle		
	1 st	2 nd	3 rd
5	0.15	0.25	0.32
10	0.12	0.18	0.43
15	0.35	0.21	0.45
20	0.31	0.56	0.46
25	0.31	0.54	0.47
30	0.31	0.52	0.48
35	0.34	0.48	0.50
40	0.32	0.39	0.53
45	0.34	0.38	0.54
50	0.33	0.39	0.61
55	0.32	0.40	0.63
60	0.31	0.43	0.72
65	0.34	0.48	0.75
70	0.35	0.41	0.82
75	0.35	0.45	0.97
80	0.45	0.39	1.50
85	0.51	0.35	2.00
90	0.55	0.31	2.50
95	0.56	0.48	3.00
100	0.62	0.52	3.50
105	0.67	0.57	5.00**
110	0.70	0.59	
115	0.73	0.60	
120	0.75	0.65	
125	0.80	0.70	
130	0.85	0.78	
135	0.86	0.85	
140	0.89	0.89	
145	0.98	0.90	
150	0.99	1.00	
155	0.97	1.50	
160	0.89	2.00	
165	0.91	2.05	
170	1.00	2.10	
175	1.10	2.50	
180	1.00	2.80	
185	0.98	3.00	
190	0.99	4.35	
195	1.10	5.00**	
200	1.20		
205	1.30		
210	1.30		
215	1.20		
220	1.50		
225	1.60		
230	1.90		
240	2.20		
245	2.50		
250	2.90		
255	3.40		
260	4.50**		

*Error limits: $[F^-] = \pm 0.2$ mg/L; **Discontinued due to poor fluoride removal

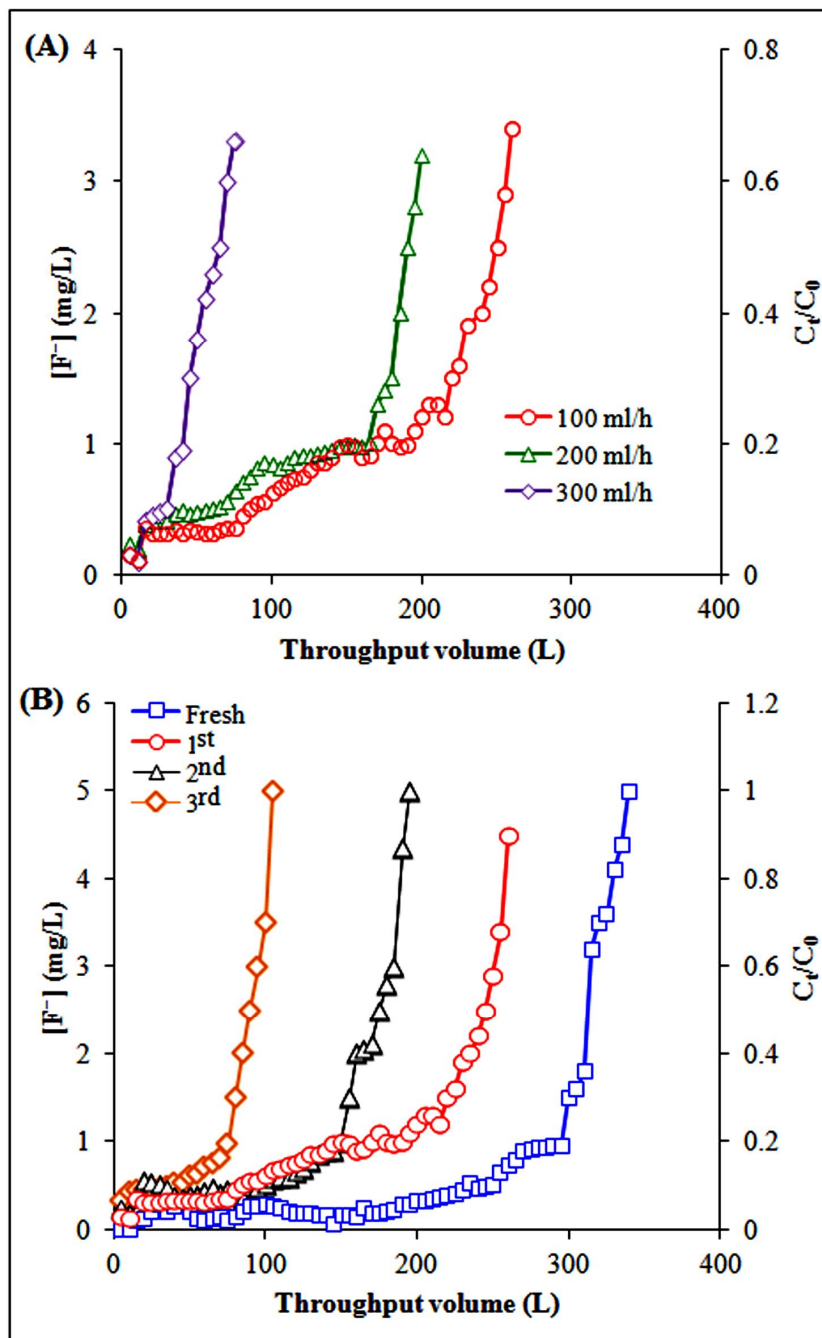


Figure 3.25. The breakthrough curves for (A) fluoride removal with first-time regenerated limestone at different flow rates; and (B) fresh limestone, and first, second and third-time regenerated limestone at a fixed flow rate of 100 ml/h with $[F^-]_0 = 5$ mg/L and $[PA]_0 = 0.01$ M.

3.3.7 Mechanism of fluoride removal

The mechanism was studied through FTIR, XRD, SEM-EDX and saturation index analyses.

3.3.7.1 FTIR analysis

The major characteristic peaks of CaCO_3 at 1430, 875 and 709 cm^{-1} are found in unused limestone²⁹⁹ (Figure 3.26A). The peaks at around 2368 cm^{-1} and 1430 cm^{-1} attributed for CO_3^{2-} ions³⁰⁵. In the precipitate obtained in the present case, the characteristics peaks at 3571 cm^{-1} and 637 cm^{-1} correspond to the OH stretching frequency¹⁹². The characteristics peak at around 1646 cm^{-1} is due to adsorbed water¹⁹³. However, absence of a peak at 1430 cm^{-1} indicating the absence of CaCO_3 in the precipitate (Figure 3.26B). On the other hand, the bands at 1089 cm^{-1} and 964 cm^{-1} are characteristics peaks for PO_4^{3-} group indicating the formation of calcium phosphate or HAP¹⁹². The peaks at around 1134 cm^{-1} and around 1226 cm^{-1} correspond to H-PO_4^{2-} stretching^{298, 310}. Moreover, a small band appears at 740 cm^{-1} can be attributed to the Ca-F stretching of CaF_2 ²⁹⁹. Thus, the FTIR of the precipitate formed in the reactor after continuous-flow PACLT method indicates the presence of calcium phosphate or HAP and sorption of fluoride by HAP.

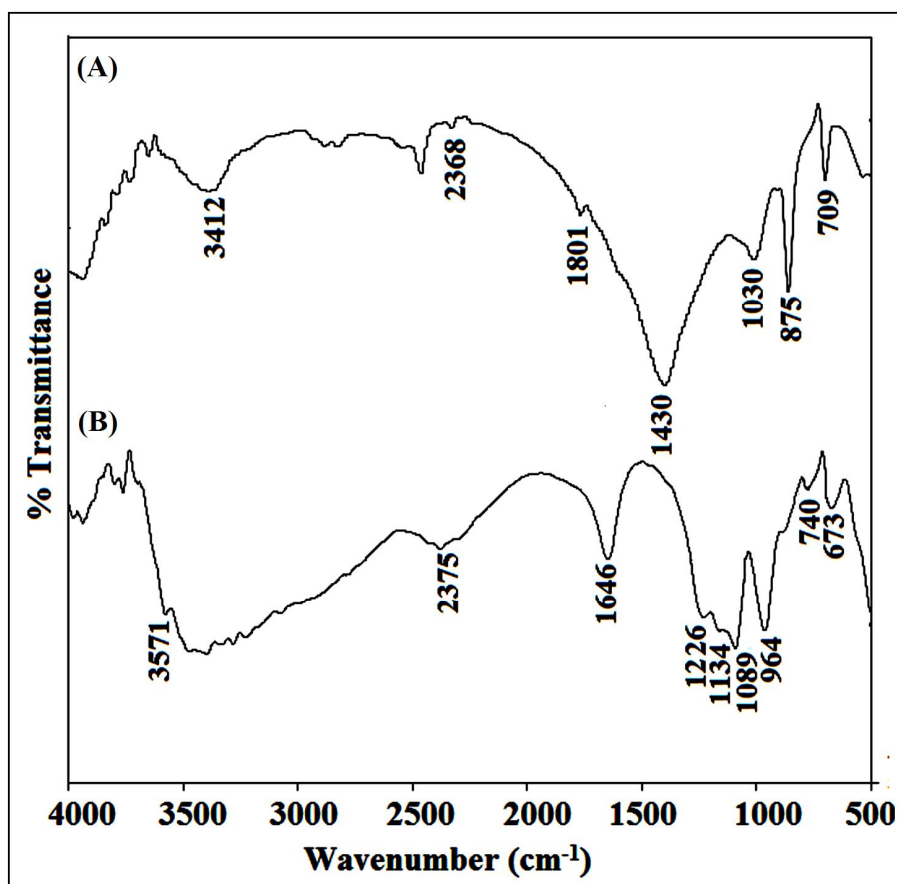


Figure 3.26. FTIR spectra of (A) unused limestone and (B) precipitate formed in the column in continuous-flow PACLT.

3.3.7.2 XRD analysis

The peaks with significant intensities at $2\theta = 29.5^\circ$ (1 0 4) (strong), 36.12° (1 1 0), 39.5° (1 1 3), 43.5° (2 0 2), 47.5° (1 0 8) and 48.5° (1 1 6) corresponding to calcite polymorph of calcium carbonate are seen in the XRD of the fresh limestone powder (Figure 3.27A). A large increase in the intensity of the XRD peak at around 47° compared to that of fresh limestone can be attributed to diffraction of plane of fluorite, CaF_2 ²⁸⁷ (Figure 3.27B). The peaks at 25.8° (0 0 2), 31.7° (2 1 1), and 50° (3 2 1) are corresponding to HAP¹⁹¹ (JCPDS card no. 89-6438). A small peak at 31.9° (2 1 1) can be attributed to diffraction from plane of FAP¹⁹² (JCPDS card no. 87-2462). Thus, sorption by HAP contributes to the fluoride removal.

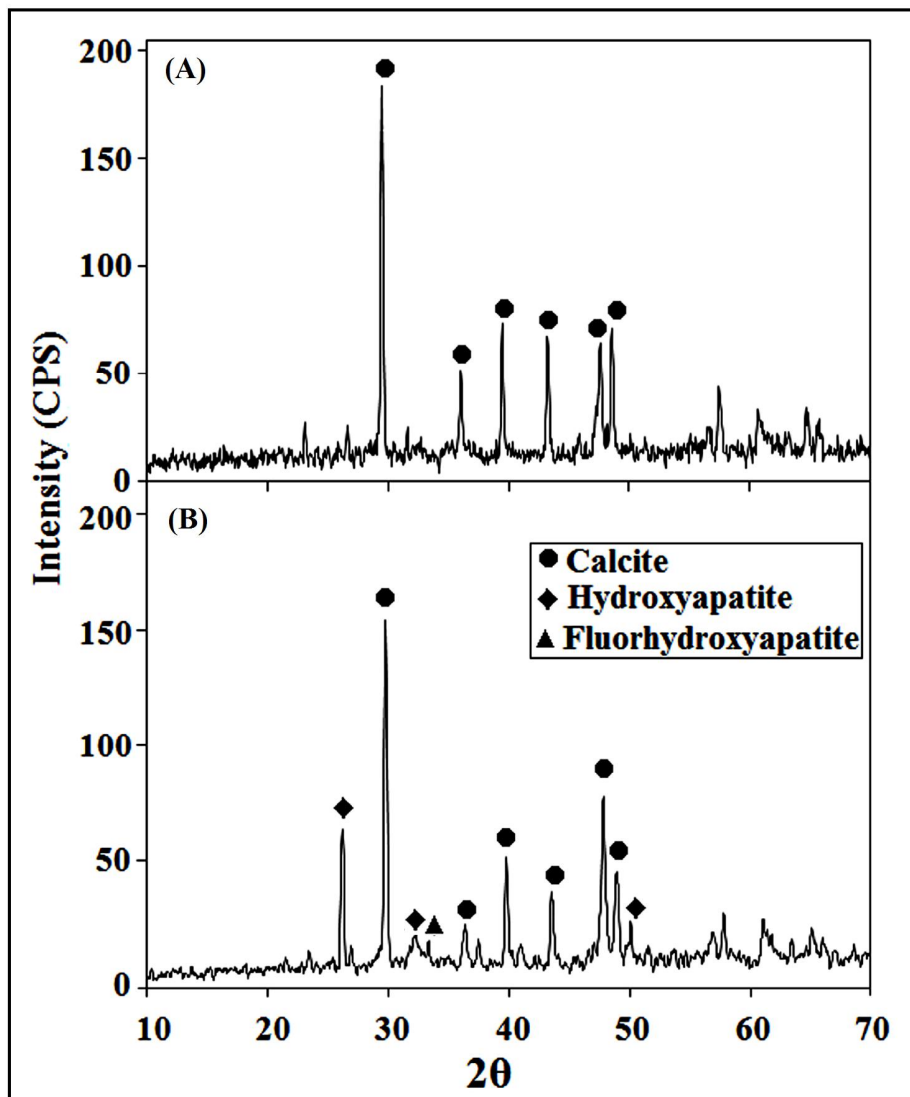


Figure 3.27. XRD spectra of (A) unused limestone and (B) the precipitate formed in the column in continuous-flow PACLT.

3.3.7.3 SEM-EDX analysis

The surface morphology and energy dispersive X-ray spectrum of unused limestone and the precipitate found after PACLT in continuous-flow mode has been studied (Figure 3.28). The surface of the precipitate was found to be rough and showed the presence of P. In the precipitate, F was not noticed which may be due to masking by large excess of HAP in the precipitate. However, a quantitative determination of fluoride content in the precipitate formed in the reactor, using a standard procedure³¹¹, showed about 1.2 mg/L F^- which confirms the sorption of fluoride by HAP.

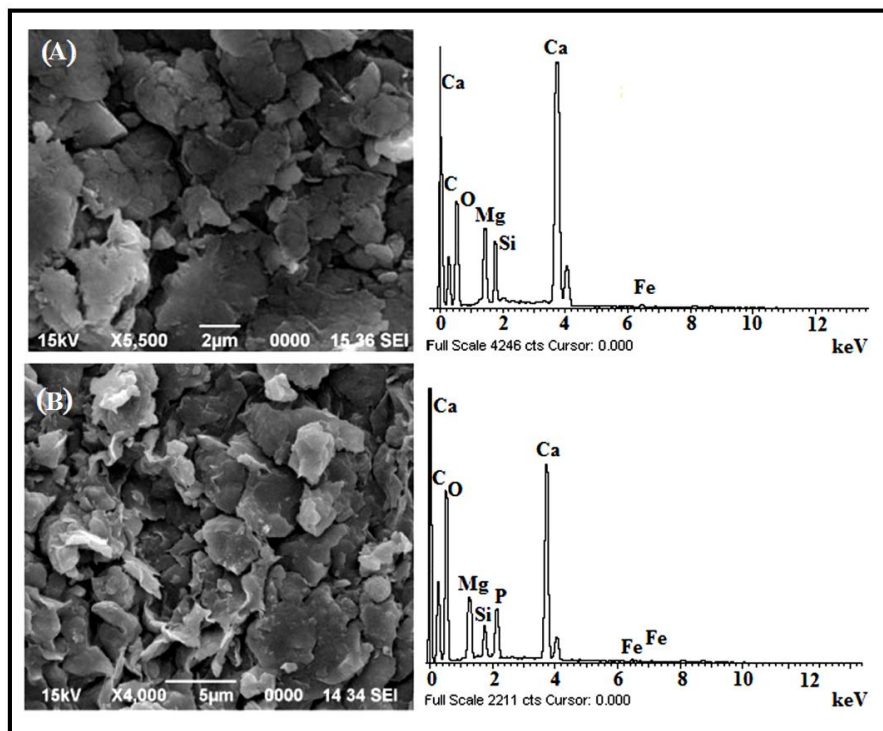


Figure 3.28. SEM-EDX of (A) unused limestone and (B) the precipitate formed in the column in continuous-flow PACLT.

3.3.7.4 Saturation index

The fluorite Saturation Index (SI_f) has been calculated using Eq. 3.3.4²⁴⁷:

$$SI_f = \log_{10} (Q/K_{sp}) \quad (3.3.4)$$

$$\text{Where, } Q = [Ca^{2+}][F^-]^2 \quad (3.3.5)$$

The results of $[F^-]$ and $[Ca^{2+}]$ present in the water after using fresh limestone and regenerated limestone in the PACLT are shown in Table 3.34 & Figure 3.29.

Table 3.34A. Remaining $[F^-]$ (mg/L) and residual $[Ca^{2+}]$ (mg/L) in the water after treatment by the PACLT at different $[PA]_0$. * $[F^-]_0 = 5$ mg/L and flow rate = 100 mL/h.

Throughput volume (L)	$[PA]_0$ (M)					
	0.01 M		0.03 M		0.05 M	
	$[F^-]_0$ (mg/L)	$[Ca^{2+}]$ (mg/L)	$[F^-]_0$ (mg/L)	$[Ca^{2+}]$ (mg/L)	$[F^-]_0$ (mg/L)	$[Ca^{2+}]$ (mg/L)
5	0.01	7.70	0.01	23.00	0.009	52.00
40	0.26	5.20	0.06	18.00	0.03	51.00
80	0.15	3.40	0.36	16.00	0.21	48.00
120	0.19	4.00	0.14	13.60	0.10	45.00
160	0.15	3.40	0.15	13.80	0.14	50.00
200	0.32	3.00	0.32	14.80	0.24	45.00
240	0.47	4.10	0.45	14.00	0.42	46.00
280	0.93	3.80	0.80	12.70	0.77	48.00
320	3.50	3.80	0.95	12.40	0.91	47.00
340	5.00**	3.00	0.96	12.10	0.96	43.00
360			0.95	11.00	0.97	42.00
400			0.98	11.00	0.98	40.00
440			3.50	10.70	1.10	37.00
460			4.80**	10.50	2.10	38.00
480					4.00	39.00
490					5.00**	32.00

*Error limits: $[F^-] = \pm 0.2$ mg/L; **Discontinued due to poor fluoride removal

Table 3.34B. Remaining $[F^-]$ (mg/L) and residual $[Ca^{2+}]$ (mg/L) present in the water after treatment with fresh limestone and first, second and third-time regenerated limestone in the PACLT. * $[PA]_0 = 0.01$ M; $[F^-]_0 = 5$ mg/L and flow rate = 100 mL/h.

Throughput volume (L)	Fresh		1 st regeneration		2 nd regeneration		3 rd regeneration	
	$[F^-]_0$ (mg/L)	$[Ca^{2+}]$ (mg/L)	$[F^-]_0$ (mg/L)	$[Ca^{2+}]$ (mg/L)	$[F^-]_0$ (mg/L)	$[Ca^{2+}]$ (mg/L)	$[F^-]_0$ (mg/L)	$[Ca^{2+}]$ (mg/L)
5	0.01	7.70	0.15	6.50	0.25	6.00	0.32	5.10
40	0.26	5.20	0.32	6.20	0.39	5.40	0.53	4.50
80	0.15	3.40	0.45	6.30	0.39	4.70	1.50	4.60
90	0.27	3.20	0.55	6.40	0.31	4.80	2.50	4.40
100	0.27	3.40	0.62	6.20	0.52	4.70	3.50**	3.00
120	0.19	4.00	0.75	5.00	0.65	4.60		
160	0.15	3.40	0.89	4.50	2.00**	4.20		
200	0.32	3.00	1.20	3.80				
240	0.47	4.10	2.20**	4.10				
280	0.93	3.80						
320	3.50	3.80						
340	5.00**	3.00						

*Error limits: $[F^-] = \pm 0.2$ mg/L; **Discontinued due to poor fluoride removal

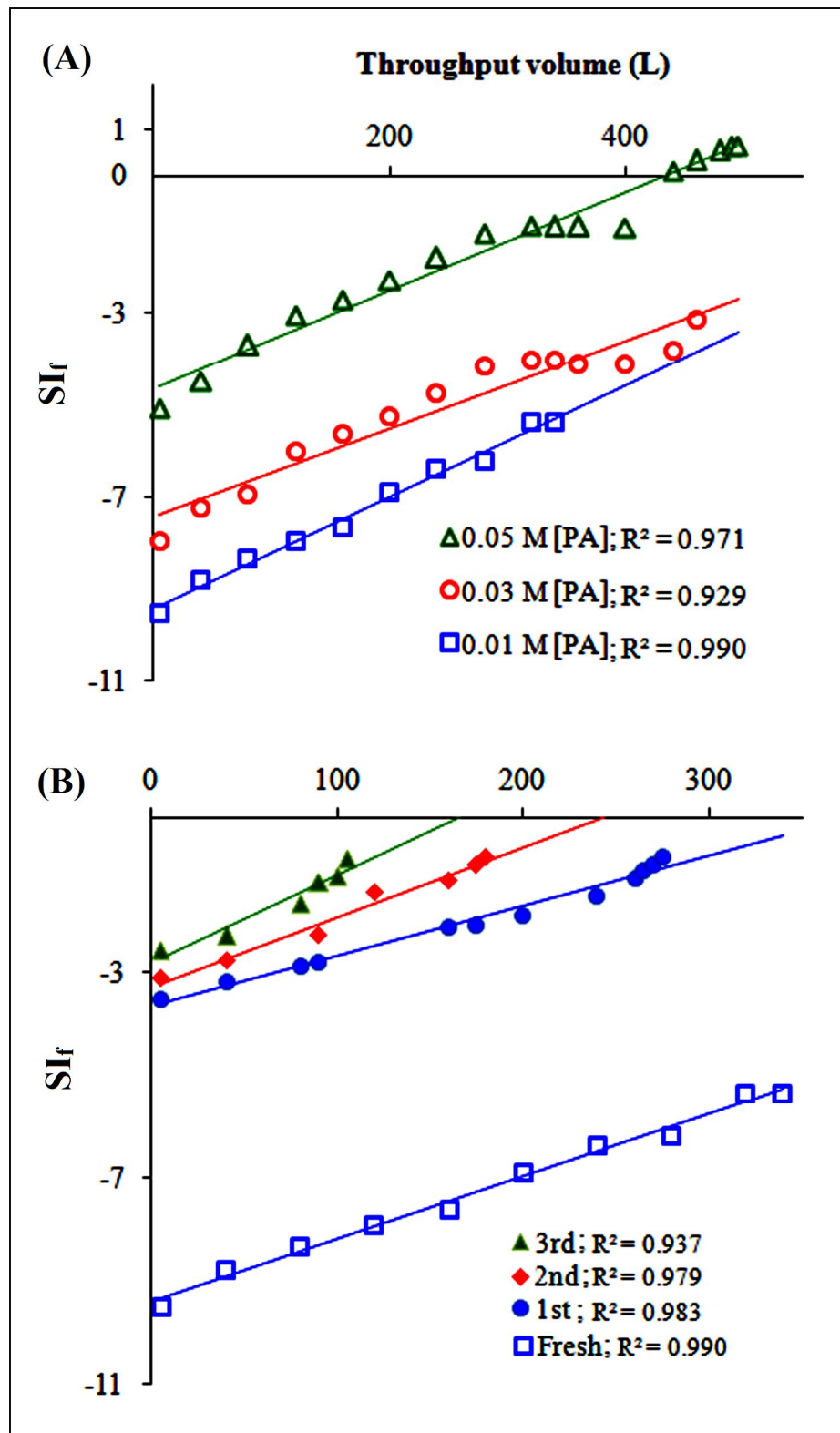


Figure 3.29. The saturation index of fluorite (SI_f) for the continuous-flow PACLT experiment: (A) with $[PA]_0$ of 0.01, 0.03 and 0.05 M; and (B) with regenerated limestone.

The SI_f of the experiment with fresh limestone at 0.01, 0.03 and 0.05 M $[PA]_0$ and with regenerated limestone (Figure 3.29) provides some interesting information:

- i. The SI_f were found to be higher with higher $[PA]_0$ which may be attributed to an increase in $[Ca^{2+}]$ in the effluent water due to an increasing dissolution of limestone at higher $[PA]_0$.
- ii. The SI_f values were negative in all cases, except towards the breakthrough with 0.05 M $[PA]_0$, indicating a dominant role of sorption of fluoride in the removal of fluoride²⁴⁶. There is a highly efficient fluoride removal, to far below 1 mg/L, at low throughput volume (Figures. 3.21-3.23A, 3.25 and 3.29). This can be attributed to sorption of fluoride in addition to precipitation as precipitation alone can remove fluoride only to below 2 mg/L as limited by the solubility product of CaF_2 ²⁴⁶. Probably, the relatively rapid precipitation²⁷⁷⁻²⁷⁹ quickly brings down the fluoride from any initial concentration to about 2 mg/L and after that the relatively slow sorption process comes into play.
- iii. The SI_f values increased almost linearly with the throughput volume. Therefore, the observed increase in the SI_f , at a fixed flow rate, is due to a decrease in sorption of fluoride and not due to any increase of the precipitation. From the linear plots of SI vs. V , the author finds

$$SI = mV + C \quad (3.3.6)$$

where, V is the measured throughput volume, and m and C are experimentally determined constants which are the characteristic of $[PA]_0$, $[F^-]_0$, flow rate and the limestone quality.

Thus, from Eqs. (3.3.4), (3.3.5) and (3.3.6) the author gets,

$$\begin{aligned} \log Q - \log K_{sp} &= mV + C \\ \Rightarrow \log ([Ca^{2+}][F^-]^2) &= mV + (C + \log K_{sp}) \\ \Rightarrow \log [F^-]^2 &= -\log [Ca^{2+}] + mV + C + \log K_{sp} \\ \Rightarrow [F^-] &= (K_{sp}e^{mVC}/[Ca^{2+}])^{1/2} \\ \text{or, } [F^-] &= (K_{sp}e^{mVC}/[Ca^{2+}])^{1/2} \end{aligned} \quad (3.3.7)$$

Therefore, the $[F^-]$ in the effluent water and hence the breakthrough point can be determined indirectly for a set of fixed conditions of the process by determining the $[Ca^{2+}]$. It may be noted that monitoring effluent $[F^-]$ through determination of $[Ca^{2+}]$

using a flame photometer in rural areas should be easier than the determination of $[F^-]$ using an ISE.

- iv. The SI_f value increased considerably after first regeneration of the column and then slightly increased after further successive regenerations. This suggests that the sorption of fluoride considerably decreased after the first regeneration and the decrease continued after subsequent regenerations.

3.3.7.5 The removal efficiency and the mechanism

It can be seen from the pattern of remaining $[F^-]$ in Figure 3.29 that the $[F^-]$, before breakthrough, increases with each regeneration. In fact, there are three different levels of fluoride removal. The first one is a very good removal to below 0.5 mg/L which is prominent with fresh limestone and towards the beginning of the use of the limestone, the second one is a moderately good removal to between 0.5 and 1 mg/L after use of the limestone for some time and the third one is a fairly good removal to between 1 and 2 mg/L towards the last stage of the activity of the limestone. It is known that precipitation alone cannot remove fluoride to below 2 mg/L²⁴⁶ whereas adsorption can remove fluoride to any low level.

Based on the present findings one can attribute the observed stages of fluoride removal as a function of the throughput volume as follows:

- i. The initial very good fluoride removal to near 0.1 mg/L may be due to an unabated precipitation of fluoride and an unabated sorption of fluoride on abundant original adsorption sites of limestone surface and by HAP.
- ii. The good fluoride removal to 0.1-0.5 mg/L may be due to an unabated precipitation and a reduced sorption by HAP and limestone surfaces renewed by precipitation.
- iii. The moderately good fluoride removal to 0.5-1.0 mg/L may be due to a gradually diminishing precipitation and sorption due to covering of limestone surface by adsorbed fluoride and deposition of inactive precipitates like $CaCO_3$.
- iv. Finally the onset of the breakthrough may be due to cessations of both the precipitation and the sorption processes.

3.3.8 Suitability Analysis

The suitability analysis was assessed in terms of safety of the process as a whole, capacity of limestone and the cost of the process.

3.3.8.1 Safety

The relevant water quality parameters of the treated water samples before and after PACLT treatment determined using standard methods³¹² are given in Table 3.35. All the water quality parameters after treatment were within the respective WHO guideline values for drinking water⁴⁹. The concentrations of most of the metal ions showed a decrease after treatment. The concentrations of Ca^{2+} and PO_4^{3-} which are components in the materials used in the present method also remained within the acceptable range that of concentration of NO_3^{2-} was slightly decreased after treatment.

Table 3.35. The relevant water quality parameters of water before and after treatment in the PACLT in the continuous-flow mode with $[\text{PA}]_0 = 0.01\text{M}$, $[\text{F}^-]_0 = 5\text{ mg/L}$ and flow rate of 100 mL/h.

Parameter in mg/L except for pH	WHO guideline Value	Before treatment	After treatment
pH	6.50-8.50 ^a	7.47	7.4-7.7
Dissolved solid	600	130	156
Suspended solid	NS ^b	10	4
Total alkalinity as CaCO_3	200	80	84
Total hardness as CaCO_3	200	86	95
Sulphate	500	6.3	6.2
Phosphate	NS	0.70	0.74
Nitrate	50	0.55	0.20
Cadmium	0.003	0.001	<0.001
Calcium	50	2.50	3.76
Chromium	0.05	ND ^c	ND
Cobalt	NS	ND	ND
Copper	2.0	1.00	1.20
Lead	0.01	ND	ND
Magnesium	NS	2.4	2.9
Manganese	0.40	0.10	0.09
Zinc	3.0	2.0	0.08
Sodium	200	60.6	60.0
Potassium	NS	1.07	ND
Iron	0.30	0.34	0.085

^aAcceptable range for drinking, ^bNS: Not specified, ^cND: Not detectable

It can be mentioned here that a toxicity characteristic leaching procedure (TCLP) test²⁹⁵ on the precipitate has shown a leaching of 0.28 mg/L which is much less than the permissible value of 150 mg/L for disposal in landfill^{295, 309}.

3.3.8.2 Capacity of limestone and cost-benefits analysis

The removal of fluoride was found to be better at the flow rate of 100 mL/h in presence of 0.01 M $[PA]_0$. Therefore, capacity of limestone and cost benefit analysis was calculated for this flow rate. A preliminary estimation has shown that the process can be adjusted to achieve 1 L/h treated water using a column containing 15 kg of crushed limestone. Regeneration with NaOH recovers about 73% of the activity of limestone. The regeneration can be repeated up to at least 3 times. Thus, a total volume of about 300 L treated water could be obtained per kg of limestone. This gives a total capacity of 3.84 mg/g of limestone which is much better than the capacity of limestone alone¹⁰⁷ and highly competitive with the other low-cost sorbents of fluoride like HAP¹¹².

Taking the cost of limestone as INR 1822 (US\$ 27) per metric ton and the market price of 85% W/V PA as INR 37 (US\$ 0.55) per litre, the cost of limestone and PA per litre of the treated water have been estimated as INR 0.0077 and 0.02 (US\$ 0.000115 and 0.0003), respectively. This gives an overall recurring cost for the PACLT in a continuous-flow mode to remove fluoride from 5 mg/L to below 1 mg/L as INR 0.03 (US\$ 0.00041) per litre of treated water, which is indeed very good. There are scopes for further reduction of the cost by improving the capacity through process optimization including design of column, lowering $[PA]_0$, etc. Thus, the PACLT in the continuous-flow mode is quite efficient and cost-effective.

3.3.9 Summary

The findings of this work can be summarised as follows:

- Fluoride can be removed efficiently from contaminated water by treatment of the water, pre-acidified with PA, in a fixed-bed crushed limestone reactor in a continuous up-flow mode.
- The present method can remove fluoride from initial 5-10 mg/L to 0.1-1.5 mg/L in presence of PA.
- The present method gives a total 300 L of defluoridated water with 0.01 M $[PA]_0$ and 1.5 kg of 1.0-1.5 cm crushed limestone at a flow rate of 100 mL/h.
- The breakthrough volume increases with increase in $[PA]_0$ from 0.01 M to 0.05 M.
- The breakthrough occurs sooner with higher flow rate.
- Both precipitation and sorption of fluoride contribute in fluoride removal.

- The precipitation quickly brings down the fluoride concentration from any initial level to about 2 mg/L and after that the sorption of fluoride by in situ produced HAP and the limestone surface takes place which brings down fluoride to 0.1-1.5 mg/L.
- The inhibitory effect of competing anions on the fluoride removal by the present method is very small except SO_4^{2-} and increases in the order $\text{NO}_3^- < \text{Cl}^- < \text{Br}^- < \text{SO}_4^{2-}$.
- The method gives potable water consistent with the WHO guideline values.
- The used exhausted limestone can be regenerated with NaOH to recover 73% of the capacity and the regeneration can be repeated for at least 3 times giving a total fluoride removal capacity of limestone as 3.84 mg/g.
- The recurring cost of the present method has been estimated as US\$ 0.00041 (INR 0.03) per litre of treated water.

3.4 Fluoride removal by phosphoric acid-crushed limestone treatment:

A laboratory pilot test

A laboratory-scale pilot test of fluoride removal by PA-crushed limestone treatment (PACLT) in plug-flow mode has been carried out for examining its fluoride removal performance under field conditions. The plug-flow mode has been chosen mainly because of its convenience over continuous-flow mode for application in rural set up. The effects of variation in $[F^-]_0$, $[PA]_0$, co-existing ions and regeneration of limestone have been addressed. One way analysis of variance (one-way ANOVA) was performed using SPSS 16 to examine the real variations amongst the results of treatments under different conditions by calculating the least significant difference (LSD) amongst the data of fluoride removal with $[F^-]_0$, and $[PA]_0$. An attempt has been made also to throw more light on the mechanisms of fluoride removal through analysis of the solids and the treated water. The results of the laboratory-scale pilot test including the fluoride removal performance, statistical analysis of fluoride removal, mechanism of fluoride removal, regeneration of limestone and suitability study have been presented and discussed in this section. The suitability of the PACLT has also been discussed in the light of the pilot test results in terms of safety, acceptability, capacity and cost.

3.4.1 The fluoride removal performance

The fluoride removal performance of the laboratory pilot unit was studied using different $[PA]_0$ as described in the section, *2.4.4 Methods of the laboratory-scale pilot test of PACLT*. About 5 L treated water was collected after every cycle of treatment. The results of the pilot test performed with synthetic groundwater containing 10 mg/L $[F^-]_0$ and varying $[PA]_0$ at residence time of 3 h are shown in Table 3.36. The method can remove fluoride from $[F^-]_0$ of 10 mg/L to below 0.01-1.0 mg/L in presence of 0.01 M $[PA]_0$. It can be seen from the Figure 3.30 that the method removes fluoride efficiently from $[F^-]_0$ of 10 mg/L to below 1.5 mg/L up to 130 times which gives almost 660 L, i.e., total discharged water volume in presence of 0.01 M $[PA]_0$ using the same limestone bed.

Table 3.36. Remaining $[F^-]$ (mg/L) and final pH of water after treatment by the PACLT in the pilot experiment with a residence time of 3 h and $[F^-]_0 = 10$ mg/L with different $[PA]_0$.*

n [†]	$[PA]_0$ (M)					
	0.01 M		0.005 M		0.001 M	
	$[F^-]$ (mg/L)	pH	$[F^-]$ (mg/L)	pH	$[F^-]$ (mg/L)	pH
1	0.12	7.32	0.33	7.52	0.94	7.79
2	0.01	7.32	0.23	7.54	0.89	7.75
3	0.11	7.31	0.22	7.54	0.89	7.75
4	0.01	7.29	0.23	7.59	0.63	7.78
5	0.008	7.34	0.25	7.58	0.73	7.77
6	0.01	7.34	0.32	7.59	0.78	7.76
7	0.005	7.35	0.29	7.62	0.73	7.81
8	0.009	7.37	0.30	7.51	0.71	7.81
9	0.06	7.26	0.32	7.52	0.78	7.82
10	0.04	7.34	0.31	7.55	0.75	7.84
11	0.03	7.37	0.35	7.53	0.82	7.64
12	0.03	7.41	0.35	7.49	0.81	7.78
13	0.33	7.45	0.21	7.48	0.80	7.75
14	0.15	7.49	0.23	7.46	0.78	7.71
15	0.13	7.49	0.23	7.49	0.74	7.53
16	0.46	7.50	0.22	7.51	0.63	7.55
17	0.06	7.54	0.18	7.51	0.67	7.56
18	0.03	7.43	0.19	7.34	0.65	7.57
19	0.03	7.41	0.18	7.41	0.64	7.56
20	0.03	7.42	0.18	7.46	0.78	7.57
21	0.02	7.52	0.18	7.52	0.71	7.55
22	0.02	7.55	0.16	7.53	0.79	7.55
23	0.20	7.35	0.17	7.51	0.74	7.56
24	0.01	7.24	0.15	7.48	0.72	7.54
25	0.01	7.12	0.14	7.42	0.70	7.56
26	0.006	7.11	0.15	7.36	0.89	7.54
27	0.007	7.10	0.17	7.31	0.91	7.56
28	0.008	6.78	0.23	7.32	0.95	7.53
29	0.009	6.55	0.15	7.31	1.10	7.55
30	0.05	6.59	0.15	7.41	1.10	7.56
31	0.01	6.44	0.14	7.41	1.20	7.59
32	0.05	6.5	0.21	7.45	1.40	7.53
33	0.01	6.52	0.25	7.43	1.30	7.53
34	0.007	6.54	0.27	7.41	1.50	7.59
35	0	6.54	0.28	7.43	1.40	7.61
36	0	6.57	0.29	7.32	1.60	7.62
37	0	6.45	0.29	7.32	1.80	7.61
38	0	6.45	0.31	7.35	1.90	7.58
39	0	6.47	0.35	7.31	2.90	7.56
40	0	6.41	0.37	7.31	3.50**	7.54
41	0	6.42	0.31	7.31		

Continued to the next page-

Continued from the previous page-

n [†]	0.01 M		0.005 M		0.001 M	
	[F ⁻] (mg/L)	pH	[F ⁻] (mg/L)	pH	[F ⁻] (mg/L)	pH
42	0	6.46	0.32	7.32		
43	0	6.48	0.34	7.33		
44	0	6.42	0.54	7.37		
45	0	6.45	0.63	7.39		
46	0	6.38	0.71	7.41		
47	0	6.34	0.74	7.41		
48	0	6.45	0.80	7.41		
49	0	6.42	0.92	7.38		
50	0	6.32	1.10	7.32		
51	0	6.42	1.30	7.36		
52	0	6.47	1.60	7.31		
53	0	6.41	1.50	7.25		
54	0	6.45	1.90	7.21		
55	0	6.49	1.80	7.31		
56	0	6.52	2.01	7.32		
57	0	6.57	2.10	7.29		
58	0	6.49	2.10	7.19		
59	0	6.42	3.20	7.15		
60	0.30	6.40	3.90**	7.12		
61	0.25	6.42				
62	0.32	6.47				
63	0.31	6.51				
64	0.14	6.54				
65	0.09	6.51				
66	0.09	6.54				
67	0.08	6.61				
68	0.12	6.58				
69	0.18	6.54				
70	0.20	6.61				
71	0.11	6.57				
72	0.19	6.59				
73	0.23	6.62				
74	0.25	6.65				
75	0.28	6.60				
76	0.24	6.57				
77	0.37	6.52				
78	0.32	6.50				
79	0.27	6.48				
80	0.26	6.54				
81	0.25	6.52				
82	0.24	6.61				
83	0.26	6.63				
84	0.26	6.71				
85	0.23	6.74				
86	0.21	6.67				
87	0.20	6.56				
88	0.21	6.61				
89	0.23	6.64				

Continued to the next page-

Continued from the previous page-

n [†]	0.01 M		0.005 M		0.001 M	
	[F ⁻] (mg/L)	pH	[F ⁻] (mg/L)	pH	[F ⁻] (mg/L)	pH
90	0.29	6.72				
91	0.31	6.69				
92	0.37	6.71				
93	0.39	6.66				
94	0.34	6.69				
95	0.38	6.74				
96	0.42	6.77				
97	0.41	6.79				
98	0.39	6.81				
99	0.35	6.76				
100	0.48	6.67				
101	0.53	6.65				
102	0.57	6.62				
103	0.59	6.55				
104	0.60	6.54				
105	0.61	6.53				
106	0.62	6.51				
107	0.63	6.52				
108	0.62	6.50				
109	0.64	6.47				
110	0.65	6.47				
110	0.65	6.47				
111	0.67	6.40				
112	0.68	6.32				
113	0.69	6.21				
114	0.71	6.19				
115	0.73	6.17				
116	0.75	6.18				
117	0.78	6.21				
118	0.77	6.23				
119	0.79	6.21				
120	0.91	5.98				
121	0.92	5.94				
122	0.93	5.93				
123	0.94	5.89				
124	0.98	5.85				
125	0.99	5.84				
126	1.01	5.82				
127	1.11	5.79				
128	0.99	5.76				
129	1.21	5.72				
130	0.98	5.74				
131	0.99	5.75				
132	1.20	5.66				
133	1.70	5.62				
134	1.81	5.69				
135	2.10	5.48				
136	2.40	5.74				

Continued to the next page-

Continued from the previous page-

n [†]	0.01 M		0.005 M		0.001 M	
	[F ⁻] (mg/L)	pH	[F ⁻] (mg/L)	pH	[F ⁻] (mg/L)	pH
137	2.50	5.59				
138	2.70	5.72				
139	2.80	5.73				
140	3.20**	5.70				

*Error limits: [F⁻] = ±0.2 mg/L and pH = ±0.1;

**Discontinued due to poor fluoride removal

†n = number of cycle or treatment

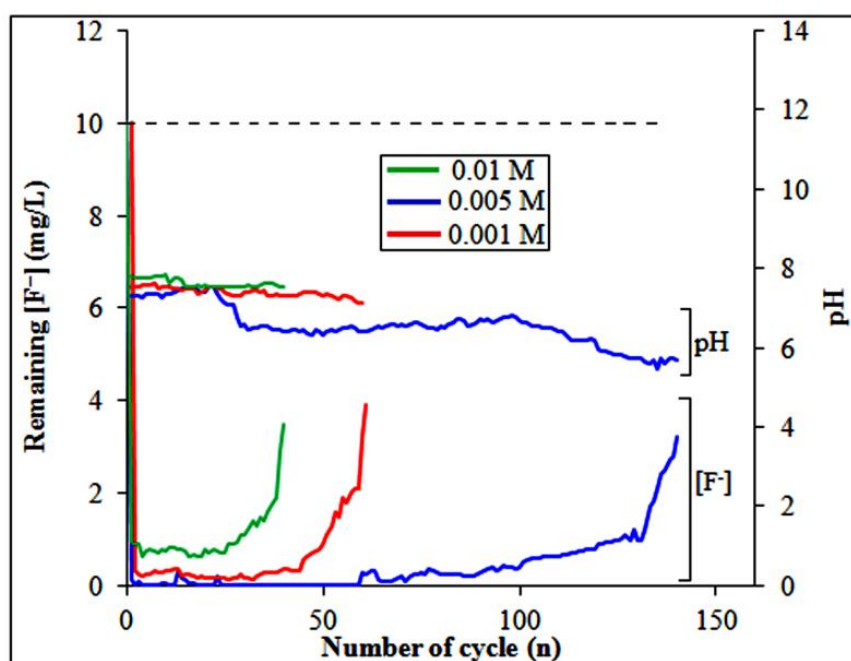


Figure 3.30. Remaining [F⁻] (mg/L) and final pH of treated water vs. number of cycle used in the pilot experiment with [F⁻]₀ of 10 mg/L (shown by horizontal dotted line), residence time of 3 h and varying [PA]₀ of 0.01 M, 0.005 M and 0.001 M.

The fluoride removal performance is found to decrease with decreasing [PA]₀ from 0.01 M to 0.001 M. About 52 and 35 number of cycles have been obtained at 0.005 and 0.001 M [PA]₀ before the [F⁻] in the effluent water reached the WHO guideline value of 1.5 mg/L. At 0.01 M [PA]₀ the author achieved almost 100% defluoridation up to 23 L and above 90% defluoridation up to 51 L of water per kg of limestone. The fluoride removal significantly increased with [PA]₀ as evident from LSD value 0.25 and p<0.05 as has been found from one-way ANOVA described in the section, 2.3 Statistical Analysis. The results are shown in Table 3.37.

Table. 3.37. The results of one-way analysis of variance of fluoride removal with different $[PA]_0$. $[F^-]_0 = 10$ mg/L and residence time = 3 h.

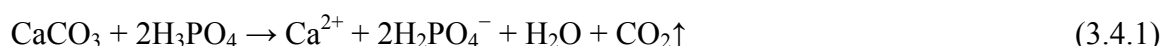
$[PA]_0$ (M)			LSD	p*
0.01	0.005	0.001		
** $[F^-]$ (mg/L)	** $[F^-]$ (mg/L)	** $[F^-]$ (mg/L)	0.25	<0.05
0.29	0.39	0.90		
0.30	0.38	0.88		
0.38	0.37	0.87		

*p- Pearson's correlation is significant at <0.05 level

**The results are average of three experiments

3.4.2 The pH of treated water

The final pH of the PA-limestone treated water was found to be in the ranges of 5.7-7.5, 7.1-7.6 and 7.5-7.8 at 0.01, 0.005 and 0.001 M $[PA]_0$, respectively (Table 3.36 and Figure 3.30). The final pH was found to increase with decreasing $[PA]_0$ from 0.01 M to 0.001 M. The neutralization of acidic water by limestone can be represented by Eq. (3.4.1):



The fluoride removal performance of limestone in presence of 0.01 M $[PA]_0$ was found to be better than that in presence of 0.005 and 0.001 M $[PA]_0$, respectively. However, the final pH of the treated water was slightly low in case of 0.01 M $[PA]_0$ compared to 0.005 and 0.001 M $[PA]_0$. But, the acidic pH can be neutralized through a sand-limestone-sand-gravel filter as shown in Figure 2.1.

3.4.3 Effect of co-existing ions

The author studied the effects of co-existing anions, *viz.*, SO_4^{2-} , NO_3^- , Br^- and Cl^- in the concentration range of 100-500 mg/L on fluoride removal from $[F^-]_0$ of 10 mg/L with $[PA]_0$ of 0.01 M (Figure 3.31). The interference by the competing anions was found to increase in the order: $NO_3^- < Cl^- < Br^- < SO_4^{2-}$. However, the net effect of these ions was negligible unlike in the cases of other edible acids, *viz.*, acetic acid, citric acid and oxalic acid²⁶⁴⁻²⁶⁶ indicating that the selective strong sorption of fluoride by the calcium phosphate or HAP is less affected by these anions.

3.4.4 Mechanism of fluoride removal

The mechanism involved in the present PACLT method was assessed by saturation index, FTIR and XRD analyses.

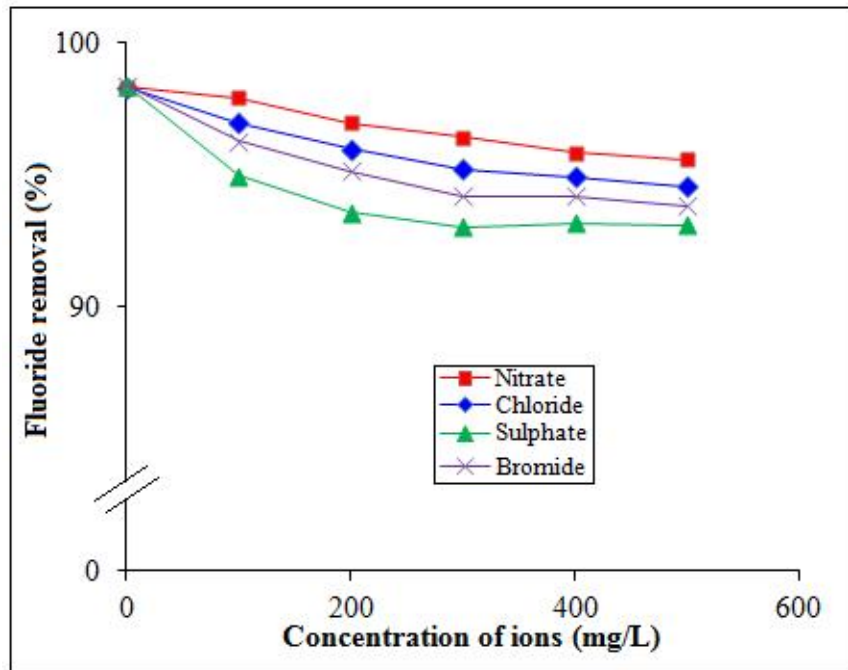


Figure 3.31. Effects of different competing anions on fluoride removal by PACLT in the laboratory-scale pilot experiment with $[F^-]_0 = 10$ mg/L, $[PA]_0 = 0.01$ M and residence time = 3 h.

3.4.4.1 Saturation index

Saturation index (SI) of fluorite (CaF_2) has been evaluated for the pilot test experiments using the Eq. (3.4.2)²⁴⁷.

$$SI_f = \log_{10} (Q/K_{sp}) \quad (3.4.2)$$

where, $Q = (\text{activity of } Ca^{2+})(\text{activity of } F^-)^2$ and K_{sp} is the solubility product of fluorite, 3.5×10^{-11} .

The results of SI of fluorite have been summarized in Table 3.38. The plot of SI of fluorite vs., n at $[PA]_0$ of 0.01 M has been shown in Figure 3.32. The SI of fluorite in the pilot test was negative though the value slightly increased with n . The negative value of SI indicates that sorption is the dominant mechanism for fluoride removal. Fluoride is removed to below 1 mg/L is due to sorption of fluoride in addition to precipitation as precipitation alone can remove fluoride only to below 2 mg/L as limited by the solubility product of CaF_2 ²⁴⁶. However, SI value slightly increased with n is due to a decrease in sorption of fluoride and not due to any increase of the precipitation.

Table 3.38. Results of saturation index of fluorite (SI_f) calculated from $[F^-]$ (mg/L) and calcium ions (mg/L) present in the treated water after treatment by the PACLT in the pilot test. †n = number of cycle or treatment

n [†]	$[F^-]$ (mg/L)	$[Ca^{2+}]$ (mg/L)	SI_f
5	0.008	146.5	-4.68
10	0.04	25.5	-4.09
16	0.46	23	-3.58
18	0.032	57	-3.88
20	0.03	59	-3.90
30	0.05	40	-3.67
32	0.05	56	-3.51
60	0.30	10	-2.78
61	0.25	18	-2.63
63	0.31	13	-2.61
69	0.18	34	-2.62
70	0.20	34	-2.52
80	0.26	18	-2.57
82	0.24	36	-2.34
84	0.26	37	-2.26
90	0.29	49	-2.04
100	0.48	60	-1.50
110	0.65	45	-1.38
120	0.91	28	-1.29
130	0.98	28	-1.23
140	3.20	4.1	-1.04

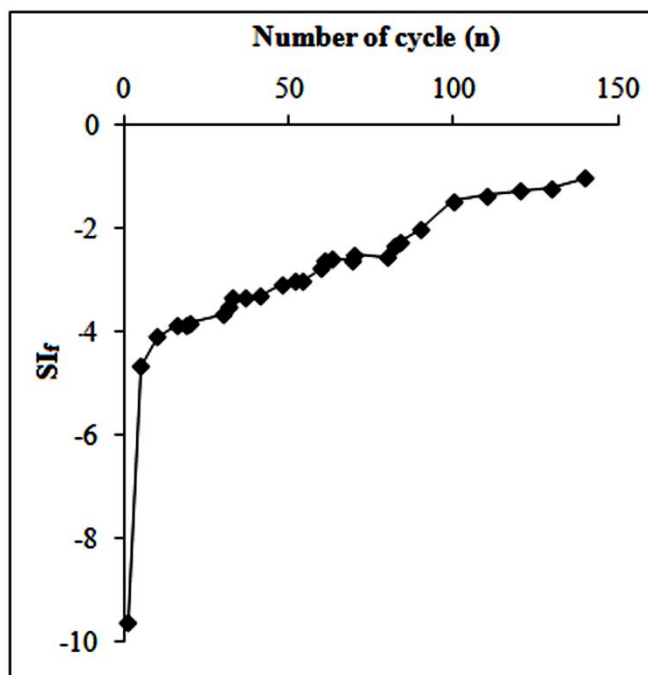


Figure 3.32. Saturation index of fluorite (SI_f) vs. number of cycle (n) for the pilot experiment with $[F^-]_0 = 10$ mg/L and $[PA]_0 = 0.01$ M.

3.4.4.2 FTIR analysis

The FTIR spectra of unused limestone and the precipitate formed in the reactor after PACLT in laboratory-scale pilot test have been shown in Figure 3.33. The main peak positions of the unused crude limestone were found to be at around 1432 cm^{-1} , 1031 cm^{-1} , 874 cm^{-1} and 708 cm^{-1} (Figure 3.33A) which indicates the presence of CaCO_3 . The peaks at around 2365 cm^{-1} correspond to CO_3^{2-} ions³⁰⁶. In the precipitate obtained in the present case, the peaks at around 3571 cm^{-1} and 634 cm^{-1} correspond to the OH stretching frequency¹⁹¹ (3.33B). The characteristic peak around 1634 cm^{-1} is due to adsorbed water. On the other hand, the bands at 1090 cm^{-1} and 978 cm^{-1} are characteristic peaks for PO_4^{3-} group indicate the formation of calcium phosphate or HAP¹⁹². The peak at around 1150 cm^{-1} corresponds to H-PO_4^{2-} stretching²⁹⁸ of HAP. Moreover, a small band appears at 740 cm^{-1} can be attributed to the formation of CaF_2 ²⁹⁹. Thus, the FTIR of the precipitate formed in the reactor after PACLT in laboratory-scale pilot experiment indicates the presence of HAP.

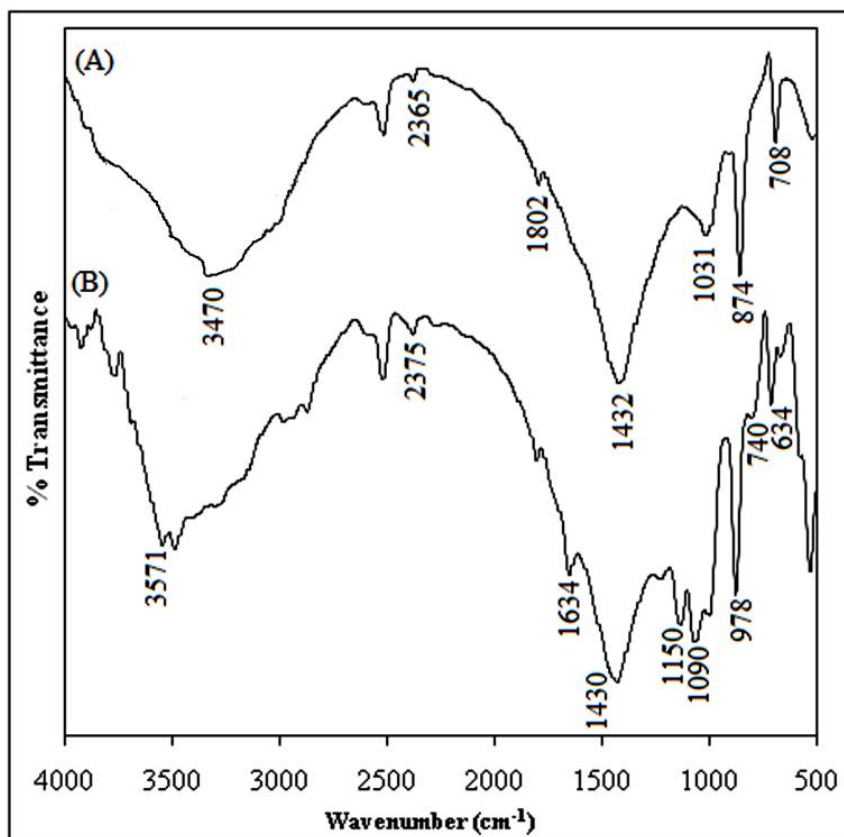


Figure 3.33. The FTIR spectra of (A) unused limestone and (B) precipitate found in bottom of the container after the pilot test. $[\text{F}^-]_0 = 10\text{ mg/L}$, $[\text{PA}]_0 = 0.01\text{ M}$.

3.4.4.3 XRD analysis

The author has studied the XRD spectra of unused limestone and precipitate found after PACLT in batch mode. The spectra are shown in Figure 3.34. The peaks with significant intensities at 29.5° , 36.12° , 39.5° , 43.5° , 47.5° , and 48.5° are corresponding to standard calcite spectra²⁷⁷⁻²⁷⁹ (Figure 3.34A). The XRD spectra of the precipitate show a large increase in the intensity of the peak at around 47° compared to that of fresh limestone which can be attributed to diffraction of plane of fluorite, CaF_2 ³⁰⁰ (Figure 3.34B). The peaks at 26° , 31.7° , and 50° correspond to HAP¹⁹² (JCPDS card no. 89-6438) indicating significant formation of HAP in situ in the reactor by reaction between the phosphate ions of PA and the calcium ions generated by the acid-dissolution of limestone. A small peak at 31.9° can be attributed to diffraction from plane of fluorhydroxyapatite (FAP)¹⁹² (JCPDS card no. 87-2462). Thus, the XRD analysis indicates a partial damage of the calcite crystalline structure during the PACLT in batch mode and the presence of CaCO_3 , HAP, FAP and a small amount of CaF_2 in the precipitate formed in the process³¹³.

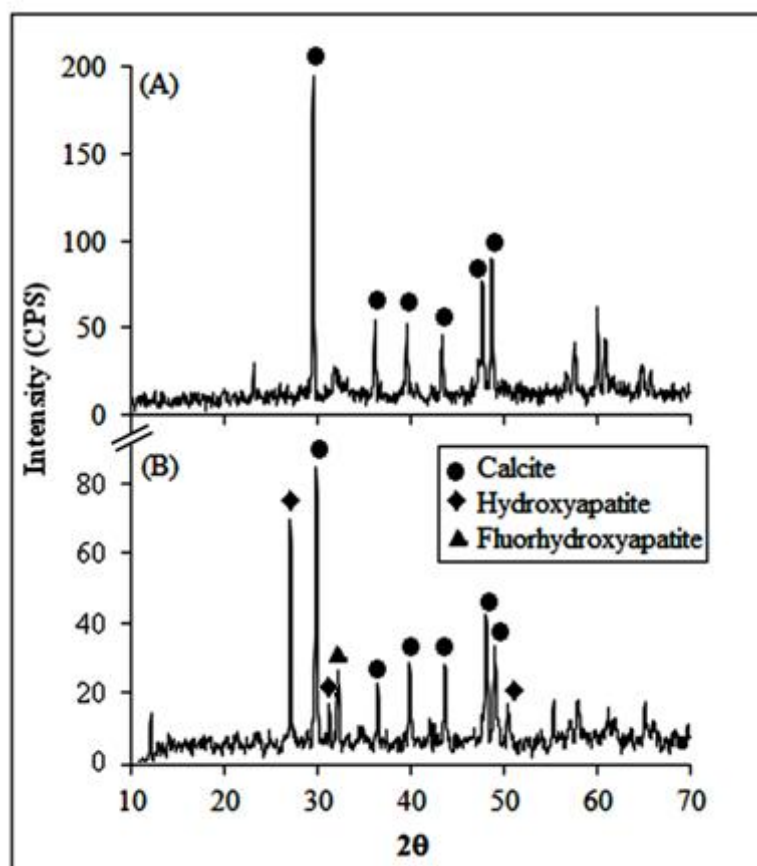
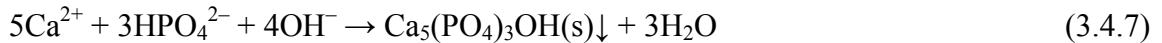
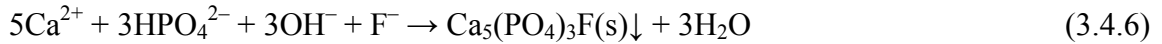


Figure 3.34. The XRD spectra of (A) unused limestone and (B) precipitate found in the container after the pilot test. $[\text{F}^-]_0 = 10 \text{ mg/L}$, $[\text{PA}]_0 = 0.01 \text{ M}$.

3.4.5 The schematic mechanism of PACLT method

The following reaction scheme may describe the major mechanism of fluoride removal in the PACLT:



Although both H_2PO_4^- ($\text{pK}_{\text{a}2} = 7.21$) and HPO_4^{2-} ($\text{pK}_{\text{a}3} = 12.35$) are present in the pH range of treated water, the former dominates below pH 7.21 and the reaction in Eq. (3.4.4) is significant only above pH 6.21. The reactions of dissolution of CaCO_3 by the triprotic PA (H_3PO_4 , $\text{pK}_{\text{a}1} = 2.12$), Eq. (3.4.3), the precipitation of CaF_2 , Eq. (3.4.5) and the precipitation of calcium phosphate fluoride (fluorapatite, FAP) and calcium phosphate hydroxide (hydroxyapatite, HAP), Eq. (3.4.6&7) are completed rapidly. Precipitation of FAP should be preferred over precipitation of HAP due to lower solubility product of FAP than that of HAP^{260, 314}. However, a high abundance of hydroxide ion in the system is also expected to precipitate HAP. The sorption or exchange of the remaining fluoride by the calcium phosphates, Eq. (3.4.8) probably continues for a longer time and completed in about 3 h as indicated by the continued increase in the fluoride removal till about 3 h. The neutralization of H_2CO_3 ($\text{pK}_{\text{a}1} = 6.35$) is probably rather slow and continues beyond 24 h as indicated by slow increase in the pH. Finally it can be stated that a dominant defluoridation through sorption of fluoride by HAP, formed in situ, in addition to the precipitation of CaF_2 , and sorption of fluoride by limestone makes the PACLT highly efficient.

3.4.6 Regeneration of used limestone

The activity of used limestone giving less than 80% removal from 10 mg/L in the pilot test, was regenerated by three different ways: (i) simple scrubbing, (ii) soaking in 0.30 M $\text{Ca}(\text{OH})_2$ for 24 h and (iii) soaking in 0.03 M NaOH for 24 h followed by rinsing with water. The results of the pilot test with 10 mg/L $[\text{F}^-]_0$ and 0.01 M $[\text{PA}]_0$ using regenerated limestone are shown in Table 3.39 and Figure 3.35.

Table 3.39. Results of remaining $[F^-]$ (mg/L) and final pH of water after treatment in the pilot test using regenerated limestone regenerated by using $Ca(OH)_2$, NaOH and by simply scrubbing and rinsing treatment.* $[PA]_0 = 0.01$ M; $[F^-]_0 = 10$ mg/L.

n [†]	Ca(OH) ₂ (M)		NaOH (M)		Rinsing & scrubbing	
	[F ⁻] (mg/L)	pH	[F ⁻] (mg/L)	pH	[F ⁻] (mg/L)	pH
1	1.30	6.65	2.20	6.98	0.25	6.02
2	0.55	6.91	0.51	7.69	0.31	6.22
3	0.34	7.07	0.28	7.65	0.48	6.17
4	0.26	6.91	0.06	7.37	0.53	6.10
5	0.18	7.21	0.35	7.21	0.62	6.00
6	0.05	7.25	0.22	7.18	0.73	6.00
7	0.21	7.22	0.32	7.13	0.59	6.05
8	0.38	7.26	0.34	7.12	0.63	6.10
9	0.23	7.29	0.25	7.11	0.71	5.97
10	0.19	6.40	0.15	6.68	0.71	5.95
11	0.16	6.13	0.21	6.52	0.62	5.94
12	0.19	6.12	0.27	6.45	0.58	5.93
13	0.32	6.02	0.42	6.42	0.59	5.94
14	0.47	5.76	0.32	6.52	0.54	5.92
15	0.48	5.66	0.33	6.41	0.52	5.90
16	0.49	5.68	0.35	6.48	0.51	5.92
17	0.38	5.64	0.38	6.52	0.5	5.93
18	0.47	6.03	0.32	6.12	0.48	5.91
19	0.54	5.91	0.41	6.21	0.47	5.92
20	0.59	5.81	0.45	6.20	0.45	5.94
21	0.62	6.25	0.50	6.17	0.42	5.95
22	0.67	6.01	0.58	6.15	0.44	5.97
23	0.68	5.64	0.82	6.14	0.42	5.94
24	0.51	5.67	0.76	6.12	0.45	5.97
25	0.52	5.68	0.74	6.09	0.64	5.92
26	0.55	5.65	0.75	6.00	0.64	5.87
27	0.57	5.63	0.70	6.08	0.65	5.88
28	0.61	5.64	0.67	6.07	0.63	5.89
29	0.67	5.62	0.59	6.05	0.67	5.80
30	0.71	5.61	0.52	6.04	0.64	5.82
31	0.72	5.62	0.50	6.03	0.65	5.80
32	0.73	5.63	0.43	6.02	0.66	5.80
33	0.81	5.62	0.43	5.96	0.67	5.79
34	0.83	5.61	0.52	5.94	0.68	5.77
35	0.85	5.6	0.62	5.91	0.69	5.74
36	0.87	5.61	0.69	5.90	0.70	5.72
37	0.87	5.62	0.71	5.89	0.70	5.77
38	0.88	5.61	0.75	5.89	0.80	5.79
39	0.95	5.62	0.74	5.87	0.80	5.78
40	0.96	5.63	0.73	5.84	0.82	5.77
41	0.97	5.63	0.74	5.86	0.83	5.62

Continued to the next page-

Continued from the previous page-

n [†]	Ca(OH) ₂ (M)		NaOH (M)		Rinsing & scrubbing	
	[F ⁻] (mg/L)	pH	[F ⁻] (mg/L)	pH	[F ⁻] (mg/L)	pH
42	0.98	5.64	0.76	5.85	0.84	5.60
43	0.98	5.62	0.77	5.84	0.85	5.50
44	0.58	5.59	0.79	5.82	0.86	5.51
45	0.56	5.58	0.78	5.80	0.87	5.49
46	0.57	5.50	0.77	5.84	0.89	5.46
47	0.64	5.40	0.79	5.82	0.90	5.44
48	0.67	5.41	0.80	5.80	0.90	5.40
49	0.69	5.42	0.81	5.79	0.92	5.42
50	0.70	5.43	0.80	5.74	0.95	5.41
51	0.74	5.40	0.78	5.74	0.71	5.43
52	0.77	5.41	0.79	5.67	0.81	5.45
53	0.80	5.39	0.81	5.65	0.82	5.47
54	0.81	5.38	0.86	5.64	0.87	5.49
55	0.82	5.41	0.87	5.55	0.90	5.50
56	0.83	5.42	0.86	5.53	0.93	5.57
57	0.85	5.42	0.86	5.50	0.96	5.58
58	0.87	5.43	0.92	5.48	0.98	5.57
59	0.88	5.38	0.95	5.51	1.70	5.42
60	0.89	5.39	1.20	5.54	1.70	5.40
61	0.94	5.31	1.30	5.48	1.80	5.35
62	1.34	5.31	1.40	5.46	1.90	5.31
63	1.37	5.32	1.50	5.43	2.00	5.32
64	1.38	5.33	1.60	5.42	2.00	5.30
65	1.49	5.34	1.60	5.41	3.80**	5.30
66	1.47	5.33	1.70	5.40		
67	1.45	5.31	1.80	5.32		
68	1.50	5.32	1.90	5.31		
69	1.40	5.29	2.50	5.23		
70	1.40	5.22	3.70**	5.21		
71	1.40	5.23				
72	1.50	5.22				
73	1.65	5.21				
74	1.90	5.20				
75	2.20	5.21				
76	2.30	5.18				
77	2.50	5.17				
78	2.60	5.16				
79	2.60	5.14				
80	2.71	5.15				
81	3.90**	5.11				

*Error limits: [F⁻] = ±0.2 mg/L and pH = ±0.1

**Discontinued due to poor fluoride removal

[†]n = number of cycle or treatment

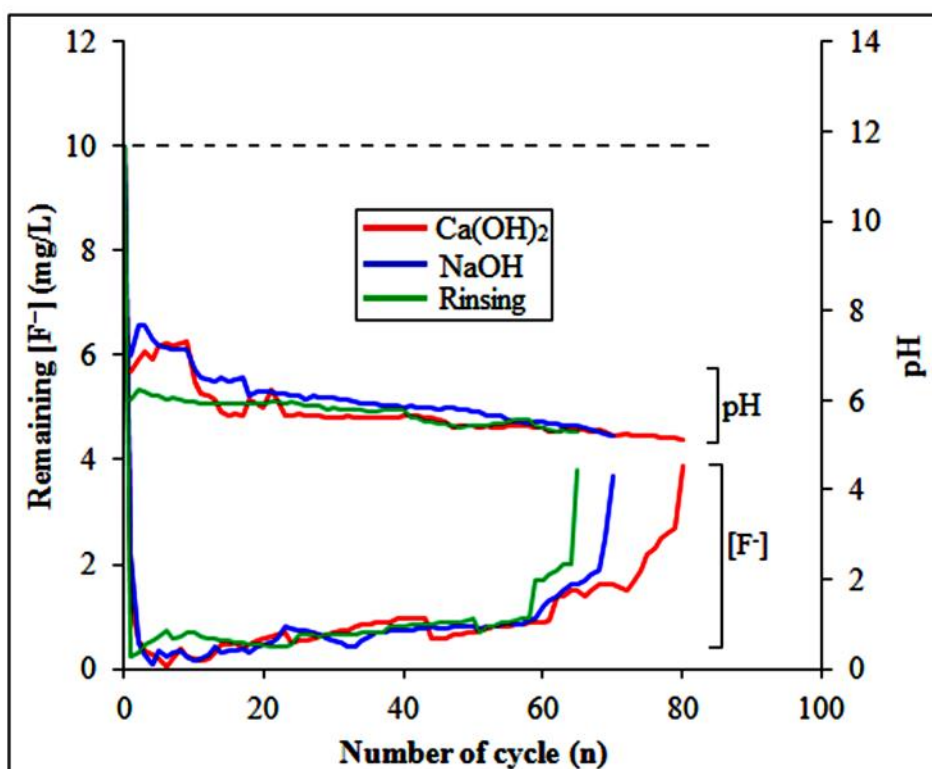


Figure 3.35. Remaining $[F^-]$ (mg/L) and final pH of water after PACLT pilot test by reusing limestone regenerated by soaking in 0.30 M $Ca(OH)_2$ and NaOH and by simply scrubbing and rinsing. $[F^-]_0 = 10$ mg/L (shown by horizontal dotted line) and $[PA]_0 = 0.01$ M.

Interestingly, the regenerated limestone obtained by all three methods showed almost equal ($\approx 50\%$) regeneration of activity. The weight loss of limestone during the regeneration by scrubbing and rinsing was $\approx 5\%$. The regeneration by simple scrubbing and rinsing may be preferable as it gives competitive results without using any chemical.

3.4.7 Suitability analysis

The suitability was analyzed in terms of safety of the process, capacity of limestone and the cost of the process.

3.4.7.1 Safety

For safety assessment, the final pH, the potability with respect to the relevant water quality parameters and disposal of the sludge were considered.

3.4.7.1.1 Other water quality parameters of treated water

The water quality parameters of the treated water samples before and after PACLT treatment in laboratory-scale pilot study were determined using standard methods³¹². The results are presented in Table 3.40. All the water quality parameters after treatment were within the respective WHO guideline values for drinking water⁴⁹. The concentrations of most of the metal ions decreased after treatment. The lower concentrations of Ca^{2+} and PO_4^{3-} are expected from low solubility product of calcium phosphate. The PACLT is unlikely to increase microorganism in the water as the water is treated with an acid.

Table 3.40. The relevant water quality parameters of water before and after treatment in the PACLT in laboratory-scale pilot study. $[\text{PA}]_0 = 0.01\text{M}$; $[\text{F}^-]_0 = 10 \text{ mg/L}$ and residence time = 3 h.

Parameter in mg/L except for pH	WHO guideline value	Before treatment	After treatment
pH	6.50-8.50 ^a	7.47	5.7-7.5
Dissolved solid	600	132	149
Suspended solid	NS ^b	12	6
Total alkalinity as CaCO_3	200	80	86
Total hardness as CaCO_3	200	82	84
Sulphate	500	6.7	6.0
Phosphate	NS	0.71	0.80
Nitrate	50	0.59	0.24
Cadmium	0.003	0.001	<0.001
Calcium	50	2.50	<50*
Chromium	0.05	ND ^c	ND
Cobalt	NS	ND	ND
Copper	2.0	1.00	1.10
Lead	0.01	ND	ND
Magnesium	NS	2.4	2.9
Manganese	0.40	0.10	0.08
Zinc	3.0	2.3	0.09
Sodium	200	62.6	62.0
Potassium	NS	1.2	ND
Iron	0.30	0.36	0.09

^aAcceptable range for drinking, ^bNS: Not specified, ^cND: Not detectable

*Average value

3.4.7.1.2 Toxicity characteristic leaching procedure (TCLP) test

A toxicity characteristic leaching procedure (TCLP) test was performed on the precipitate obtained from the PACLT using a standard method²⁹⁵. The method showed <0.4 mg/L fluoride in the leachate which is much below than the maximum permissible level 150 mg/L for disposal at land-fill³⁰⁹. The used limestone may be used in cement manufacturing or in construction of roads. Lastly, PA is easily acceptable to people as it is an edible acid and a common ingredient in many popular beverages. Thus, the PACLT is a safe method.

3.4.7.2 Capacity

The capacity and cost have been estimated from the laboratory-scale pilot test. With 50% recovery of the limestone during regeneration, a total of 106 L of water can be defluoridated per kg of limestone, which gives a capacity of limestone in the PACLT as 1.01 mg/g. This capacity is as such better than the capacity of 0.39 mg/g reported for limestone alone¹¹² and comparable to that reported for activated alumina (1.08 mg/g) (Maliyekkal et al.¹¹⁸), activated carbon (1.10 mg/g) (Ramos et al.³¹⁵) and bone char (1.4 mg/g) (Dahi and Nielsen²²⁴). The capacity of limestone in the present case has been found to be lower than that of HAP nanoparticles (5.5 mg/g) (Poiner et al.¹⁹²). However, the practical fluoride removal capacity of limestone obtained from the present pilot study cannot be compared as such with the ideal monolayer adsorption capacities of the adsorbents available in the literature^{112, 118, 192, 224, 315}. However, there are scopes for increasing the capacity through process optimization, e.g., using still lower $[PA]_0$ in the beginning, stepwise increase of the dose of $[PA]_0$, further crushing of the limestone chips after use, etc.

3.4.7.3 Cost estimation

The cost of limestone is INR 1822 (US\$ \approx 27) per metric ton. Taking the fluoride removal capacity of limestone as 1.01 mg/g, the cost of limestone for fluoride removal from 10 mg/L to \leq 1 mg/L at 0.01 M PA, has been estimated as INR 0.014 (US\$ \approx 0.00021) per liter of treated water. Using the market price of PA as INR 37 (US\$ \approx 0.55) per liter, the cost for PA has been calculated as INR 0.025 (US\$ \approx 0.00037) per liter when used at 0.01M PA. This gives an overall recurring cost for the PACLT to remove fluoride

from 10 mg/L to below 1 mg/L at 0.01 M [PA]₀ as INR 0.04 (US\$ 0.00058) per litre of water which is indeed very good. An additional sand-limestone-gravel filter for correction of pH and removing Fe, Mn and SS will add a little to the recurring cost. This estimated overall recurring cost of PACLT is much lower than that of AELD with acetic acid INR 0.81 (US\$ 0.012), citric acid INR 3.24 (US\$ 0.048) and oxalic acid INR 9.37 (US\$ 0.139) per litre of water and may be further improved through process optimization. The recurring cost of the present method is however slightly greater than INR 0.03 (US\$ 0.00041) per litre estimated for the PACLT in continuous-flow mode.

Interestingly, the author does not observed any clogging during the laboratory-scale pilot tests as was reported²⁴¹ which make the laboratory-scale pilot test suitable for the PACLT. Such a process is preferable for rural applications over a continuous-flow process which requires more sophistication and power for regulating flow of water.

3.4.8 Summary

The findings of the pilot test can be summarised as follows:

- Addition of dilute PA to the influent water before treatment with crushed limestone efficiently removes fluoride from water. Fluoride removal from initial fluoride concentrations of 10 mg/L to about 0.01-1.0 mg/L along with near neutral pH of the treated water has been achieved with 0.01 M [PA]₀ in 3 h. The performance of PA in the PACLT has been found to be much better than that of other edible acids, *viz.*, acetic acid, citric acid and oxalic acid, reported earlier.
- The exhausted limestone can be regenerated by simple scrubbing and rinsing with water and by lime or NaOH solution treatment. All the three regeneration methods show about 50% regeneration of the activity of the used limestone.
- All relevant water quality parameters including pH of the treated water remain within the acceptable range and/or the WHO guideline values for drinking water.
- The present study also indicates sorption of fluoride by HAP produced in the reactor as the dominant mechanism of fluoride removal while precipitation of FAP and CaF₂, and sorption of fluoride by limestone also contribute to the fluoride removal.

- Addition of PA increases the fluoride removal capacity of limestone from 0.39 to 1.01 mg/g. The recurring cost has been estimated as INR 0.04 (US\$ 0.00058) per litre of treated water.
- Finally, the present laboratory-scale pilot test clearly demonstrates the PACLT technique as an efficient, low-cost, safe, environment-friendly and simple technique with great potential for rural application for fluoride removal from contaminated water.

3.5 Field study of fluoride removal by phosphoric acid-crushed limestone treatment:

Fluoride Nilogon

The promising results of the laboratory scale pilot test of the phosphoric acid-crushed limestone treatment (PACLT) in plug-flow mode has justified a field trial of the method. The method was named as '*Fluoride Nilogon*' ('*Nilogon*' for removal in Assamese) for better acceptability by user. The field trial was started in a phased manner at six sites. This included one small community unit with 220 L water holding capacity at Dengaon and five household units with 15 L capacity each at five different sites, viz., Napakling, Kehang Inglang, Sarik Teron and Kat Tisso villages in Bagpani area in Karbi Anglong district of Assam, India. At Dengaon, the drinking water supplied by the Public Health Engineering Department (PHED) was also found to have excess fluoride of 4.8 mg/L. Most people in the Bagpani area have been using groundwater for drinking from hand tube wells contaminated with excess fluoride up to 20 mg/L. The author noticed moderate to severe dental fluorosis in the people in these areas. Prior to starting the field units, the author had carried out a PA-dose optimization in the laboratory with fluoride containing groundwater from field source using a replica of the proposed field units as described in section, 2.4.5.2 *Methods of fluoride removal from groundwater model unit*. The author has also carried out experiments using the replica to pre-assess the performances of the field units under the field conditions. The results of the dose optimization, pre-assessment of the field units and the field trial have been presented here.

3.5.1 Optimization of PA dose

The fluoride removal from fluoride containing groundwater collected from field source having 4.8 mg/L fluoride has been examined at 0.001 M [PA]₀ in the feed. Results of fluoride removal vs. number of cycle (n) used have been shown in Table 3.41. The fluoride removal was found to be somewhat poor initially but started to increase after 10 cycles of use and excellent after 16 cycles (Figure 3.36). The observed initial slightly poor fluoride removal may be attributed to a possible presence of CaO impurity in the limestone and a higher alkalinity of the field water compared to synthetic groundwater.

The factors were not strong enough to influence the fluoride removal at higher initial PA concentration described in the section 3.4.1 *The fluoride removal performance* in the pilot test. The alkalinity (as CaCO₃) in the field water sample was 150 mg/L whereas that of the synthetic groundwater was 80 mg/L. Due to the presence of high alkalinity, a part of PA is neutralized and become unavailable for contributing to fluoride removal. The presence of slightly higher concentrations of sulphate (60 mg/L) and chloride (20 mg/L) ions in the field water than that of sulphate (6.7 mg/L) and chloride (5 mg/L) ions in the synthetic water did not have any noticeable influence on the fluoride removal. The author did not observe any initial poor fluoride removal at higher [PA]₀ (e.g., 0.01M) of the feed during the pilot test as can be seen in Figure 3.30 of the pilot test results. Therefore, it was decided to pre-treat the crushed limestone bed with 0.01 M [PA]₀ before using lower dose of feed PA.

Table. 3.41. Remaining [F⁻] and final pH of the water after treatment by the replica unit using field water containing 4.8 mg/L initial [F⁻].

n	[PA] ₀ = 0.001 M	
	[F ⁻] (mg/L)	pH
1	2.10	6.46
2	1.80	6.66
3	1.30	6.69
4	1.10	6.68
5	0.89	6.68
6	0.89	6.69
7	0.89	6.62
8	0.89	6.84
9	0.89	6.87
10	0.89	6.89
11	0.75	6.89
12	0.58	6.99
13	0.47	6.99
14	0.33	6.89
15	0.23	6.84
16	0.21	6.84
17	0.15	6.83
18	0.12	6.82
19	0.11	6.83
20	0.11	6.82

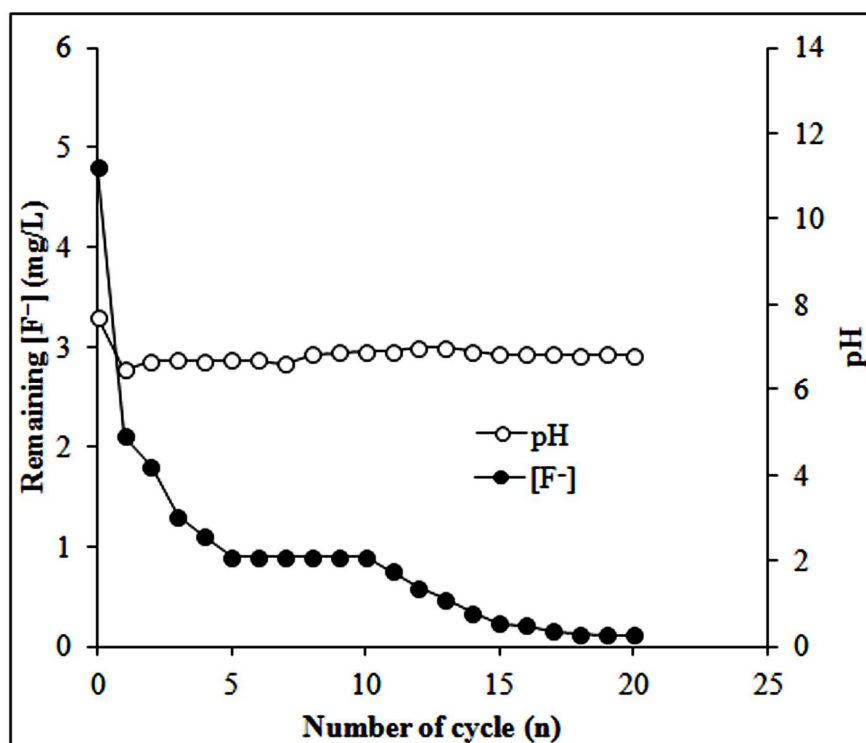


Figure 3.36. Plots of remaining $[F^-]$ with pH vs. number of cycle (n) used in PACLT for fluoride removal in the replica unit from field water with 0.001 M $[PA]_0$. $[F^-]_0 = 4.8 \pm 0.2$ mg/L.

Fluoride removal by the replica unit with the field water ($[F^-]_0 = 4.8 \pm 0.2$ mg/L) was also studied with varying $[PA]_0$ in order to determine the optimum $[PA]_0$ dose for the field trial. For this experiment the limestone bed of 1.0-1.5 cm chip size was pre-treated with 0.01 M PA initially to neutralise any lime (CaO) present with limestone. Then fluoride removal from the field water by the replica unit was measured at varying $[PA]_0$ in the range from 0.01 M to 0.5 mM. The results are shown in Table 3.42 and Figure 3.37. In presence of 0.01 M $[PA]_0$, fluoride is removed from initial 4.8 mg/L to final 0.01 mg/L which is much below the WHO guideline value. Such a low concentration of fluoride in drinking water may have some negative effects on tooth such as tooth carries for which the WHO have suggested fluoridation of around 0.5-1.0 mg/L for water deficient in fluoride⁴². On lowering $[PA]_0$ from 0.01 M to 0.7 mM, the effluent fluoride concentration slowly increased from 0.01 mg/L to 0.41 mg/L, still well below the fluoridation value. On further decreasing the $[PA]_0$ to 0.6 mM also gave a higher effluent fluoride concentration of 0.91 mg/L. Therefore, a $[PA]_0$ concentration of 0.68 mM, which

gave the effluent $[F^-]$ of 0.65 mg/L, was chosen as the optimum initial concentration of PA for the field trial.

Table 3.42. Remaining $[F^-]$, initial pH (pH_0) of water pre-acidified with different $[PA]_0$ and final pH (pH_f) of the treated water after treatment in the replica unit including the four layered filter with field water having 4.8 ± 0.2 mg/L of $[F^-]_0$.

$[PA]_0$ (mM)	$[F^-]$ (mg/L)	pH_0	pH_f
10	0.85	2.34	6.27
10	0.01	2.34	6.27
7.0	0.30	2.55	6.31
5.0	0.39	2.94	6.32
3.5	0.38	3.60	6.65
3.0	0.39	4.56	6.68
2.5	0.38	5.12	6.91
1.0	0.39	5.59	6.98
0.70	0.41	5.79	6.99
0.68	0.65	5.89	7.16
0.60	0.91	6.22	7.45
0.50	1.60	6.45	7.74

Error limits: $[F^-] = \pm 0.2$ mg/L and $pH = \pm 0.1$

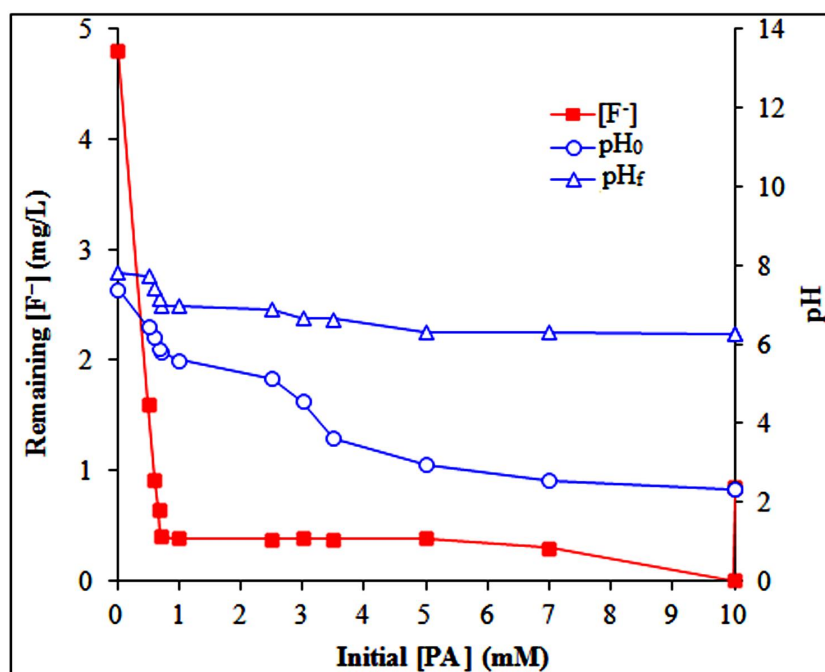


Figure 3.37. Plots of remaining $[F^-]$ and pH of water before (pH_0) and after (pH_f) treatment in presence of varying $[PA]_0$ in the replica unit with field water having 4.8 ± 0.2 mg/L of $[F^-]_0$.

3.5.1.1 Influence of pH on fluoride removal

The pH of the water, before and after the treatment, has also been included in Table 3.42 and Figure 3.37 for $[PA]_0$ in the range of 0.01 M to 0.5 mM. The initial pH of the feed water gradually increased from 2.34 to 5.89 on decreasing $[PA]_0$ from 0.01 M to 0.68 mM. The pH increased after the treatment with limestone and the four layered sand-limestone-sand-gravel filter (Figure 2.3.a). However, the effluent pH was below 6.5, the minimum acceptable limit for drinking water, with $[PA]_0$ in the range of 0.01 M to 5.0 mM. The effluent pH increased above 6.5 at $[PA]_0$ of 3.5 mM and below. Influent water with $[PA]_0$ of 0.6 mM and below (with an initial pH of 6.22 and above) also showed high effluent fluoride concentration to 0.91 mg/L and higher. An initial PA concentration of 0.68 mM gave both effluent fluoride concentration and pH suitable for drinking water and therefore this optimum initial PA concentration was chosen for the subsequent studies of the PACLT in the field.

3.5.2 Pre-assessment of limestone capacity

The results of the experiment with the replica unit for a pre-assessment of the capacity of limestone for the field groundwater are shown in Table 3.43 and Figure 3.38. These results were for the treated water after four layered sand-limestone-sand-gravel filtration in the replica unit. A higher concentration of $[PA]_0 = 0.01$ M was used in the first two cycles in order to neutralize the possible CaO impurities of limestone. In the first cycle the effluent fluoride and pH were found to be 0.81 mg/L and 6.01, respectively. In the second cycle the effluent fluoride concentration became 0.29 mg/L which was lower than desired and the pH was 6.12 which was below the acceptable range for drinking.

The optimized $[PA]_0$ of 0.68 mM was used from the third cycle onwards. The effluent fluoride concentration as well as the effluent pH gradually improved with number of cycles and soon settled at 0.66 ± 0.2 mg/L and 7.6 ± 0.2 , respectively. The effluent fluoride concentration and the pH remained so consistently up to 250 cycles giving 83 L defluoridated water per kg of limestone. A breakthrough was observed after 250 cycles. Overall, the performance of the replica unit with water from the field source has been found to be much better than that observed in the laboratory-pilot test which may be attributed to the lower $[F^-]_0$ (4.8 mg/L) of the field water in the present case than 10 mg/L in the pilot test.

Table 3.43. Remaining $[F^-]$ (in mg/L) and final pH of the water after treatment in the replica unit. * $[F^-]_0 = 4.8 \pm 0.2$ mg/L; $[PA]_0 = 0.68$ mM and residence time = 3 h.

n^\dagger	$[F^-]$ (mg/L)	pH	n^\dagger	$[F^-]$ (mg/L)	pH	n^\dagger	$[F^-]$ (mg/L)	pH
1	0.81	6.01	44	0.74	7.58	87	0.72	7.74
2	0.29	6.12	45	0.75	7.58	88	0.73	7.75
3	0.65	7.45	46	0.77	7.58	89	0.72	7.75
4	0.65	7.45	47	0.78	7.58	90	0.70	7.75
5	0.46	7.51	48	0.77	7.61	91	0.69	7.71
6	0.63	7.52	49	0.78	7.61	92	0.72	7.72
7	0.77	7.55	50	0.79	7.62	93	0.71	7.72
8	0.67	7.54	51	0.79	7.63	94	0.72	7.72
9	0.68	7.54	52	0.80	7.63	95	0.73	7.72
10	0.69	7.54	53	0.81	7.64	96	0.73	7.72
11	0.70	7.55	54	0.82	7.64	97	0.72	7.73
12	0.74	7.55	55	0.83	7.65	98	0.72	7.73
13	0.75	7.54	56	0.81	7.65	99	0.73	7.73
14	0.80	7.59	57	0.82	7.66	100	0.71	7.72
15	0.78	7.48	58	0.83	7.67	101	0.72	7.71
16	0.76	7.49	59	0.84	7.67	102	0.70	7.72
17	0.75	7.48	60	0.79	7.67	103	0.71	7.72
18	0.75	7.47	61	0.79	7.67	104	0.72	7.72
19	0.74	7.47	62	0.80	7.68	105	0.73	7.72
20	0.74	7.46	63	0.81	7.68	106	0.75	7.73
21	0.65	7.45	64	0.82	7.68	107	0.76	7.73
22	0.64	7.51	65	0.83	7.64	108	0.77	7.73
23	0.65	7.54	66	0.81	7.54	109	0.78	7.74
24	0.67	7.54	67	0.82	7.64	110	0.80	7.72
25	0.68	7.54	68	0.83	7.65	111	0.80	7.72
26	0.69	7.51	69	0.84	7.65	112	0.79	7.72
27	0.70	7.52	70	0.84	7.65	113	0.80	7.72
28	0.71	7.55	71	0.80	7.66	114	0.72	7.72
29	0.72	7.59	72	0.83	7.67	115	0.73	7.72
30	0.73	7.58	73	0.82	7.67	116	0.72	7.72
31	0.74	7.59	74	0.81	7.68	117	0.70	7.72
32	0.65	7.59	75	0.80	7.69	118	0.69	7.71
33	0.67	7.59	76	0.75	7.79	119	0.72	7.72
34	0.65	7.58	77	0.78	7.79	120	0.71	7.75
35	0.64	7.59	78	0.79	7.75	121	0.72	7.76
36	0.65	7.59	79	0.70	7.75	122	0.73	7.77
37	0.67	7.59	80	0.72	7.78	123	0.73	7.78
38	0.68	7.59	81	0.74	7.73	124	0.72	7.78
39	0.69	7.56	82	0.73	7.74	125	0.72	7.78
40	0.70	7.57	83	0.72	7.74	126	0.73	7.78
41	0.71	7.57	84	0.71	7.74	127	0.71	7.77
42	0.72	7.57	85	0.70	7.75	128	0.80	7.79
43	0.73	7.57	86	0.71	7.75	129	0.72	7.78

Continued to the next page-

Continued from the previous page-

n [†]	[F ⁻] (mg/L)	pH	n [†]	[F ⁻] (mg/L)	pH	n [†]	[F ⁻] (mg/L)	pH
130	0.73	7.79	172	0.67	7.78	214	0.86	7.72
131	0.72	7.74	173	0.68	7.78	215	0.85	7.72
132	0.70	7.71	174	0.67	7.74	216	0.86	7.69
133	0.69	7.71	175	0.65	7.73	217	0.86	7.72
134	0.79	7.71	176	0.68	7.73	218	0.86	7.72
135	0.75	7.71	177	0.68	7.72	219	0.86	7.72
136	0.75	7.72	178	0.69	7.72	220	0.85	7.72
137	0.74	7.72	179	0.71	7.72	221	0.85	7.73
138	0.73	7.72	180	0.72	7.71	222	0.86	7.71
139	0.72	7.73	181	0.73	7.72	223	0.86	7.69
140	0.71	7.73	182	0.72	7.75	224	0.87	7.71
141	0.70	7.74	183	0.73	7.76	225	0.86	7.72
142	0.71	7.75	184	0.72	7.77	226	0.86	7.72
143	0.70	7.75	185	0.74	7.78	227	0.83	7.72
144	0.72	7.75	186	0.73	7.78	228	0.84	7.69
145	0.70	7.76	187	0.77	7.72	229	0.85	7.72
146	0.70	7.77	188	0.78	7.72	230	0.85	7.72
147	0.71	7.78	189	0.75	7.73	231	0.85	7.69
148	0.72	7.78	190	0.77	7.73	232	0.86	7.65
149	0.73	7.78	191	0.78	7.73	233	0.86	7.75
150	0.74	7.74	192	0.78	7.74	234	0.85	7.76
151	0.75	7.73	193	0.77	7.72	235	0.86	7.77
152	0.71	7.74	194	0.76	7.72	236	0.86	7.78
153	0.70	7.74	195	0.77	7.72	237	0.83	7.78
154	0.72	7.74	196	0.75	7.72	238	0.84	7.71
155	0.70	7.74	197	0.75	7.72	239	0.85	7.71
156	0.70	7.75	198	0.76	7.76	240	0.85	7.71
157	0.71	7.75	199	0.77	7.77	241	0.86	7.71
158	0.72	7.75	200	0.78	7.78	242	0.85	7.72
159	0.73	7.76	201	0.79	7.69	243	0.86	7.72
160	0.74	7.76	202	0.79	7.72	244	0.86	7.72
161	0.75	7.77	203	0.80	7.72	245	0.85	7.73
162	0.74	7.77	204	0.81	7.72	246	0.85	7.73
163	0.73	7.77	205	0.82	7.72	247	0.85	7.72
164	0.72	7.78	206	0.82	7.73	248	0.86	7.77
165	0.73	7.78	207	0.83	7.72	249	0.85	7.72
166	0.73	7.65	208	0.83	7.72	250	1.11	7.69
167	0.72	7.75	209	0.84	7.72	251	1.90	7.65
168	0.71	7.76	210	0.85	7.72	252	2.10	7.78
169	0.70	7.77	211	0.85	7.71	253	2.51	7.77
170	0.72	7.78	212	0.85	7.72	254	2.82	7.72
171	0.69	7.78	213	0.86	7.72	255	3.13**	7.78

*Error limits: [F⁻] = ±0.2 mg/L and pH = ±0.1

**Discontinued due to poor fluoride removal

†n = number of cycle or treatment

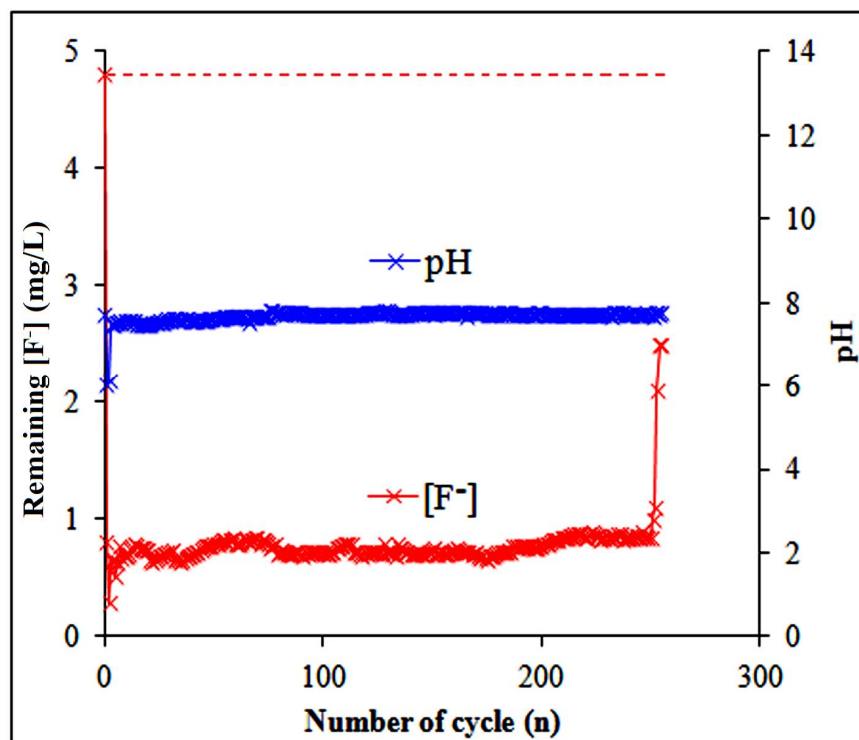


Figure 3.38. Plots of $[F^-]$ and pH of the treated water vs. n in the replica unit. $[F^-]_0 = 4.8$ mg/L (shown by horizontal dotted line), $[PA]_0 = 0.68$ mM and residence time = 3 h.

3.5.3 Regeneration of used limestone

The author regenerated the exhausted limestone obtained from the pre-assessment experiment with the replica unit. The regeneration was done by two ways, i.e., soaking in 0.30 M $\text{Ca}(\text{OH})_2$ solution and simple scrubbing followed by rinsing with water. The results are shown in Table 3.44A and 3.44B and Figure 3.39. Regeneration was not done with NaOH solution as it gave almost same results with $\text{Ca}(\text{OH})_2$. The limestone regenerated with $\text{Ca}(\text{OH})_2$ treatment and by simple scrubbing and rinsing showed showed about 57% and 45% regeneration of activity, respectively. The activity of regenerated limestone gradually decreased with repeated regeneration. Though regenerated limestone gave better results in $\text{Ca}(\text{OH})_2$ treatment, simple scrubbing and rinsing treatment has been considered preferable as it does not require any chemicals.

Table 3.44A. $[F^-]$ and pH of treated water treated in the replica unit using limestone regenerated with $Ca(OH)_2$ up to three times. * $[F^-]_0 = 4.8$ mg/L; $[PA]_0 = 0.68$ mM and residence time = 3 h.

n [†]	Regeneration cycle					
	1 st		2 nd		3 rd	
	$[F^-]$ (mg/L)	pH	$[F^-]$ (mg/L)	pH	$[F^-]$ (mg/L)	pH
1	0.85	7.83	0.89	7.75	0.94	7.70
2	0.52	7.85	0.90	7.75	0.87	7.74
3	0.67	7.80	0.62	7.76	0.76	7.74
4	0.69	7.79	0.67	7.76	0.74	7.74
5	0.70	7.79	0.68	7.76	0.73	7.74
6	0.71	7.79	0.72	7.76	0.74	7.74
7	0.65	7.79	0.75	7.76	0.77	7.74
8	0.68	7.78	0.76	7.77	0.78	7.74
9	0.71	7.78	0.77	7.77	0.76	7.74
10	0.69	7.78	0.78	7.75	0.77	7.74
11	0.68	7.78	0.77	7.76	0.76	7.74
12	0.65	7.78	0.76	7.76	0.74	7.73
13	0.66	7.78	0.75	7.76	0.73	7.73
14	0.67	7.78	0.74	7.77	0.74	7.72
15	0.65	7.78	0.73	7.70	0.75	7.72
16	0.66	7.77	0.74	7.69	0.76	7.72
17	0.67	7.76	0.73	7.65	0.77	7.72
18	0.71	7.76	0.75	7.61	0.75	7.71
19	0.72	7.76	0.74	7.60	0.74	7.65
20	0.73	7.76	0.76	7.54	0.71	7.62
21	0.74	7.76	0.77	7.54	0.70	7.61
22	0.73	7.76	0.78	7.32	0.75	7.61
23	0.72	7.76	0.77	7.32	0.77	7.52
24	0.71	7.75	0.76	7.32	0.76	7.51
25	0.70	7.74	0.71	7.32	0.78	7.47
26	0.72	7.74	0.72	7.32	0.77	7.41
27	0.73	7.74	0.73	7.32	0.74	7.40
28	0.74	7.74	0.74	7.33	0.76	7.39
29	0.72	7.75	0.73	7.34	0.74	7.34
30	0.71	7.75	0.72	7.33	0.85	7.33
31	0.70	7.75	0.73	7.33	1.20	7.32
32	0.71	7.75	0.74	7.33	1.50	7.28
33	0.72	7.75	0.75	7.33	2.10	7.28
34	0.73	7.75	0.72	7.30	2.50**	7.28

Continued to the next page-

Continued from the previous page-

n [†]	1 st		2 nd		3 rd	
	[F ⁻] (mg/L)	pH	[F ⁻] (mg/L)	pH	[F ⁻] (mg/L)	pH
35	0.74	7.74	0.73	7.31		
36	0.73	7.74	0.74	7.31		
37	0.72	7.74	0.75	7.31		
38	0.71	7.73	0.76	7.32		
39	0.72	7.73	0.77	7.32		
40	0.73	7.73	0.74	7.32		
41	0.74	7.72	0.75	7.32		
42	0.72	7.72	0.77	7.33		
43	0.71	7.73	0.76	7.32		
44	0.70	7.70	0.74	7.32		
45	0.75	7.74	0.75	7.31		
46	0.72	7.74	0.73	7.32		
47	0.73	7.7	0.72	7.32		
48	0.71	7.74	0.69	7.32		
49	0.70	7.74	0.73	7.32		
50	0.72	7.74	0.74	7.31		
51	0.74	7.74	0.75	7.31		
52	0.75	7.74	0.76	7.32		
53	0.74	7.74	0.75	7.31		
54	0.71	7.74	0.74	7.32		
55	0.73	7.75	0.73	7.32		
56	0.71	7.75	0.74	7.31		
57	0.72	7.75	0.75	7.31		
58	0.69	7.75	0.74	7.31		
59	0.71	7.74	0.76	7.31		
60	0.74	7.74	0.75	7.30		
61	0.75	7.74	0.76	7.29		
62	0.71	7.74	0.74	7.29		
63	0.72	7.74	0.75	7.29		
64	0.73	7.74	0.76	7.31		
65	0.75	7.75	0.77	7.29		
66	0.76	7.74	0.78	7.29		
67	0.71	7.74	0.79	7.29		
68	0.70	7.74	0.76	7.29		
69	0.72	7.74	0.78	7.29		
70	0.73	7.74	0.77	7.29		
71	0.74	7.73	0.74	7.29		
72	0.71	7.74	0.76	7.29		
73	0.69	7.74	0.77	7.29		
74	0.72	7.74	0.76	7.28		
75	0.75	7.74	0.79	7.28		

Continued to the next page-

Continued from the previous page-

n [†]	1 st		2 nd		3 rd	
	[F ⁻] (mg/L)	pH	[F ⁻] (mg/L)	pH	[F ⁻] (mg/L)	pH
76	0.76	7.73	0.84	7.27		
77	0.77	7.73	0.92	7.27		
78	0.75	7.73	1.50	7.27		
79	0.76	7.73	2.50	7.27		
80	0.74	7.73	2.80**	7.26		
81	0.72	7.73				
82	0.73	7.73				
83	0.74	7.73				
84	0.75	7.73				
85	0.78	7.72				
86	0.75	7.73				
87	0.76	7.73				
88	0.78	7.73				
89	0.77	7.73				
90	0.79	7.73				
91	0.75	7.73				
92	0.76	7.73				
93	0.77	7.74				
94	0.74	7.73				
95	0.78	7.73				
96	0.77	7.75				
97	0.76	7.73				
98	0.77	7.73				
99	0.75	7.73				
100	0.79	7.73				
101	0.78	7.73				
102	0.77	7.73				
103	0.76	7.73				
104	0.65	7.72				
105	0.62	7.72				
106	0.64	7.72				
107	0.65	7.69				
108	0.63	7.64				
109	0.71	7.63				
110	0.75	7.63				
111	0.74	7.64				
112	0.71	7.64				
113	0.70	7.63				
114	0.69	7.63				
115	0.68	7.63				
116	0.69	7.63				

Continued to the next page-

Continued from the previous page-

n [†]	1 st		2 nd		3 rd	
	[F ⁻] (mg/L)	pH	[F ⁻] (mg/L)	pH	[F ⁻] (mg/L)	pH
117	0.67	7.63				
118	0.68	7.63				
119	0.69	7.62				
120	0.71	7.62				
121	0.72	7.61				
122	0.73	7.61				
123	0.72	7.58				
124	0.75	7.56				
125	0.78	7.54				
126	0.77	7.54				
127	0.76	7.54				
128	0.75	7.51				
129	0.76	7.51				
130	0.77	7.51				
131	0.78	7.51				
132	0.79	7.53				
133	0.80	7.53				
134	0.81	7.54				
135	0.80	7.55				
136	0.82	7.54				
138	0.87	7.54				
139	0.89	7.47				
140	0.82	7.43				
141	0.85	7.41				
142	0.90	7.41				
143	1.50	7.41				
144	1.60	7.40				
145	1.70	7.40				
146	1.80	7.41				
147	1.90	7.41				
148	2.00	7.41				
149	2.10	7.39				
150	2.10	7.41				
151	2.20	7.40				
152	2.30	7.41				
153	2.40	7.40				
154	2.42	7.40				
155	2.50**	7.40				

*Error limits: [F⁻] = ±0.2 mg/L and pH = ±0.1

**Discontinued due to poor fluoride removal;

†n = number of cycle or treatment

Table 3.44B. Remaining $[F^-]$ (in mg/L) and final pH of treated water after reusing limestone regenerated by scrubbing and rinsing with water up to three times after completion of each cycle in the PACLT method. * $[F^-]_0 = 4.8 \pm 0.2$ mg/L; $[PA]_0 = 0.68$ mM and residence time = 3 h.

n [†]	Regeneration cycle					
	1 st		2 nd		3 rd	
	$[F^-]$ (mg/L)	pH	$[F^-]$ (mg/L)	pH	$[F^-]$ (mg/L)	pH
1	0.99	7.74	0.87	7.54	0.86	7.27
2	0.89	7.68	0.84	7.54	0.84	7.27
3	0.86	7.69	0.83	7.53	0.82	7.27
4	0.84	7.68	0.82	7.53	0.80	7.27
5	0.76	7.68	0.81	7.54	0.85	7.27
6	0.75	7.68	0.79	7.54	0.75	7.27
7	0.76	7.68	0.75	7.54	0.74	7.26
8	0.78	7.68	0.76	7.54	0.73	7.25
9	0.72	7.68	0.74	7.54	0.70	7.25
10	0.82	7.68	0.79	7.56	0.74	7.25
11	0.84	7.68	0.76	7.56	0.72	7.25
12	0.86	7.68	0.77	7.59	0.7	7.24
13	0.75	7.68	0.74	7.59	0.73	7.24
14	0.75	7.67	0.72	7.59	0.72	7.24
15	0.72	7.67	0.73	7.59	0.71	7.24
16	0.71	7.67	0.72	7.58	0.74	7.24
17	0.70	7.67	0.74	7.56	0.72	7.24
18	0.69	7.67	0.75	7.56	0.65	7.23
19	0.75	7.67	0.69	7.56	0.62	7.23
20	0.81	7.67	0.62	7.56	0.69	7.23
21	0.82	7.67	0.68	7.56	0.72	7.24
22	0.76	7.67	0.67	7.56	0.73	7.24
23	0.79	7.67	0.65	7.56	0.74	7.24
24	0.75	7.67	0.64	7.56	0.71	7.24
25	0.76	7.67	0.62	7.56	0.75	7.23
26	0.78	7.67	0.63	7.56	0.84	7.24
27	0.77	7.67	0.62	7.56	0.82	7.24
28	0.76	7.67	0.64	7.54	0.79	7.24
29	0.75	7.67	0.63	7.54	0.92	7.24
30	0.75	7.67	0.64	7.54	1.50	7.24
31	0.72	7.65	0.61	7.54	2.50	7.24
32	0.56	7.56	0.59	7.54	3.10**	7.23
33	0.58	7.56	0.55	7.54		
34	0.59	7.56	0.58	7.54		
35	0.62	7.56	0.59	7.54		

Continued to the next page-

Continued from the previous page-

n [†]	1 st		2 nd		3 rd	
	[F ⁻] (mg/L)	pH	[F ⁻] (mg/L)	pH	[F ⁻] (mg/L)	pH
36	0.64	7.56	0.62	7.54		
37	0.67	7.54	0.64	7.54		
38	0.68	7.54	0.62	7.54		
39	0.69	7.54	0.67	7.54		
40	0.72	7.54	0.69	7.54		
41	0.75	7.54	0.71	7.48		
42	0.74	7.54	0.72	7.48		
43	0.72	7.54	0.74	7.47		
44	0.73	7.54	0.69	7.46		
45	0.74	7.54	0.73	7.47		
46	0.73	7.54	0.75	7.48		
47	0.71	7.54	0.81	7.49		
48	0.76	7.54	0.84	7.48		
49	0.74	7.54	0.89	7.47		
50	0.72	7.67	0.85	7.48		
51	0.75	7.67	0.71	7.48		
52	0.72	7.67	0.78	7.48		
53	0.74	7.67	0.79	7.49		
54	0.69	7.67	0.81	7.49		
55	0.68	7.67	0.89	7.49		
56	0.65	7.67	1.50	7.34		
57	0.64	7.67	2.50	7.34		
58	0.62	7.67	3.10**	7.34		
59	0.63	7.67				
60	0.65	7.67				
61	0.67	7.67				
62	0.69	7.56				
63	0.68	7.56				
64	0.67	7.54				
65	0.64	7.54				
66	0.65	7.54				
67	0.64	7.54				
68	0.63	7.54				
69	0.62	7.54				
70	0.74	7.54				
71	0.71	7.54				
72	0.73	7.54				
73	0.75	7.54				
74	0.74	7.54				
75	0.71	7.54				
76	0.69	7.54				
77	0.68	7.67				

Continued to the next page-

Continued from the previous page-

n [†]	1 st		2 nd		3 rd	
	[F ⁻] (mg/L)	pH	[F ⁻] (mg/L)	pH	[F ⁻] (mg/L)	pH
78	0.65	7.67				
79	0.67	7.67				
80	0.75	7.67				
81	0.74	7.67				
82	0.73	7.67				
83	0.72	7.67				
84	0.76	7.67				
85	0.75	7.67				
86	0.74	7.67				
87	0.76	7.67				
88	0.77	7.56				
89	0.73	7.56				
90	0.73	7.54				
91	0.74	7.54				
92	0.72	7.54				
93	0.78	7.54				
94	0.79	7.54				
95	0.69	7.54				
96	0.71	7.54				
97	0.74	7.54				
98	0.75	7.54				
99	0.72	7.53				
100	0.77	7.53				
101	0.75	7.52				
102	0.74	7.56				
103	0.69	7.48				
104	0.68	7.47				
105	0.67	7.46				
106	0.66	7.46				
107	0.69	7.46				
108	0.89	7.45				
109	0.94	7.35				
110	1.50	7.32				
111	2.10	7.33				
112	2.50	7.32				
113	3.10**	7.32				

*Error limits: [F⁻] = ±0.2 mg/L and pH = ±0.1

**Discontinued due to poor fluoride removal

†n = number of cycle or treatment

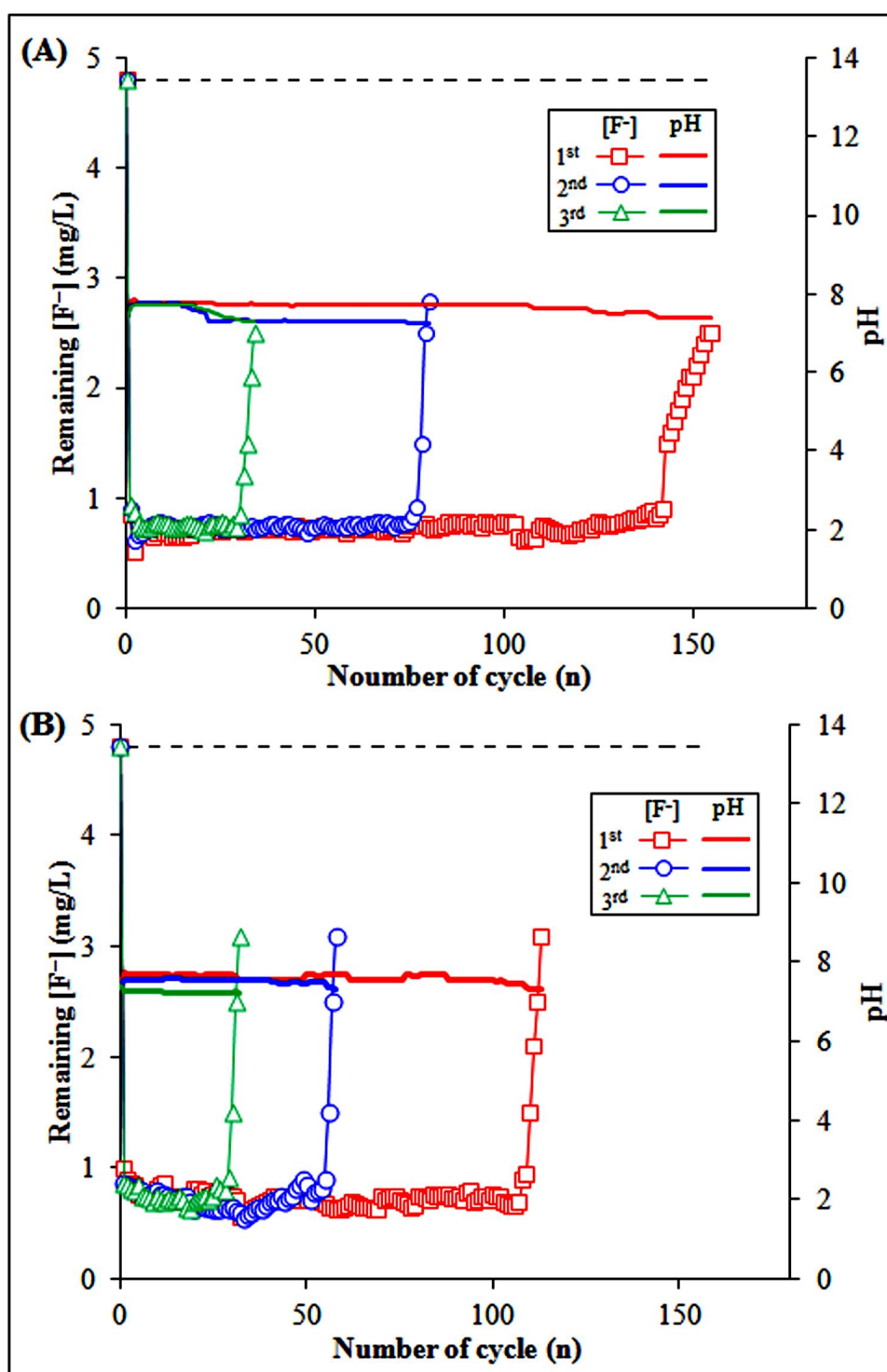


Figure 3.39. $[F^-]$ and pH of treated water vs. number of cycle (n) used in the replica unit after 1st, 2nd and 3rd regeneration of limestone: (A) with 0.30 M $Ca(OH)_2$ and (B) by scrubbing and rinsing. $[F^-]_0 = 4.8$ mg/L (dotted line) and $[PA]_0 = 0.68$ mM.

3.5.4 Performance of the small community unit

The 500 L food grade plastic reactor used in the small community unit, started on 16 March 2013 at Dengaon, Karbi Anglong, had a pore volume (water holding capacity) of 220 L. It was filled with crushed limestone of size 0.2 to 2.0 cm. This size range was chosen for practical reasons acceptable for the users. The first cycle treatment was done with feed water having 0.01 M of $[PA]_0$. A feed $[PA]_0$ of 0.68 mM was used for all subsequent cycles of treatments. PA purchased for the field trial was 85% W/V. The author supplied a ten times diluted, i.e., 8.5% (1.47 M) PA to the villagers for safety reason. The dose of PA to give 0.68 M initial PA concentration in 220 L was calculated as 101.8 mL. The author used a positively rounded dose of 105 mL instead of 101.8 mL. The residence time in the reactor was 3 h. The first 220 L water filled the pore volume of the four layered filter and so remained within the filter. Treated water could be collected from the filter only from the second cycle onwards. The treated water therefore had an actual residence time of at least 6 h. The water is used by three families for drinking and cooking purposes regularly since the beginning till date. They have been doing the treatment (dosing) on their own without any difficulty. They also have been collecting the treated water sample after each and every use and giving to us for evaluation and monitoring purposes. The results of fluoride removal and the final pH of water after treatment and filtration through the four layered filter in the small community unit are shown in Table 3.45 and Figure 3.40.

The effluent fluoride concentration have been found to be 0.65 ± 0.2 mg/L right from the first cycle up to a total of 270 cycles treated till date (9 March 2016). Remaining fluoride concentration is in close conformity to 0.7 mg/L, the WHO prescribed range for fluoridation of fluoride deficient water⁴². The fluoride removal performance of the small community unit of the PACLT in the plug-flow mode in the field has been found to be better than that predicted from the replica test. The observed better performance of the field unit than that of the replica unit can be attributed to smaller particle size of limestone, i.e., 0.2 to 2.0 cm used in the field trial experiment. Crushed limestone chips of 1.0-1.5 cm size range was used in the laboratory replica test as it was started before facing the practical difficulty of choosing a narrow size range. The lowering the particle size of limestone increases its effective surface area of limestone increasing the capacity of fluoride removal. It is expected to continue for some more cycles till the breakthrough point.

Table 3.45. Remaining $[F^-]$ and final pH in the water after treatment in small community unit. * $[F^-]_0 = 4.8 \pm 0.2$ mg/L; $[PA]_0 = 0.68$ mM and residence time = 3 h.

n [†]	$[F^-]$ (mg/L)	pH	n [†]	$[F^-]$ (mg/L)	pH	n [†]	$[F^-]$ (mg/L)	pH
1	0.79	6.15	46	0.72	7.77	91	0.84	7.78
2	0.57	7.21	47	0.75	7.76	92	0.74	7.80
3	0.64	7.20	48	0.79	7.78	93	0.75	7.82
4	0.65	7.25	49	0.77	7.78	94	0.77	7.82
5	0.68	7.22	50	0.78	7.78	95	0.76	7.82
6	0.54	7.64	51	0.64	7.74	96	0.78	7.83
7	0.55	7.74	52	0.70	7.78	97	0.75	7.83
8	0.54	7.70	53	0.72	7.77	98	0.74	7.82
9	0.56	7.79	54	0.74	7.76	99	0.78	7.83
10	0.54	7.77	55	0.75	7.78	100	0.76	7.83
11	0.55	7.89	56	0.78	7.77	101	0.75	7.82
12	0.57	7.86	57	0.76	7.78	102	0.77	7.80
13	0.57	7.81	58	0.73	7.75	103	0.78	7.81
14	0.55	7.89	59	0.77	7.78	104	0.80	7.81
15	0.52	7.84	60	0.79	7.80	105	0.81	7.79
16	0.50	7.85	61	0.78	7.80	106	0.80	7.82
17	0.54	7.79	62	0.80	7.77	107	0.79	7.78
18	0.57	7.81	63	0.81	7.77	108	0.80	7.79
19	0.62	7.71	64	0.79	7.87	109	0.81	7.82
20	0.64	7.63	65	0.71	7.84	110	0.82	7.78
21	0.54	7.73	66	0.78	7.78	111	0.83	7.79
22	0.56	7.75	67	0.75	7.80	112	0.84	7.78
23	0.54	7.78	68	0.80	7.82	113	0.81	7.78
24	0.55	7.79	69	0.81	7.79	114	0.80	7.83
25	0.57	7.81	70	0.83	7.79	115	0.80	7.83
26	0.57	7.77	71	0.85	7.80	116	0.79	7.84
27	0.55	7.75	72	0.80	7.90	117	0.77	7.78
28	0.52	7.78	73	0.82	7.85	118	0.75	7.79
29	0.45	7.79	74	0.81	7.75	119	0.74	7.78
30	0.54	7.81	75	0.80	7.75	120	0.74	7.78
31	0.57	7.91	76	0.79	7.77	121	0.76	7.81
32	0.62	7.73	77	0.80	7.78	122	0.77	7.97
33	0.64	7.87	78	0.83	7.74	123	0.78	7.84
34	0.67	7.91	79	0.82	7.82	124	0.79	7.82
35	0.52	7.75	80	0.81	7.81	125	0.80	7.83
36	0.50	7.74	81	0.83	7.97	126	0.80	7.84
37	0.65	7.75	82	0.82	7.84	127	0.81	7.78
38	0.57	7.74	83	0.80	7.82	128	0.82	7.79
39	0.62	7.76	84	0.78	7.83	129	0.83	7.78
40	0.64	7.73	85	0.79	7.84	130	0.82	7.78
41	0.70	7.75	86	0.77	7.78	131	0.84	7.78
42	0.77	7.78	87	0.79	7.79	132	0.83	7.79
43	0.80	7.76	88	0.81	7.78	133	0.82	7.78
44	0.79	7.76	89	0.85	7.78	134	0.81	7.78
45	0.70	7.77	90	0.83	7.78	135	0.82	7.75

Continued to the next page-

Continued from the previous page-

n [†]	[F ⁻] (mg/L)	pH	n [†]	[F ⁻] (mg/L)	pH	n [†]	[F ⁻] (mg/L)	pH
136	0.84	7.81	181	0.69	7.79	226	0.65	7.81
137	0.81	7.97	182	0.70	7.78	227	0.64	7.97
138	0.83	7.84	183	0.72	7.78	228	0.63	7.84
139	0.82	7.82	184	0.71	7.81	229	0.62	7.82
140	0.83	7.83	185	0.69	7.97	230	0.61	7.83
141	0.80	7.84	186	0.68	7.84	231	0.64	7.84
142	0.75	7.78	187	0.71	7.75	232	0.62	7.78
143	0.65	7.79	188	0.70	7.79	233	0.71	7.79
144	0.61	7.78	189	0.72	7.78	234	0.69	7.78
145	0.58	7.78	190	0.71	7.78	235	0.68	7.78
146	0.75	7.81	191	0.73	7.81	236	0.71	7.81
147	0.65	7.97	192	0.71	7.97	237	0.70	7.97
148	0.61	7.84	193	0.70	7.84	238	0.72	7.84
149	0.58	7.82	194	0.69	7.75	239	0.71	7.82
150	0.67	7.83	195	0.65	7.74	240	0.73	7.83
151	0.68	7.84	196	0.64	7.75	241	0.67	7.79
152	0.67	7.78	197	0.65	7.76	242	0.69	7.78
153	0.69	7.79	198	0.71	7.74	243	0.71	7.84
154	0.67	7.78	199	0.72	7.78	244	0.70	7.80
155	0.65	7.78	200	0.65	7.79	245	0.74	7.78
156	0.61	7.81	201	0.64	7.81	246	0.75	7.77
157	0.52	7.97	202	0.64	7.77	247	0.66	7.75
158	0.54	7.84	203	0.65	7.75	248	0.72	7.78
159	0.57	7.82	204	0.64	7.78	249	0.74	7.79
160	0.61	7.83	205	0.63	7.79	250	0.68	7.79
161	0.67	7.84	206	0.62	7.81	251	0.54	7.77
162	0.68	7.78	207	0.61	7.91	252	0.63	7.79
163	0.67	7.79	208	0.64	7.73	253	0.67	7.80
164	0.69	7.78	209	0.62	7.87	254	0.64	7.70
165	0.67	7.78	210	0.61	7.91	255	0.62	7.76
166	0.71	7.81	211	0.63	7.75	256	0.65	7.78
167	0.72	7.97	212	0.62	7.74	257	0.66	7.77
168	0.73	7.84	213	0.64	7.74	258	0.68	7.78
169	0.71	7.82	214	0.61	7.75	259	0.67	7.79
170	0.69	7.83	215	0.70	7.76	260	0.70	7.77
171	0.70	7.84	216	0.68	7.74	261	0.69	7.80
172	0.72	7.78	217	0.68	7.78	262	0.69	7.81
173	0.74	7.79	218	0.75	7.75	263	0.58	7.74
174	0.71	7.78	219	0.73	7.82	264	0.65	7.74
175	0.72	7.78	220	0.65	7.83	265	0.69	7.77
176	0.75	7.78	221	0.71	7.84	266	0.68	7.74
177	0.67	7.79	222	0.72	7.78	267	0.65	7.73
178	0.64	7.78	223	0.65	7.79	268	0.69	7.74
179	0.62	7.78	224	0.64	7.78	269	0.64	7.75
180	0.67	7.78	225	0.64	7.78	270	0.63	7.76

*Error limits: [F⁻] = ±0.2 mg/L and pH = ±0.1.[†]n = number of cycle or treatment.[#]The unit is still continuing without regeneration as the limestone is not yet exhausted.

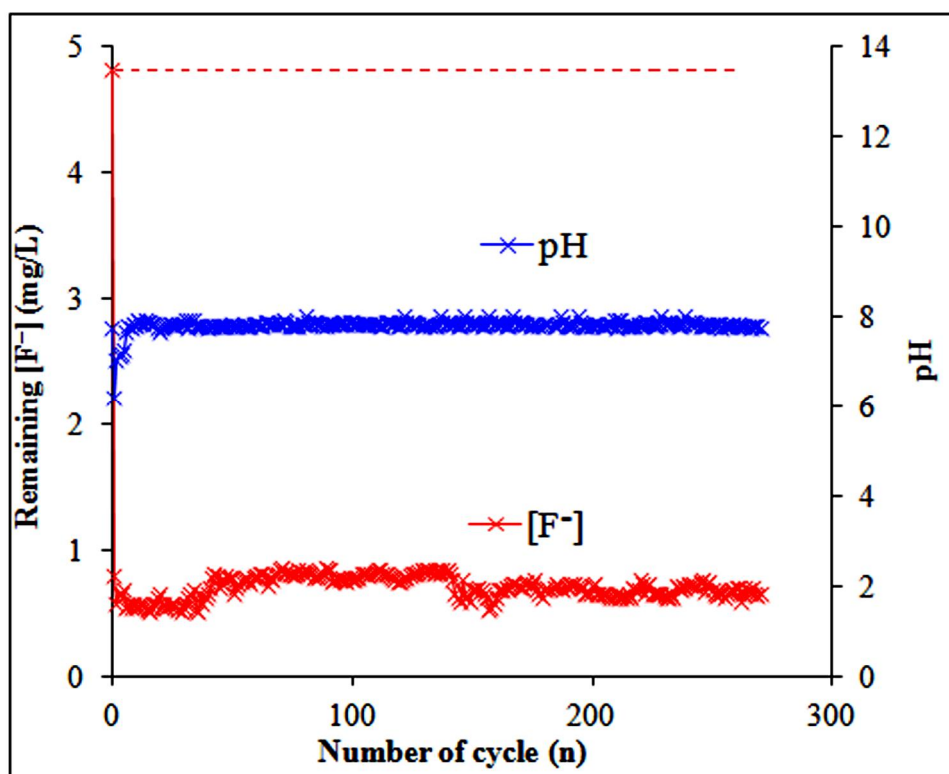


Figure 3.40. Plots of $[F^-]$ and pH in the treated water vs. n for the small community unit. $[F^-]_0 = 4.8$ mg/L (shown by horizontal dotted line); $[PA]_0 = 0.68$ mM and residence time = 3 h. The unit is still continuing as the limestone is not yet exhausted.

The pH of the field water was 7.40. The pH of the water after the first cycle, measured after the filtration with the four layered filter, was found to be 6.15. The final effluent pH after the filtration observed from second cycle of treatment was 7.2. The pH slightly increased after the subsequent treatments and soon settled in the range between 7.6 and 7.9 in a range acceptable for drinking. Such variations in the effluent pH within ± 0.3 and also in the effluent $[F^-]$ within ± 0.2 mg/L can be attributed to neutralization of possible CaO impurities present in the limestone. On continuous use of the limestone the limestone surface is continuously renewed exposing different amounts of CaO impurities every cycle. This difference may lead to the small variations in the effluent $[F^-]$ and pH.

The unit is still continuing without needing regeneration of limestone. It was initially planned at least to see how long the limestone works before becoming exhausted, which was expected around $n = 250$. However, the unit has been giving consistent results even after $n = 270$ without showing any indication of the limestone getting exhausted. Therefore, the author has been forced to be content with reporting in this thesis the

performance of the small community unit till the last possible date, i.e., 9 March 2016 instead of waiting till exhaustion of the limestone.

3.5.5 Performance of the domestic units

The results of effluent fluoride and the final pH of water after treatment and filtration through four layered filters for the households units with 15 L water holding capacity (pore volume) installed by us at the villages of Napakling (H1), Kehang Inglang (H2), Sarik Teron (H3) and Kat Tisso (H4) are shown in Table 3.46 and Figure 3.41. The results of another household unit installed at the village of Napakling (H5) by a villager, trained by us at Tezpur University, has also been included in Table 3.46 and Figure 3.41. H1 was started on 12 October 2014, H2, H3 and H4 were started on 6 December 2014 and H5 was started on 15 October 2015. The $[F^-]_0$ of the groundwater of sources H1, H2, H3, H4 and H5, which were all hand tube wells, were 5.0, 20, 2.8, 5.2 and 4.2 mg/L, respectively.

The author performed the treatment in the domestic units following the same procedure as was done in the small community unit. The calculated dose of 8.5% PA, provided to the users, required for 15 L of water was 6.94 mL. However, for convenience the author has decided to round it positively at 7 mL and instructed the users to add that quantity of acid for every use. The residence time of water in the limestone reactor was 3 h.

The results from all five domestic units have been given in Table 3.46. The units showed effluent fluoride concentration data and pH data within the ranges of 0.50-0.80 mg/L and 7.4-7.7, respectively. While the effluent fluoride concentrations are in close conformity with the WHO prescribed value for fluoridation of fluoride deficient drinking water, the effluent pH is almost in the middle of the acceptable range for drinking water. It is very interesting to note the consistency of the fluoride removal and the effluent pH data obtained from all five domestic units (Figure 3.41).

The average values of effluent $[F^-]$ and pH obtained from community and five household systems are also presented in Table 3.47. The average values were calculated considering all data collected till date. From the table it can be seen that in C1, H1, H2, H3, H4 and H5 units, where the $[F^-]_0$ were 4.8, 5.0, 20, 2.8, 5.2 and 4.2 mg/L, respectively showed average effluent $[F^-]$ as 0.70, 0.62, 0.59, 0.55, 0.67 and 0.62 mg/L, respectively.

Table 3.46. $[F^-]$ and pH of water after treatment in the five households units, H1 (started on 12 October 2014); H2, H3 and H4 (started on 6 December 2014); and H5 (started on 15 October 2015).*^ψ

H1								
n [†]	$[F^-]$ (mg/L)	pH	n [†]	$[F^-]$ (mg/L)	pH	n [†]	$[F^-]$ (mg/L)	pH
3	0.69	7.60	39	0.61	7.61	75	0.61	7.71
6	0.72	7.61	42	0.63	7.71	78	0.63	7.69
9	0.71	7.71	45	0.64	7.69	81	0.64	7.61
12	0.70	7.69	48	0.64	7.61	84	0.64	7.62
15	0.69	7.61	51	0.62	7.62	87	0.62	7.64
18	0.71	7.71	54	0.68	7.69	90	0.63	7.64
21	0.54	7.69	57	0.67	7.61	93	0.62	7.65
24	0.52	7.61	60	0.59	7.62	96	0.67	7.66
27	0.59	7.62	63	0.61	7.61	99	0.68	7.65
30	0.61	7.64	66	0.61	7.66	102	0.70	7.67
33	0.62	7.71	69	0.62	7.69	105	0.69#	7.66
36	0.65	7.69	72	0.65	7.61			
H2								
n [†]	$[F^-]$ (mg/L)	pH	n [†]	$[F^-]$ (mg/L)	pH	n [†]	$[F^-]$ (mg/L)	pH
3	0.85	7.54	39	0.61	7.71	72	0.58	7.71
6	0.62	7.64	42	0.59	7.69	75	0.57	7.69
9	0.54	7.65	45	0.58	7.61	78	0.63	7.68
12	0.61	7.64	48	0.57	7.62	81	0.64	7.69
15	0.65	7.65	51	0.54	7.64	84	0.54	7.67
18	0.64	7.65	54	0.52	7.71	87	0.56	7.66
21	0.63	7.65	57	0.61	7.62	90	0.52	7.68
24	0.62	7.66	60	0.64	7.64	93	0.51	7.69
27	0.62	7.66	63	0.59	7.71	96	0.58#	7.66
33	0.64	7.69	66	0.61	7.69			
36	0.59	7.61	69	0.59	7.61			
H3								
n [†]	$[F^-]$ (mg/L)	pH	n [†]	$[F^-]$ (mg/L)	pH	n [†]	$[F^-]$ (mg/L)	pH
3	0.72	7.51	57	0.51	7.43	111	0.52	7.42
6	0.68	7.55	60	0.54	7.44	114	0.54	7.43
9	0.71	7.58	63	0.53	7.41	117	0.52	7.42
12	0.62	7.45	66	0.52	7.45	120	0.50	7.43
15	0.60	7.45	69	0.54	7.45	123	0.49	7.41
18	0.59	7.42	72	0.52	7.42	126	0.48	7.41
21	0.65	7.43	75	0.50	7.43	129	0.54	7.45
24	0.67	7.43	78	0.49	7.42	132	0.55	7.46
27	0.68	7.44	81	0.48	7.43	135	0.60	7.44
30	0.66	7.41	84	0.61	7.43	138	0.64	7.46
33	0.54	7.41	87	0.62	7.44	141	0.63	7.43
36	0.62	7.51	90	0.59	7.41	144	0.64	7.46
39	0.58	7.55	93	0.62	7.41	147	0.62	7.45
42	0.54	7.58	96	0.59	7.51	150	0.63	7.46
45	0.61	7.45	99	0.52	7.44	153	0.51	7.45
48	0.59	7.45	102	0.51	7.40	156	0.49	7.44
51	0.54	7.42	105	0.54	7.45	159	0.52	7.46
54	0.52	7.43	108	0.53	7.45	162	0.52#	7.47
H4								
n [†]	$[F^-]$ (mg/L)	pH	n [†]	$[F^-]$ (mg/L)	pH	n [†]	$[F^-]$ (mg/L)	pH
3	0.70	7.45	9	0.80	7.47	15	0.78	7.50
6	0.76	7.51	12	0.75	7.47	18	0.77	7.56

Continued to the next page-

Continued from the previous page-

n^\dagger	$[F^-]$ (mg/L)	pH	n^\dagger	$[F^-]$ (mg/L)	pH	n^\dagger	$[F^-]$ (mg/L)	pH
21	0.74	7.55	30	0.65	7.45	36	0.71	7.51
24	0.62	7.54	33	0.68	7.48	39	0.72 [#]	7.52

H5								
n^\dagger	$[F^-]$ (mg/L)	pH	n^\dagger	$[F^-]$ (mg/L)	pH	n^\dagger	$[F^-]$ (mg/L)	pH
3	0.71	7.62	15	0.54	7.68	27	0.64	7.72
6	0.70	7.64	18	0.61	7.68	30	0.65 [#]	7.73
9	0.69	7.71	21	0.60	7.69			
12	0.71	7.69	24	0.62	7.7			

*Error limits: $[F^-] = \pm 0.2$ mg/L and $\text{pH} = \pm 0.1$; $^\dagger n$ = number of cycle or treatment.

^ψThe samples have been collected after every third treatment.

[#]The unit is still continuing without regeneration as the limestone is not yet exhausted.

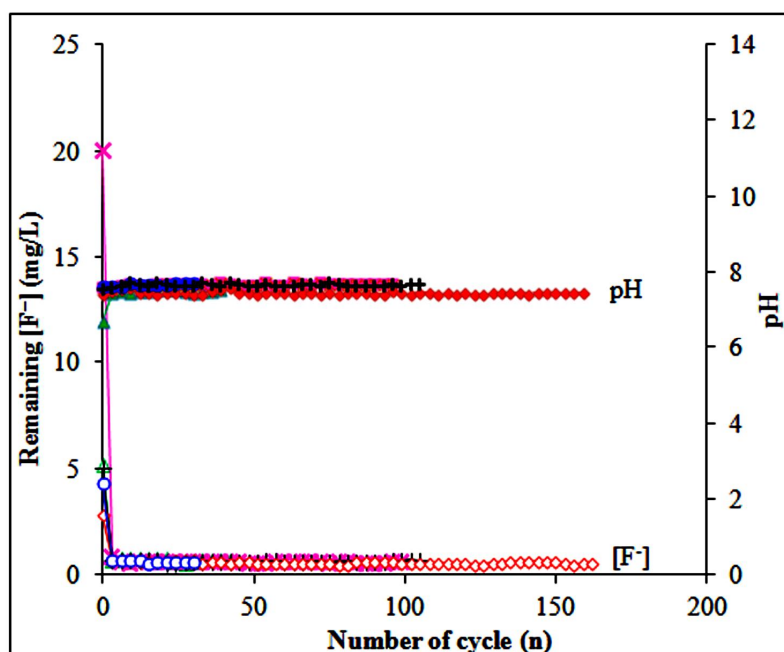


Figure 3.41. Results of $[F^-]$ before and after treatment along with final pH vs. number of cycle (n) of the household units: H1 (black), H2 (pink), H3 (red), H4 (green) and H5 (blue). $[PA]_0 = 0.68$ mM and residence time = 3 h.

It is interesting to note the lowering of fluoride concentration from initial 20 mg/L to an average of 0.59 mg/L in the domestic unit H2. This indicates that the performance of the present plug-flow PACLT method is almost independent of initial fluoride concentration at least up to 20 mg/L.

In Figure 3.42, where the average effluent $[F^-]$ and pH have been shown with expanded X-axis, indicates small variations in the effluent $[F^-]$ and the pH with the number of cycles. These variations can be attributed to variation in dissolution of small CaO impurity present in the limestone which is exposed to the surface nonuniformly.

Table 3.47. $[F^-]$ and pH of water before and after treatment and the total alkalinity of raw water collected from field source at small community (C) and households (H).

Field unit & source ^a	Total alkalinity (mg/L)	$[F^-]$ (mg/L)			pH	
		Before	After		Before	After
			\bar{a}	n		
C1	150	4.8	0.70	270	7.40	7.80
H1	125	5.0	0.62	105	7.52	7.65
H2	115	20	0.59	96	7.60	7.66
H3	104	2.8	0.55	162	7.41	7.44
H4	131	5.2	0.67	39	6.72	7.51
H5	129	4.2	0.62	30	7.01	7.70

^aC1 - the community unit at Dengaon, H1-H4 – household units at Napakling, Kehang Inglang, Sarik Teron and Kat Tisso villages installed by us and H5 – at Napakling household unit installed by a villager.

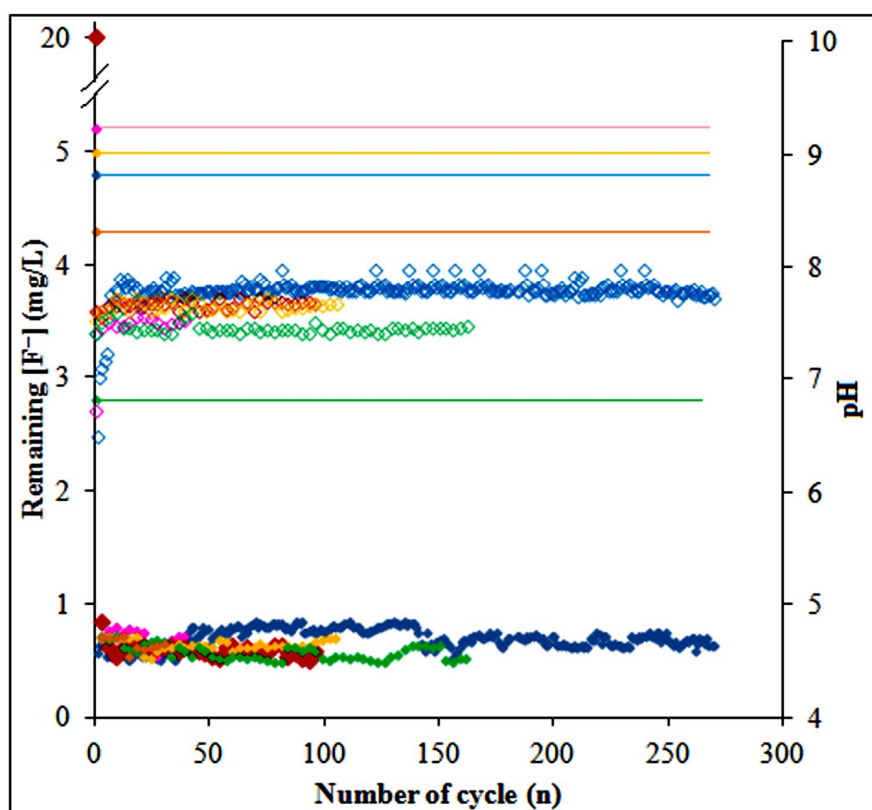


Figure 3.42. The average remaining $[F^-]$ and final pH of treated water with expanded X-axis for all six field units. C1 (blue), H1 (yellow), H2 (pink), H3 (green), H4 (red) and H5 (brown). $[PA]_0 = 0.68$ mM and residence time = 3 h. The $[F^-]_0$ of the units are shown with horizontal lines of respective colours.

The plots of average effluent $[F^-]$ and pH vs. total alkalinity of the source water showed a strong positive correlation between the effluent $[F^-]$ and the total alkalinity of the source water (Figure 3.43). However, there was only a very weak positive correlation between the effluent pH and the alkalinity. It may be noted here that the effluent pH is expected to increase with longer residence time in the reactor and the four layered filter. The effluent water of the small community unit had longer residence time in the filter.

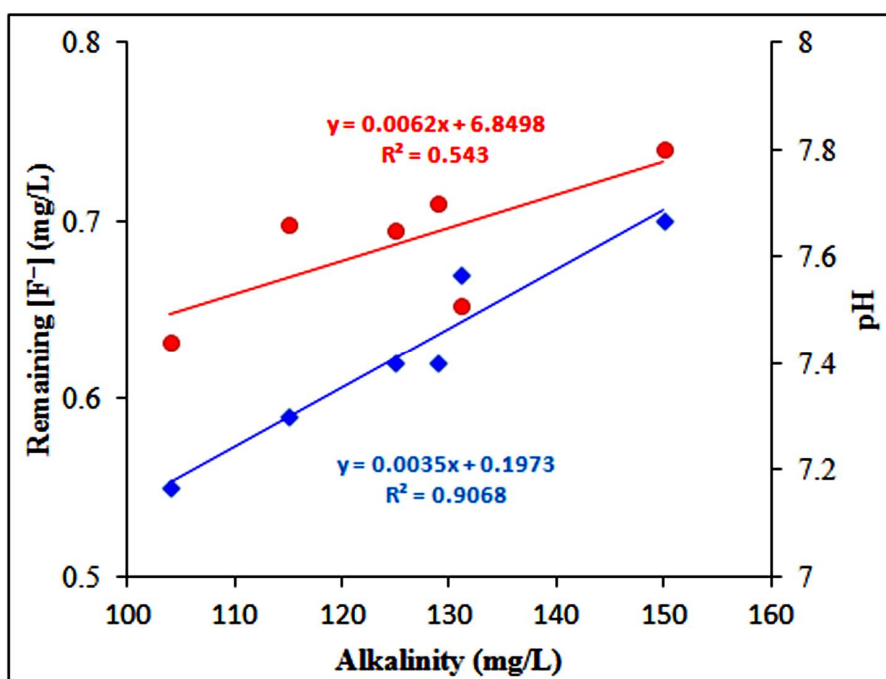


Figure 3.43. A plot of average value of remaining $[F^-]$ and final pH of treated water after the PACLT in the six field units vs. total alkalinity as $CaCO_3$ of the influent water.

3.5.6 A remark on the mechanism of fluoride removal

The observed fluoride removal which is independent of the initial fluoride concentration can be explained with the help of the combined precipitation and sorption mechanisms of fluoride removal. The precipitation which is quicker than the sorption first brings down the fluoride concentration to a level, say about 1-2 mg/L from any initial concentration²⁴⁷. Thereafter, the slower subsequent sorption therefore starts removing fluoride practically from similar concentrations giving almost the same effluent fluoride concentration in water from all sources.

3.5.7 Potability of treated water

The relevant water quality parameters of the water before and after treatment by the PACLT in plug-flow field units measured using standard method³¹² have been presented in Table 3.48. The results show that all the water quality parameters after treatment were within the respective WHO guideline values for drinking water⁴⁹. The concentrations of most of the metal ions have showed a small decrease after treatment. The concentrations of Ca^{2+} and PO_4^{3-} ions which are the main components in the materials used in the present method also remained within the WHO guideline values.

Table 3.48. Concentrations of metal ions and anions in sample before and after treatment by the PACLT. $[\text{PA}]_0 = 0.68 \text{ mM}$; $[\text{F}^-]_0 = 4.8 \pm 0.2 \text{ mg/L}$; source of water sample: water supply by PHED.

Parameter in mg/L except for pH	WHO guideline Value	Before treatment	After treatment
pH	6.50-8.50 ^a	7.40	7.80
Dissolved solid	600	175	240
Suspended solid	NS ^b	12	8
Total alkalinity as CaCO_3	200	150	154
Total hardness as CaCO_3	200	155	160
Calcium	50	10.8	12.1
Phosphate	NS	0.14	0.11
Sulfate	500	60	62
Chloride	250	20	7
Nitrate	50	0.45	0.27
Cadmium	0.003	<0.001	<0.001
Chromium	0.05	ND ^c	ND
Cobalt	NS	ND	ND
Copper	2.0	<1.00	<1.00
Lead	0.01	<0.001	<0.001
Magnesium	NS	2.81	3.40
Manganese	0.40	<0.001	<0.001
Zinc	3.0	2.5	0.07
Sodium	200	94.69	85.96
Potassium	NS	4.22	3.12
Iron	0.30	0.013	<0.001

^aAcceptable range for drinking, ^bNS: Not specified, ^cND: Not detectable

3.5.8 Suitability of the method

3.5.8.1 Capacity

The author has analyzed the capacity of limestone and done a cost- benefit analysis from the laboratory experiments done using the replica unit as the field trials experiments are still in progress without needing regeneration. With 45% recovery of the limestone after scrubbing and rinsing regeneration, a total of 149 L of water can be defluoridated per kg of limestone, which gives a capacity of limestone in the PACLT method as 1.20 mg/g. It may be noted here that this is a practical capacity estimated from actual fluoride removal and therefore cannot be compared with theoretical monolayer adsorption capacity. The capacity of limestone here was found to be slightly better than that estimated from the laboratory-scale pilot test.

3.5.8.2 Cost estimation

A cost estimation, estimated following the same procedure with that used in the pilot test (*Section 3.4.7.3 Cost estimation*), taking into account the dose of PA used in the field trial and periodic regeneration/replacement of limestone has shown the recurring cost of the present method as INR 0.016 (US\$ 0.00023) per liter of water which is lower than that of INR 0.04 (US\$ 0.00058) estimated from the pilot study. The capital cost depends on personal choice and requirement of the users.

A TCLP test was done on the precipitate produced in situ in the reactor which showed only 0.35 mg/L fluoride in the leached water. The leaching of fluoride from the precipitate in the present case is much lower than the maximum leaching of 150 mg/L allowed for land-fill dumping by the US-EPA³⁰⁹.

The field trial has proven the present method as an efficient, low-cost, safe and environment friendly. Non requirement of energy is another advantage. The acceptance of the method by the rural users and the ability of the rural people to use the method shows the simplicity of the method. Thus, the field trial has clearly proven the of the present PACLT in plug-flow mode method as suitable for rural applications in fluoride affected areas both at domestic and small community scale.

3.5.9 Summary

The findings of the pilot test can be summarised as follows:

- The field trial has shown excellent and consistent fluoride removal by small community and domestic units of the PACLT in plug-flow mode.
- The method removes fluoride from initial 2.8-20 mg/L to 0.5-0.8 mg/L with a dose of just 0.68 mM PA. The removal is almost independent of initial fluoride concentration.
- In this method, the precipitation rapidly brings down the fluoride concentration from any high level up to at least 20 mg/L to a moderate level of 1-2 mg/L controlled by solubility product, whereafter sorption removes the rest fluoride to finally give the desired 0.5-0.8 mg/L in the effluent water.
- The relevant water quality parameters after treatment remain within the WHO guideline values for drinking water. The pH of the treated water also remains within the range of 7.4-7.8 which is in the middle of the acceptable range for drinking water, i.e., 6.5-8.5.
- The pre-assessment with the replica test gave 83 L of treated fluoride-free water per kg of crushed limestone but the field small community unit has been giving more treated water than that. The regenerated limestone shows almost 45% and 57% activity using simple scrubbing-rinsing and lime solution treatment, respectively, as found from the replica test. There is no need for frequent replacement or replenishment of limestone in the units.
- The actual fluoride removal capacity of limestone in the PACLT in plug-flow mode has been found to be 1.20 mg/g from the pre-assessment experiment with the replica unit. The recurring cost of the PACLT method including the costs of limestone and PA has been estimated to be INR 0.016 (US\$ 0.00023) per liter of water.
- The acceptance of the method by the rural users and the ability of the rural people to use the method shows its simplicity of the method which can be operated without electricity.
- The field trial has clearly proven the present PACLT in plug-flow mode method as an efficient, low-cost, safe, environment-friendly and user-friendly method suitable for rural applications in fluoride affected areas.